A FINITE ELEMENT MODEL FOR DYNAMIC ANALYSIS OF MOORING CABLES

by

Per I. Johansson

Sivilingeniør (S.M.) The Technical University of Norway
1969

Cand. Real. (S.M.) University of Oslo
1972

Submitted in partial fulfillment of the requirements
for the degree of Doctor of Philosophy

at the

Massachusetts Institute of Technology
January, 1976

Signature of Author .....
Department of Ocean Engineering
14, January, 1976

Certified by .....
Thesis Supervisor

Accepted by .....
Chairman, Departmental
Committee on Graduate Students

AUG 16 1976

A FINITE ELEMENT MODEL FOR DYNAMIC ANALYSIS OF MOORING CABLES

by

Per I. Johansson

Submitted to the Department of Ocean Engineering January 1976, in partial fulfillment of the requirements for the degree of Doctor of Philosophy.

ABSTRACT

A finite element model has been constructed for numerical analysis of the dynamic response of mooring cables. The model is non-linear, taking into account the velocity squared dependence of the drag force, large deviations away from equilibrium and the effect of tension variation in the equations of motion. The solution method is deterministic in the time domain and is intended for analyzing transient phenomena. The equations of motion are formulated in matrix form. Normal modes are defined for small amplitude oscillations about equilibrium, and the equations of motion are transformed to normal coordinates.

A new (to our knowledge) method for integrating approximately the coupled equations of motion numerically was developed as a variation of Newmark's method. The coupled force terms are decoupled by assuming each as a function of time only over short intervals of time and a trial and error process is used to estimate the state at the end of the interval.

The mode of excitation particularly studied here is that of a forced motion of one end of the cable (the upper point of fixation to the moored vehicle). Several examples are analyzed. Some of these are of a theoretical nature, allowing correlations with analytical solutions. Finally two examples of mooring lines are analyzed, under transient pull from rest in equilibrium and under harmonic forced motion of the upper end.

Thesis Supervisor: Edward C. Kern

Title: Assistant Professor of Ocean Engineering

ACKNOWLEDGEMENTS

I gratefully appreciate the advice of my thesis supervisor, Professor E. C. Kern and the efforts of the other members of my committee, Professor J. N. Newman of MIT, H. O. Berteaux of Woods Hole Oceanographic Institution and Dr. D. E. Cummings of Draper Laboratories.

Further, I am thankful to Norges Teknisk-naturvitenskapelige Forskningsråd (The Norwegian Council for Technology and Science) and my employer, Det norske Veritas, for the financial support which permitted my studies at MIT.

I also wish to thank Mrs. Annette Pearson for her excellent typing work.

TABLE OF CONTENTS

		Page
Title Page		1
Abstract		2
Acknowledgements		3
Table of Contents		4
Table of Figures		6
Ch. 1	INTRODUCTION	8
1.1	Technical Background	8
1.2	Review of Literature	11
Ch. 2	FORCES AND EQUILIBRIUM OF CABLE SEGMENT	21
2.1	Geometric Relations	21
2.2	Forces on an Infinitesimal Segment of a Continuous Cable. Equilibrium Relations	26
2.3	Forces on a Finite Element	38
Ch. 3	STATIC EQUILIBRIUM CONFIGURATION	58
3.1	General Method	58
3.2	Equilibrium Conditions at the Nodes	60
Ch. 4	FORCES DUE TO DEVIATIONS FROM EQUILIBRIUM	63
4.1	Tension Force Deviations	63
4.2	Inertia Forces	72
4.3	Other Forces	77
Ch. 5	FINITE ELEMENT MODEL FOR TOTAL SYSTEM	78
5.1	The Total Cable System	78
5.2	Total Dynamic Equilibrium	82
5.3	Boundary Conditions	83
5.4	Eigenfrequencies and Mode Shapes	86
5.5	Normal Form of the Equations of Motion	90
5.6	A Linear Damping Term	91
Ch. 6	INTEGRATION OF THE EQUATIONS OF MOTION	93
6.1	General Requirements to Integrals	93
6.2	Various Methods in Use	94
6.3	The Present Method	99

		Page
Ch. 7	COMPUTER PROGRAM -	104
Ch. 8	CALCULATION EXAMPLES	110
8.1	Natural Vibrations of Cable Suspended in One End	111
8.2	Transverse Waves on a Straight String . .	117
8.3	Response of a Taut String with Current Suddenly Applied at t=0	124
8.4	Wave Propagation on String with Damping .	131
8.5	Analysis of Mooring Lines	145
Ch. 9	SUMMARY AND REVIEW	185
9.1	Review of Calculation Model	185
9.2	Review of Calculation Results	194
9.3	Suggestions for Further Work	200
APPENDIX A:	Computer Listing of MAIN Program and Subroutine TIMINT.	202
REFERENCES		211
BIOGRAPHICAL NOTE		214

LIST OF FIGURES

Fig. 1.2.1 Discrete Element Types--14

1.2.2 Configurations for Incremental Integration--19

2.1.1 Geometry of Cable--21

2.2.1 Geometry of Cable Segment--26

2.2.2 Static Forces on Cable Segment--28

2.2.3 Dynamic Forces on Cable Segment--34

2.2.4 Kelvin Viscoelastic Model--36

2.3.1 Distributed Force on Finite Element--41

3.2.1 Two Adjoining Finite Elements--60

4.1.1 Displaced State of Finite Element--63

4.2.1 Dynamic Variables--73

5.1.1 Total Finite Element Model--78

5.3.1 Analogous Two-mass System--85

7.1.1 Macro Flow Chart Program DYNLIN--108

7.1.2 Flow Chart Subroutine TIMINT--109

8.1.1 Finite Element Models--113

8.1.2 Natural Mode Shapes of Model I and Analytic Solution--116

8.2.1 Taut, Straight String--117

8.2.2 Initial Conditions--119

8.2.3a,b String Shape as Function of Time--122

8.3.1 String in Homogeneous Current--126

8.3.2 Modal and Midpoint Response--129

8.4.1 Finite Element Model of String--138

Fig. 8.4.2 Response Parameters of String--138

8.4.3a,b String Shape as a Function of Time--143

8.5.1 Mooring Configuration--147

8.5.2 Shape of Mooring Line at 500 m Depth--150

8.5.3 Shape of Mooring Line at 200 m Depth--151

8.5.4a Natural Mode Shapes--Transverse Modes--154

8.5.4b Natural Mode Shapes--Longitudinal Modes--155

8.5.5a Pull Test Response--500 m Depth Cable--158

8.5.5b Pull Test Response--200 m Depth Cable--159

8.5.5c Force Balance in Initial Motion--162

8.5.6 Harmonic Time Dependent Response--165

8.5.7a-d Harmonic Time Dependent Response--Modes 1-18--167

8.5.8 Tension Variation Amplitudes as Function of T_e. 500 m Depth Cable--171

8.5.9 Tension Variation Amplitudes as Function of T_e, 200 m Depth Cable--172

8.5.10 Response as Function of Excitation Amplitude--175

9.2.1 Tension Response for Different Excitation Amplitudes--197

9.2.2 Simple Oscillator Analogy for Transverse Motion--199

CHAPTER 1. Introduction.

1.1 Technical Background.

Mooring is technically a method for keeping a vehicle (platform) on station at or below the sea surface. Another method developed for this purpose in recent years is dynamic positioning. From a technical point of view, mooring may look like the simpler method, requiring basically only a mooring cable and an anchor, while dynamic positioning utilizes a system of thrusters and is controlled by a sophisticated computer system. However, a comparison between the two systems should be more detailed in specifying operational parameters like accuracy requirements of position, convenience in relocating, cost of operation, and desired lifetime.

One can assume that a vehicle, e.g. a mineral or petroleum production platform, which is required to remain permanently at a specific location, may favour the mooring concept. A vehicle, e.g. a drilling ship, which is required to shift position from time to time, sometimes even on short notice, may be more likely to choose the dynamic positioning concept.

One can distinguish two important aspects of the dynamic behavior of a moored system. One is the so-called slow drift motion, connected with the horizontal, low frequency forces imposed upon the vehicle by the momentum content of the irregular waves. In an irregular sea these forces have a period of

variation several times the wave period. When the vehicle is restrained by mooring lines, we have an oscillation system moving under these slowly varying forces. For a heavy body with long mooring lines will the vehicle-mooring system have a relatively long natural period and under certain circumstances can the slow drift forces give a resonance excitation of the system. See e.g. [20]* for a discussion of slow drift.

The other aspect is the more rapid oscillatory behavior of the body among the waves. This corresponds to the phenomenon normally treated in Naval Architecture as the sea-keeping problem. It appears to be accepted engineering practice to assume that the wave motion of heavy vehicles is practically not influenced by the presence of the mooring lines. For lighter bodies, e.g. buoys, is the mutual coupling between the cable and the vehicle more important.

It also seems to be accepted practice to treat the two phenomena of slow drift motion and wave motion as uncoupled. This implies that in analyzing the slow drift motion, the response of the mooring cables can be assumed to be practically static, so that the non-linear restoring force as a function of displacement can be estimated by a statical analysis. In analyzing the response of the cable to the rapid excitation, a more detailed consideration must be made of the forces acting on the cable, particularly the interaction between the tension, drag and inertia forces in determining the motion of the cable.

---

*Numbers in [] refer to References at the end.

One should also be able to determine the response of the cable to transient conditions, e.g. as due to a single, large wave imposed upon the vehicle.

The main aspect of the present thesis is the analysis of a mooring cable to a given time dependent excitation of the upper fixation point to the vehicle.

1.2 Review of Literature.

1.2.1 Survey of methods of analysis.

An early formulation of a dynamic model of cables and chains was given by E. J. Routh [5]. Consider a small segment ds of the cable, whose parametric trajectory in terms of cartesian coordinates x,y,z is x(s), y(s), z(s) where s is the trajectory curve length. Let $d\sigma$ be the unstretched length of ds, so that $ds = d\sigma(1+\varepsilon)$, where ε is the local strain. R is the tension at the lower end of ds, and the resolved components along x,y,z axes are

$$R\frac{dx}{ds}\ ,\ R\frac{dy}{ds}\ ,\ R\frac{dz}{ds}$$

At the upper end the resolved tension components are:

$$R\frac{dx}{ds} + \frac{d}{ds}\left(R\frac{dx}{ds}\right)ds,\ \text{etc.}$$

so that the net tension force components are:

$$\frac{d}{ds}\left(R\frac{dx}{ds}\right)ds = \frac{d}{d\sigma}\left(R\frac{dx}{ds}\right)d\sigma,\ \text{etc.}$$

Let m be the mass per unit length of unstretched cable, and X,Y,Z external force components per unit of unstretched length. Further, let u,v,w be the components of the segment velocity. Then the equations of motion can be written:

$$(1.2.1) \qquad m \frac{\partial u}{\partial t} = \frac{\partial}{\partial \sigma} \left(R \frac{\partial x}{\partial s}\right) + X \ ,$$

with corresponding equations for the y and z directions. t represents time. For the cable in water, the hydrodynamic forces are included in X,Y,Z.

For two-dimensional problems, the equations may be expressed in terms of local tangential and normal components in the form

$$(1.2.2) \qquad \begin{aligned} m\left(\frac{\partial u}{\partial t} - v \frac{\partial \phi}{\partial t}\right) &= P + \frac{\partial T}{\partial \sigma} \\ m\left(\frac{\partial v}{\partial t} + u \frac{\partial \phi}{\partial t}\right) &= Q + \frac{T}{\rho} \frac{\partial s}{\partial \sigma} \end{aligned}$$

where P,Q are tangential and normal components of the external force, u,v represents the tangential and normal velocities and ϕ is the angle between the tangent and the horizontal plane or some other fixed direction in the cable plane.

Although Routh does not refer specifically to moorings, the fundamental equations (1.2.1) or (1.2.2) form the basis for many later attempts at an analytical solution for the dynamic behavior of cables.

In a recent survey paper Choo and Masarella [25] make the following classification of current analytical and numerical methods for solving the equations of motion:

1. method of characteristics,
2. finite element methods,
3. linearization methods,
4. other methods.

The method of characteristics is a direct mathematical solution of equations of motion of the form (1.2.1) or (1.2.2), by integrating the partial differential equations along characteristic lines in x,y,z,t-space. Although the method gives exact analytical solutions for simple examples like straight strings, real mooring problems require a stepwise computerized solution method. With this method, the equations of motion are "exact", but some approximation is normally involved in the mathematical solution. Patton [13] has given an extensive account of the formulation and solution of cable problems in terms of characteristics.

Under the concept of finite element methods, are classified several schemes for conceptually modifying the physical system before the mathematical formulation. Some examples of finite element models are shown in Fig. 1.1.1. a) represents a model of an inelastic cable where the mass of the cable is assumed lumped at several nodes, which are assumed connected by massless and inextensible strings. Such models were used by Walton and Polacheck [26] and Dominguez and Smith [12]. In type b) the connecting segments are represented as springs, so

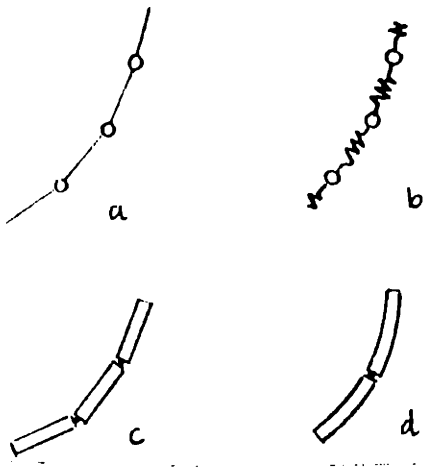

Fig. 1.2.1

Discrete Element Types

that elongation can be taken into account. In type c) the cable is modeled as a series of straight bars with distributed mass, which are connected by joints at the nodal points. Equations of motion can be formulated for each element. In the general three-dimensional formulation, six equations are required for each element. Alternatively, as will be done in this thesis, one can reduce the element properties to equivalent nodal properties and formulate the equations of motion for each node. In the former case, one must solve a number of simultaneous differential equations, while in the latter case, the problem can be approached by the methods of matrix algebra. Element type d) is similar to c) with the addition of internal curvature so that slope continuity can be represented in the model, while in c) the slope varies discontinuously at the nodes. A more detailed discussion of finite element methods will be given in Sec. 1.2.2.

With the linearization method, the equations of motion of cable-vehicle systems are linearized in order to study stability and frequency response. The motion of the system is assumed to consist of small deviations from the state of equilibrium. Then the non-linear partial differential equations are reduced to linear partial differential equations with curve length s or σ as the space variable. Usually the perturbations are assumed to be harmonic oscillations with frequency equal to some excitation frequency. Then the time derivatives may be eliminated from the equations, which become ordinary differential equations in s. The equations are still not easy for explicit solution in the general case, but may be solved for certain special cases. Examples of this type of formulation are Reid [14] and Hoffman, Geller and Niederman [15].

One problem in connection with the linearization method is to what extent solutions to the linearized equations are representative of the real physical problem. This question comes up in view of the non-linear dependence of the drag force on velocity.

A different approach, which does not approach the problem via equations of the form (1.2.1) or (1.2.2) is given by Tsai [16]. He formulates the problem by the bond graph method in terms of power and energy variables and accounts for energy supply, storage, and dissipation throughout the system, based on fundamental physical conditions.

1.2.2 Previous work using the finite element method.

The finite element concept discussed in Sec. 1.2.1 is slightly more general than what is usually understood by the finite element method (see e.g. Zienkiewicz [9]). In the displacement method, a structure is modelled as a continuous system, but the total displacement field is assumed to be described by the displacements at a finite number of nodes. At internal points, interpolation rules are used to describe the displacement field. By this description stresses and strains are normally not continuous across the boundaries between elements.

If the model displacements are interpreted as generalized coordinates, corresponding generalized forces may be defined in terms of the real forces on the structure by using the principle of virtual work. The total analysis of the structure can thus be reduced to a system with a finite number of degrees of freedom.

Some attempts have been made in recent years to formulate finite element models, and this section will review some of these. These models are similar in the formulation of the equations of motion, but the solution methods differ.

Dominguez and Smith [12] used a set of n equations of motion, for a system with n degrees of freedom, of the form

$$\underline{m}\ddot{\underline{q}} + \underline{c}\dot{\underline{q}} + \underline{k}\underline{q} = \underline{f}(t) \qquad (1.2.3)$$

$$(\underline{U} - \lambda \underline{I})\underline{\phi} = 0, \tag{1.2.6}$$

where $\lambda=\alpha^{-1}$ and $\underline{\phi}$ are either real or complex quantities and

$$U = \begin{pmatrix} \underline{O} & \underline{I} \\ -\underline{\underline{am}} & -\underline{\underline{ac}} \end{pmatrix}$$

where $\underline{a} = \underline{k}^{-1}$ is the flexibility matrix. Equation (1.2.6) can be solved for 2n eigenvalues λ and corresponding eigenvectors $\underline{\phi}$.

When $\underline{a},\underline{m},\underline{c}$ are symmetric, a linear transformation matrix $\underline{T}$ may be constructed from the eigenvectors, such that in terms of new coordinates $\underline{\xi}$ given by

$$\underline{z} = \underline{T}\,\underline{\xi}$$

the equations (1.2.5) become uncoupled.

This method seems to give a good method for analyzing cables. However, a few seeming restrictions should be mentioned. From (1.2.3) it seems that the damping is assumed to be linear and also that the forcing function $\underline{f}(t)$ is a given function of time. Hence the effect of velocity squared damping has not been taken into account.

In [17] Leonard and Recker use a solution technique, based on the theory of incremental deformations. The governing non-linear equations are reduced to a system of quasi-linear equations, which are dependent on the prior history of the

system. To reach its current position, the cable is assumed to have under-gone non-linear displacements from its initial configuration Γ^O to its present reference configuration Γ^I and then further small displacements to its current position Γ^J. The relation between the various configurations is shown in Fig. 1.2.2. With the cable in configuration Γ^J, it is

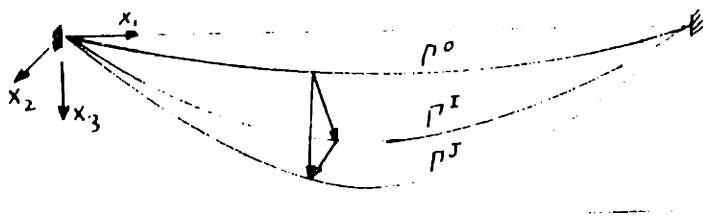

Fig. 1.2.2

Configurations for Incremental Integration

assumed to be divided into N elements. A simple linear variation of the displacement field over the element is assumed, although more complex variations could have been admitted if more nodes or nodal variables had been defined. From Γ^I, considered as a reference configuration, the solution is proceeded in a short time increment, and the configuration after this step is then taken as reference configuration for the next increment. The equation of motion for the current configuration Γ^J, referred to Γ^I, is derived by Hamilton's principle.

In this way non-linear behavior is modeled as a sequence of quasi-linear steps by successively updating the reference configuration for a subsequent period.

In [18] Leonard extends the work in [17] by allowing elements to have internal curvature and slope continuity at the nodes. With this formulation, a smaller number of elements may be used for the same accuracy than by using straight elements.

In [17] and [18] the element model may be changed for each new reference configuration.

Webster [19] obtains an equation of motion of the form

$$\underline{\underline{M}}\,\ddot{\underline{q}} + \underline{\underline{K}}(\underline{q},\underline{f})\underline{q} = \underline{f}(\underline{q},\dot{\underline{q}},t) \ ,$$

where the stiffness matrix $\underline{\underline{K}}$ may depend on the current configuration $\underline{q}$ and the force $\underline{f}$. For solution he uses an iterative technique based on Newmark's method [29], but a linearized incremental technique, similar to [17], may also be used.

CHAPTER 2. Forces and Equilibrium of a Cable Segment.

2.1 Geometric Relations.

2.1.1 Coordinates.

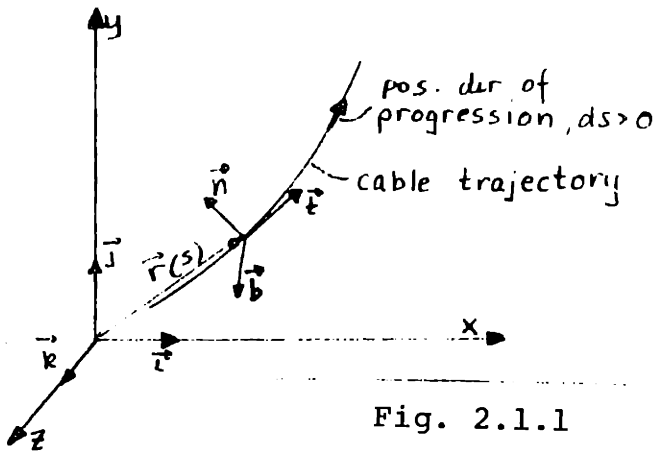

Fig. 2.1.1

Geometry of Cable

We consider the cable embedded in a cartesian coordinate system xyz with unit vectors $\vec{i},\vec{j},\vec{k}$ along the axes, Fig. 2.1.1. Using the cable trajectory length s as parameter, points on the trajectory can be represented by the radius vector $\vec{r}(s)$, or $\vec{r}(s,t)$, if the configuration is dependent on time t.

When the trajectory is time dependent, it is useful to label points on the trajectory such that an individual particle in the cable always has the same coordinate. We then introduce the Lagrangian coordinate s_o, which can be interpreted as the trajectory length parameter in some standard situation, e.g. in a completely unstretched state or under some given state of tension, e.g. in equilibrium. In terms

of s_o the length $L_o=\int ds_o$ is independent of the state of the cable, while $L=\int ds$ represents the total cable length and is time dependent. In terms of s a particle may have a variable coordinate value under dynamic conditions.

For a short segment ds_o, strain is defined by

$$(2.1.1) \qquad \varepsilon = \frac{ds-ds_o}{ds_o} \quad .$$

For a simple elastic material there is a relation between tension and strain

$$(2.1.2a) \qquad R = R(\varepsilon) \quad .$$

Most materials have some internal damping, which can most simply be expressed in the form

$$(2.1.2b) \qquad R = R(\varepsilon,\dot{\varepsilon}),$$

depending also on the time rate of change of strain, $\dot{\varepsilon}$.

The relation between s_o and s can also be expressed as

$$ds = ds_o(1+\varepsilon).$$

Hence we can also then write the cable trajectory in the forms

$$\vec{r}(s_o) \text{ or } \vec{r}(s_o,t) \quad .$$

Instead of using the cartesian coordinates xyz, it may be

convenient to express various parameters of the cable, e.g. displacements away from equilibrium or forces acting on the cable, in terms of directions tangential and normal to the local cable direction. We can do this by using the theory of space curves (Hildebrand [3], ch. 6). We start from the parametric equation of the trajectory

$$\vec{r}(s) = x(s)\vec{i} + y(s)\vec{j} + z(s)\vec{k}.$$

The tangent vector is

$$\vec{t} = \frac{d\vec{r}}{ds} = \frac{dx}{ds}\vec{i} + \frac{dy}{ds}\vec{j} + \frac{dz}{ds}\vec{k} = \alpha_1\vec{i} + \alpha_2\vec{j} + \alpha_3\vec{k},$$

The principal normal vector is

$$\vec{n} = \rho\frac{d\vec{t}}{ds} = \rho\left(\frac{d^2x}{ds^2}\vec{i} + \frac{d^2y}{ds^2}\vec{j} + \frac{d^2z}{ds^2}\vec{k}\right) = \beta_1\vec{i}+\beta_2\vec{j}+\beta_3\vec{k}$$

where ρ is the local radius of curvature

$$\rho = \left(\left(\frac{d^2x}{ds^2}\right)^2 + \left(\frac{d^2y}{ds^2}\right)^2 + \left(\frac{d^2z}{ds^2}\right)^2\right)^{-1/2} .$$

Since $\vec{t}\cdot\vec{t}=1$, it follows by differention that $\vec{t}\cdot\frac{d\vec{t}}{ds} = \frac{1}{\rho}\vec{t}\cdot\vec{n} = 0$ i.e. that $\vec{t}$ and $\vec{n}$ are normal, assuming $\vec{n}\neq 0$. We can finally define the bi-normal vector $\vec{b}$ by

$$\vec{b} = \vec{t}\times\vec{n} = \gamma_1\vec{i} + \gamma_2\vec{j} + \gamma_3\vec{k} ,$$

so that the triad $\vec{t},\vec{n},\vec{b}$ defines a right-handed orthonormal intrinsic coordinate system at each point of the trajectory.

In general $\vec{t},\vec{n},\vec{b}$ are functions of s (or s_o). For a two-dimensional configuration $\vec{t}$ and $\vec{n}$ lie in the cable plane, so that $\vec{b}$ = const represents the normal to the cable plane. In the subsequent theoretical treatment the general three-dimensional case will be discussed.

In the relations

$$\vec{t} = \alpha_1\vec{i} + \alpha_2\vec{j} + \alpha_3\vec{k}$$

(2.1.3a) $$\vec{n} = \beta_1\vec{i} + \beta_2\vec{j} + \beta_3\vec{k}$$

$$\vec{b} = \gamma_1\vec{i} + \gamma_2\vec{j} + \gamma_3\vec{k}$$

we have $\vec{t}\cdot\vec{t} = \sum_{i=1}^{3} \alpha_i^2 = 1$, $\vec{n}\cdot\vec{n} = \sum_{i=1}^{3} \beta_i^2 = 1$, $\vec{b}\cdot\vec{b} = \sum_{i=1}^{3} \gamma_i^2 = 1$,

$\vec{t}\cdot\vec{n} = \sum_{i=1}^{3} \alpha_i\beta_i = 0$, $\vec{t}\cdot\vec{b} = \sum_{i=1}^{3} \alpha_i\gamma_i = 0$, $\vec{n}\cdot\vec{b} = \sum_{i=1}^{3} \beta_i\gamma_i = 0$.

Then we can form the inverse relations:

$$\vec{i} = (\vec{i}\cdot\vec{t})\vec{t} + (\vec{i}\cdot\vec{n})\vec{n} + (\vec{i}\cdot\vec{b})\vec{b} = \alpha_1\vec{t} + \beta_1\vec{n} + \gamma_1\vec{b}$$

(2.1.3b) $$\vec{j} = \alpha_2\vec{t} + \beta_2\vec{n} + \gamma_2\vec{b}$$

$$\vec{k} = \alpha_3\vec{t} + \beta_3\vec{n} + \gamma_3\vec{b}$$

2.1.2 Transformation of vector components between cartesian and intrinsic coordinates.

Let $\vec{\rho}(\vec{r})$ be a vector defined at point $\vec{r}$ (e.g. displacement or force) with cartesian components u,v,w. Using (2.1.3a,b) we get

$$\begin{aligned}\vec{\rho} &= u\vec{i} + v\vec{j} + w\vec{k} \\ &= (u\alpha_1+v\alpha_2+w\alpha_3)\vec{t} + (u\beta_1+v\beta_2+w\beta_3)\vec{n} + (u\gamma_1+v\gamma_2+w\gamma_3)\vec{b} \\ &= \xi\vec{t} + \eta\vec{n} + \zeta\vec{b},\end{aligned}$$

where ξ,η,ζ are the intrinsic components of $\vec{\rho}$. The relation between u,v,w and ξ,η,ζ can be represented on the matrix form

$$\begin{pmatrix}\xi\\ \eta\\ \zeta\end{pmatrix} = \begin{pmatrix}\alpha_1 & \alpha_2 & \alpha_3\\ \beta_1 & \beta_2 & \beta_3\\ \gamma_1 & \gamma_2 & \gamma_3\end{pmatrix}\begin{pmatrix}u\\ v\\ w\end{pmatrix}$$

or

$$\underline{\xi} = \underline{\underline{A}}\,\underline{u}$$

where $\underline{\xi}$ and $\underline{u}$ are matrix column vectors, $\underline{\underline{A}}$ is the transformation matrix. From the relations satisfied by the coefficients $\alpha_i,\beta_i,\gamma_i$, we see that $\underline{\underline{A}}\,\underline{\underline{A}}^T=\underline{\underline{I}}$, $\underline{\underline{A}}^T=\underline{\underline{A}}^{-1}\underline{\underline{I}}=\underline{\underline{A}}^{-1}$, where $\underline{\underline{A}}^T$ is the transpose of $\underline{\underline{A}}$.

Hence the inverse $\underline{\underline{A}}^{-1}=\underline{\underline{A}}^T$ and $\underline{u}=\underline{\underline{A}}^{-1}\underline{\xi}=\underline{\underline{A}}^T\underline{\xi}$.

2.2 Forces on an Infinitesimal Segment of a Continuous Cable. Equilibrium Relations.

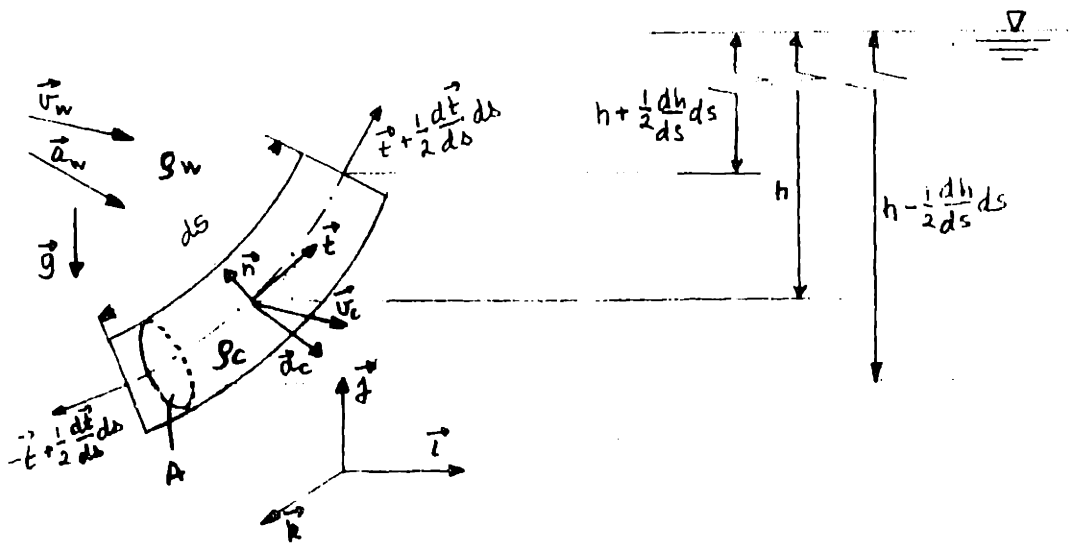

Fig. 2.2.1

Geometry of Cable Segment

We consider the situation shown in Fig. 2.2.1. The infinitesimal segment of length ds and cross section A at length parameter coordinate s is considered cut from the cable. The forces on this segment are to be determined. Several parameters contribute to determine the forces. Geometric parameters of the cable are cross sectional area and shape. Physical properties of the cable are density, elastic modulus, and internal viscous coefficient. Configuration and state of motion are represented by the cable direction, velocity and acceleration. The properties of the surrounding water are determined by the density, velocity

and acceleration. The interaction between cable and water is described by the normal and tangential drag coefficients and the hydrodynamic mass coefficient. The state of deformation is given by the strain ε and strain rate of change $\dot{\varepsilon}$, the state of stress is given by the tension R. Further the properties of the trajectory enters via the tangent direction $\vec{t}$ and the curvature κ. Further parameters are the acceleration of gravity and the depth below the surface.

We make a somewhat arbitrary distinction between static and dynamic forces, the former including the forces that occur when the cable is static, while the latter are the forces which occur only in a dynamic situation. Of course, the forces classified as static also occur in dynamics, but may have different expressions.

In Fig. 2.2.1 the following symbols are used:

$\vec{v}_w$: water velocity

$\vec{a}_w$: water acceleration

$\vec{v}_c$: cable velocity

$\vec{a}_c$: cable acceleration

ρ_w: water mass density

ρ_c: cable mass density

$\vec{g}=-g\vec{j}$: acceleration of gravity

h: segment depth below surface

and acceleration. The interaction between cable and water is described by the normal and tangential drag coefficients and the hydrodynamic mass coefficient. The state of deformation is given by the strain ε and strain rate of change $\dot{\varepsilon}$, the state of stress is given by the tension R. Further the properties of the trajectory enters via the tangent direction $\vec{t}$ and the curvature κ. Further parameters are the acceleration of gravity and the depth below the surface.

We make a somewhat arbitrary distinction between static and dynamic forces, the former including the forces that occur when the cable is static, while the latter are the forces which occur only in a dynamic situation. Of course, the forces classified as static also occur in dynamics, but may have different expressions.

In Fig. 2.2.1 the following symbols are used:

$\vec{v}_w$: water velocity

$\vec{a}_w$: water acceleration

$\vec{v}_c$: cable velocity

$\vec{a}_c$: cable acceleration

ρ_w: water mass density

ρ_c: cable mass density

$\vec{g}=-g\vec{j}$: acceleration of gravity

h: segment depth below surface

2.2.1 Static forces.

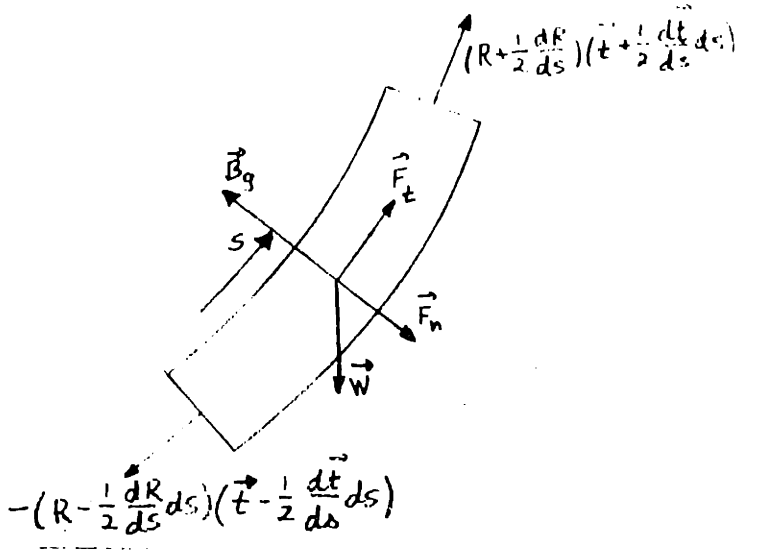

Fig. 2.2.2

Static Forces on Cable Segment

The static forces acting on the segment are shown in Fig. 2.2.2:

i) Tangential friction drag force $\vec{F}_t ds$, due to the tangential component $\vec{v}_{wt}=(\vec{v}_w\cdot\vec{t})\vec{t}$ of $\vec{v}_w$.

ii) Normal drag force $\vec{F}_n ds$, due to the normal component $\vec{v}_{wn} = \vec{v}_w-\vec{v}_{wt}$ of $\vec{v}_w$.

iii) Buoyancy force, $\vec{B}_g ds$, due to the hydrostatic pressure on the segment. Since the pressure acts only on the sides of the element and not on the end faces, the buoyancy force is not in general vertical.

iv) Gravity force, $\vec{W}ds$, due to the weight of the segment.

v) Tension forces $\pm R\vec{t}$ on the end faces. This is assumed to be the only force transmitted between neighboring segments

in the model of a completely flexible cable, so that shear forces and bending moments are disregarded. This assumption must be dropped for a cable with significant bending stiffness. Because of the curvature, the resultant of the end forces will not be in the tangent direction.

Writing the forces $\vec{F}_t ds$, $\vec{F}_n ds$, etc., we relate the force density to the current segment length ds. We can also relate force densities to the Lagrangian segment length ds_o by writing $\vec{F}_t ds = \vec{F}_t(1+\varepsilon)ds_o = \vec{F}_t^{\,o} ds_o$, et., so that the Lagrangian force density becomes $\vec{F}_t^{\,o} = \vec{F}_t(1+\varepsilon)$, etc. For dynamic problems this is advantageous, since the mass density of the cable is constant in terms of s_o, but not in terms of s. However, for many practical moorings, e.g. steel wire ropes, ε is usually small compared to 1, so that the distinction in such cases is not of large practical importance.

In the subsequent expressions, we assume that $\vec{t},\vec{n},\vec{b}$ are known in terms of $\vec{i},\vec{j},\vec{k}$, i.e. eqs. (2.1.3a,b). We further use the symbols:

c_N: normal drag coefficient

c_T: tangential friction drag coefficient

d: effective diameter of cable segment

κ: Local cable curvature, $\rho = \kappa^{-1}$: radius of curvature.

i) Tangential friction drag force.

Tangential water velocity component is $\vec{v}_{wt}=(\vec{v}_w\cdot\vec{t})\vec{t}$. The friction drag force is then:

$$(2.2.1)\qquad \vec{F}_t ds = \frac{1}{2}\rho_W c_T \pi d|\vec{v}_{wt}|\vec{v}_{wt}ds$$

If the cross section is not circular, e.g. in the case of a chain, πd can be considered as the effective circumference, upon which the value of c_T is based.

ii) Normal drag force.

Normal water velocity component is $\vec{v}_{wn}=\vec{v}_w-\vec{v}_{wt}$. The drag force is then:

$$(2.2.2)\qquad \vec{F}_n ds = \frac{1}{2}\rho_W c_N d|\vec{v}_{wn}|\vec{v}_{wn}ds.$$

If the cross section is not circular, d can be considered as the effective diameter for the value of c_N.

(iii) Buoyancy

We now consider a segment with a simple cross section, normally approximately circular. Slightly different reasoning must be used in the case of e.g. a chain.

If we use Archimedes' principle for the whole volume Ads, we must subtract the pressure integral over the end faces, which are not in contact with the water, to get the correct

pressure integral over the sides.

$$(2.2.3)\quad \vec{B}_g ds = \rho_w gAds\vec{j}+\rho_w gA(h+\frac{1}{2}\frac{dh}{ds}ds)(\vec{t}+\frac{1}{2}\frac{d\vec{t}}{ds})$$

$$- \rho_w gA(h-\frac{1}{2}\frac{dh}{ds}ds)(\vec{t}-\frac{1}{2}\frac{d\vec{t}}{ds}ds)$$

$$= \rho_w gAds(\vec{j}+\frac{dh}{ds}\vec{t}+h\frac{d\vec{t}}{ds})$$

$$= \rho_w Ads(-\vec{t}x(\vec{g}x\vec{t})+gh\kappa\vec{n}),$$

since $g\frac{dh}{ds} = \vec{g}\cdot\vec{t}$ and $\vec{t}x(\vec{g}x\vec{t}) = \vec{g}-(\vec{g}\cdot\vec{t})\vec{t} = \vec{g}_n$, where $\vec{g}_n$ is the component of $\vec{g}$ normal to $\vec{t}$. This expression gives the buoyancy force as the sum of one component along $-\vec{g}_n$ and one component, involving the curvature κ, along $\vec{n}$. $\vec{g}_n$ is always in the vertical plane, while generally $\vec{n}$ can have any direction. The term involving $h\kappa\vec{n}$ expresses a contribution due to the absolute pressure $\rho_w gh=p$ and the curvature κ. In any case, $\vec{B}_g$ has no component along $\vec{t}$. In a two-dimensional cable in a vertical plane, $\vec{g}_n$ and $\vec{n}$ will have the same or opposite direction.

iv) Gravity force.

This can be expressed as

$$(2.2.4)\quad \vec{W}_g ds = \rho_c Ads\vec{g}\ .$$

v) Tension force.

At the upper end the tension force is:

$$\vec{R}_1 = (R+ \frac{1}{2} \frac{dR}{ds} ds)(\vec{t}+ \frac{1}{2} \frac{d\vec{t}}{ds} ds)$$

where R is the tension at the segment midpoint, $\vec{t}$ is the tangent at the segment midpoint. At the lower end we have:

$$\vec{R}_2 = -(R- \frac{1}{2} \frac{dR}{ds} ds)(\vec{t}- \frac{1}{2} \frac{d\vec{t}}{ds} ds) \ .$$

Hence, the net tension force on the segment is, neglecting terms small of second order ds^2:

$$(2.2.5) \qquad \vec{F}_R ds = \vec{R}_1+\vec{R}_2 = (\frac{dR}{ds} \vec{t}+R \frac{d\vec{t}}{ds})ds = (\frac{dR}{ds} \vec{t}+R\kappa \vec{n})ds.$$

2.2.2 Dynamic forces.

The following symbols are introduced:

$\vec{V} = \vec{v}_w-\vec{v}_c$: relative water velocity to the cable

$\vec{a} = \vec{a}_w-\vec{a}_c$: relative water acceleration to the cable

C_M: hydrodynamic mass coefficient of the cable

E: Modulus of elasticity

C_V: Internal viscous coefficient of the cable.

$\vec{V}$ and $\vec{a}$ have tangential components $\vec{V}_t=(\vec{V}\cdot\vec{t})\vec{t}$ and $\vec{a}_t=(\vec{a}\cdot\vec{t})\vec{t}$. The normal components are $\vec{V}_n=\vec{V}-\vec{V}_t$ and $\vec{a}_n=\vec{a}-\vec{a}_t$.

When the cable is moving, the tangential drag and normal drag forces can be expressed by (2.2.1) and (2.2.2), when $\vec{v}_{wt}$ and $\vec{v}_{wn}$ are replaced by the relative velocities $\vec{V}_t$ and $\vec{V}_n$. The buoyancy, gravity and net tension resultant remain unchanged. Tension here means elastic tension.

In dynamics we must also consider the following forces:

i) Inertia reaction of the cable, $\vec{I}_c$, due to the acceleration $\vec{a}_c$.

ii) Inertia reaction of the water, $\vec{I}_w$, due to the relative acceleration, $-\vec{a}$, of the cable, relative to the water.

iii) When there is acceleration of the water, an additional pressure gradient will exist. This produces an unsymmetric pressure distribution over the cable sides. This can be represented by a fictitious (by d'Alembert's principle) force field $-\rho_w\vec{a}_w$, similar to the gravity force $\rho_w\vec{g}$. A corresponding fictitious buoyancy force $\vec{B}_w$ is induced by this pressure field. The details of this fictitious buoyancy is discussed in Batchelor [4], ch. 6.

iv) If the cable is assumed to have a longitudinal force, dependent on the rate of change of strain, this force $\vec{V}$ can be represented in an appropriate viscoelastic model.

The various forces are again taken as they act on the cable, the inertia forces being defined by d'Alembert's

principle. The dynamic forces are shown in Fig. 2.2.3.

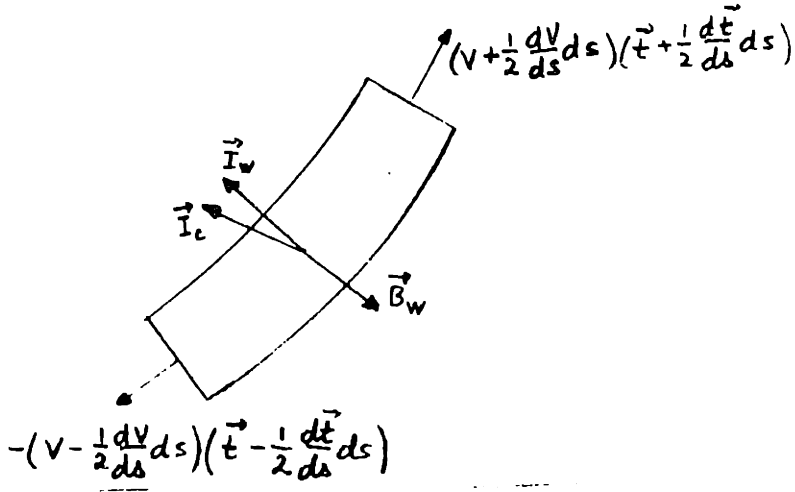

Fig. 2.2.3

Dynamic Forces on Cable Segment

i) According to d'Alembert's principle, the inertia reaction of the cable segment is:

$$(2.2.6) \qquad \vec{I}_c ds = -\rho_c A ds \vec{a}_c \ .$$

ii) We take the inertia reaction, $\vec{I}_w$, of the water as proportional to the normal component of the cable acceleration relative to the water, i.e. $-\vec{a}_n$, and as opposing this relative acceleration:

$$(2.2.7) \qquad \vec{I}_w ds = -c_M \rho_w A ds(-\vec{a}_n) = c_M \rho_w A ds(\vec{a}_{wn} - \vec{a}_{cn}),$$

with the normal components $\vec{a}_{wn} = \vec{a}_w - (\vec{a}_w \cdot \vec{t})\vec{t}$, $\vec{a}_{wc} = \vec{a}_c - (\vec{a}_c \cdot \vec{t})\vec{t}$.

iii) According to Batchelor [4], (2.2.7) describes the inertia reaction as seen from a coordinate system accelerating with the water acceleration $\vec{a}_w$. The effect of the fictitious force field $-\rho_w\vec{a}_w$ can be expressed, similarly to the buoyancy force $\vec{B}_g$ in (2.2.3), by the fictitious buoyancy $\vec{B}_w$. We substitute $-\vec{a}_w$ for $\vec{g}$ in (2.2.3):

$$(2.2.8)\qquad \vec{B}_w ds = \rho_w A ds(\vec{t}x(\vec{a}_w x\vec{t})) =$$

$$= \rho_w A ds(\vec{a}_w-(\vec{a}_w\cdot\vec{t})\vec{t}) = \rho_w A ds\vec{a}_{wn}.$$

The effect of curvature can also be included by substituting the absolute pressure p for $\rho_w gh$ in (2.2.3).

Adding (2.2.6), (2.2.7) and (2.2.8), we get the total inertia force

$$\vec{I}ds = (\vec{I}_c+\vec{I}_w+\vec{B}_w)ds = -Ads[(\rho_c+c_M\rho_w)\vec{a}_{cn}+\rho_c\vec{a}_{ct}-(1+c_M)\rho_w\vec{a}_{wn}],$$

where $\vec{a}_{ct}=(\vec{a}_c\cdot\vec{t})\vec{t}$ is the tangential component of the cable acceleration, $\vec{a}_{cn}=\vec{a}_c-\vec{a}_{ct}$ is the normal component.

Contributions can also be written for inertia reactions of the water to longitudinal acceleration of the cable. However, these forces are considered practically negligible, compared to the e.g. the tension force.

iv) The simplest model to represent a strain rate of change dependent force is the Kelvin (or Voight) viscoelastic

model, as shown in Fig. 2.2.4. This is represented as a

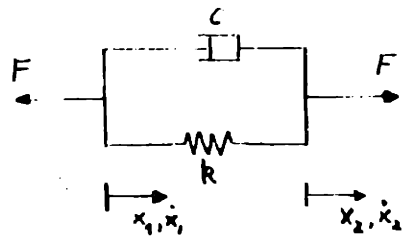

Fig. 2.2.4

Kelvin Viscoelastic Model

parallel coupling of a linear spring k and a viscous dashpot c. When x_1, x_2 are the end point displacements, $\dot{x}_1, \dot{x}_2$ the velocities, the force F is

$$F = k(x_2-x_1)+c(\dot{x}_2-\dot{x}_1)$$

For an infinitesimal segment ds_o, we make the correspondences

$$x_2-x_1 \to \varepsilon ds_o, \quad \dot{x}_2-\dot{x}_1 = \dot{\varepsilon} ds_o .$$

For a linear elastic material we have $k(x_2-x_1) \to EA\varepsilon$. Further the linear viscous force can be represented by $c(\dot{x}_2-\dot{x}_1) \to C_V A\dot{\varepsilon}$. Hence we can write the force over the viscoelastic cable segment:

$$F \to EA\varepsilon + C_V A\dot{\varepsilon}$$

Hence the net visco-elastic force on the segment ds is

$$(2.2.9) \qquad \vec{V}ds = \frac{\partial}{\partial s}(C_V A\dot{\varepsilon}\vec{t})ds = C_V A(\frac{\partial \dot{\varepsilon}}{\partial s}\vec{t} + \dot{\varepsilon}\frac{\partial \vec{t}}{\partial s})ds.$$

The elastic force is (cf. (2.2.5)):

$$(2.2.10)\quad \vec{F}_R ds = \frac{\partial}{\partial s}(EA\varepsilon\vec{t})ds = EA(\frac{\partial\varepsilon}{\partial s}\vec{t} + \varepsilon\frac{\partial\vec{t}}{\partial s})ds.$$

(2.2.9) and (2.2.10) are constitutive relations for the cable, relating internal forces to displacements. Above we have used the name tension only for the elastic part of the axial force.

2.2.3 Equilibrium relations.

We are now in position to express the conditions for equilibrium for the segment. We consider dynamic equilibrium first and specialize to static equilibrium afterwards.

Setting the sum of all forces (2.2.1-9), we get the condition of dynamic equilibrium:

$$(2.2.11a)\quad \vec{F}_t+\vec{F}_n+\vec{B}_g+\vec{W}_g+\vec{F}_R+\vec{I}_C+\vec{I}_W+\vec{B}_W+\vec{V} = 0$$

If we transpose all the inertia terms $\vec{i}=\vec{I}_C+\vec{I}_W+\vec{B}_W$, we have the form:

$$(2.2.11b)\quad A[(\rho_C+C_M\rho_W)\vec{a}_{cn}+\rho_c\vec{a}_{ct}-(1+C_M)\rho_W\vec{a}_{Wn}]$$
$$= \vec{F}_t+\vec{F}_n+\vec{B}_g+\vec{W}_g+\vec{F}_R+\vec{V}\ .$$

In the static case $\vec{a}_c=\vec{a}_w=\vec{v}_c=0$, $\dot{\varepsilon}=0$. We then have the static relation:

$$(2.2.12) \qquad \vec{F}_t+\vec{F}_n+\vec{B}_g+\vec{W}_g+\vec{F}_R = 0$$

This can also be written in terms of components along the $\vec{t},\vec{n},\vec{b}$ directions. We write $\vec{F}_t=F_t\vec{t}$.

Tangential direction:

$$(2.2.13a) \qquad F_t+\rho_c A\vec{g}\cdot\vec{t} + \frac{dR}{ds} = 0$$

Normal direction:

$$(2.2.13b) \qquad \vec{F}_n\cdot\vec{n}+ghA\kappa\rho_w+(\rho_c-\rho_w)A\vec{g}\cdot\vec{n} + R\kappa = 0,$$

Binormal direction:

$$(2.2.13c) \qquad \vec{F}_n\cdot\vec{b} + (\rho_c-\rho_w)A\vec{g}\cdot\vec{b} = 0.$$

2.3 Forces on a Finite Element.

In this section the force expressions and equilibrium relations are adapted to a form suitable for the finite element method. The analyses here will be concerned with one single element, deferring the treatment of a total system to Ch. 5.

In the present treatment a finite element will be assumed as a straight segment of finite length L, extending between

terminal nodes i and j. Each node has three displacement degrees of freedom, hence a total of six degrees of freedom for each element. More general formulations can be obtained by using elements with additional internal nodes and/or with more degrees of freedom at each node. Although one can obtain results of the same accuracy with fewer elements by using more complicated element structures, it is not obvious that a saving can be obtained in computational effort, since the amount of computation is related to the total number of degrees of freedom, rather than the number of elements.

After defining the nodes, one needs to define the internal structure of the element. This is done by interpolation functions, which express the position of any point in the element in terms of the nodal positions. In the present formulation the interpolation to interior points will be linear functions between the nodal positions. In addition to position variables, and hence also velocity and acceleration, other variables may be specified as nodal values and interpolated linearly to internal points, e.g. water current and force densities.

Remark about notations.

In expressing relations for a finite element, both matrix algebra and vector algebra are used. Two different notations,

which are used to represent various variables, should be pointed out.

Vectors, like position $\vec{r}$ and force $\vec{f}$, represent three-dimensional variables in space. In a cartesian frame, these vectors can be expressed in terms of their orthogonal components along the x,y,z directions, e.g. r_x, r_y, r_z and the basic unit vectors $\vec{i}, \vec{j}, \vec{k}$, thus

$$\vec{r} = r_x\vec{i} + r_y\vec{j} + r_z\vec{k} \ .$$

However, the components r_x, r_y, r_z can also be compiled into a column matrix (3x1):

$$\underline{r} = \begin{pmatrix} r_x \\ r_y \\ r_z \end{pmatrix} = (r_x \ r_y \ r_z)^T \ .$$

$\underline{r}$ is denoted a matrix vector or sometimes only a vector. Since $\vec{r}$ and $\underline{r}$ belong to different branches of mathematics, it may be misleading to use the name vector for both. We shall here use the name vector (or possibly space vector) for $\vec{r}$ and matrix vector or column vector for $\underline{r}$.

A general matrix is denoted by $\underline{\underline{A}}$. $\underline{\underline{A}}^n_m$ may be used to stress that $\underline{\underline{A}}$ has n lines and m columns.

Equivalent nodal forces.

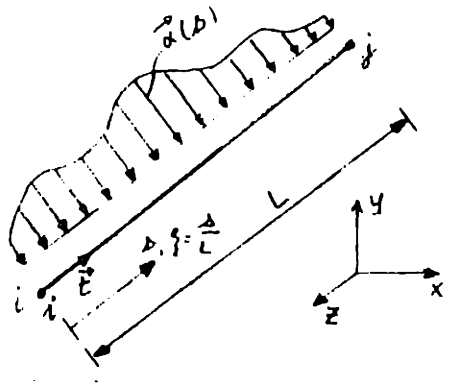

Fig. 2.3.1

Distributed Force on Finite Element

Consider the straight element shown in Fig. 2.3.1, extending from node i to node j. The element has length L. If s is the length from node i to a point of the element, we define the dimensionless coordinate $\xi=s/L$. $\vec{t}$ is a unit vector along the element from node i to j.

$\vec{\alpha}(s)$ is some force distribution along the element. We reduce this force distribution to nodal forces $\vec{f}_{\alpha i}$ and $\vec{f}_{\alpha j}$, which are "equivalent" to $\vec{\alpha}$. Two methods can be used for this:

i) By the principle of virtual work, we consider virtual displacements $\vec{\delta}_i$ and $\vec{\delta}_j$ of the nodes. The virtual work δW_1 by the forces $\vec{f}_{\alpha i}$ and $\vec{f}_{\alpha j}$ is then equal to the work δW_2 of $\vec{\alpha}$.

ii) Using a simple static reasoning, we determine $\vec{f}_{\alpha i}$, $\vec{f}_{\alpha j}$ such that their resultant and moment are the same as

those of $\vec{\alpha}$.

We consider both methods.

i) Under the virtual displacements $\vec{\delta}_i$ and $\vec{\delta}_j$, the virtual work of $\vec{f}_{\alpha i}$ and $\vec{f}_{\alpha j}$ is

$$\delta W_1 = \vec{f}_{\alpha i} \cdot \vec{\delta}_i + \vec{f}_{\alpha j} \cdot \vec{\delta}_j$$

At the point ξ of the element, the corresponding virtual displacement is $\vec{\delta}(\xi) = \vec{\delta}_i(1-\xi)+\vec{\delta}_2\xi$. Hence the virtual work of $\vec{\alpha}$ is

$$\delta W_2 = \int_0^1 \vec{\alpha} \cdot \vec{\delta} L d\xi = (\int_0^1 \vec{\alpha}(1-\xi) L d\xi) \cdot \vec{\delta}_i + (\int_0^1 \vec{\alpha}\xi L d\xi) \cdot \vec{\delta}_j$$

To have $\delta W_1 = \delta W_2$ for arbitrary $\vec{\delta}_i, \vec{\delta}_j$, we must have

$$\vec{f}_{\alpha i} = L \int_0^1 \vec{\alpha} \cdot (1-\xi) d\xi$$

(2.3.1)

$$\vec{f}_{\alpha j} = L \int_0^1 \vec{\alpha}\xi d\xi$$

ii) Statical equivalence of the resultant requires:

$$\vec{f}_{\alpha i} + \vec{f}_{\alpha j} = \int_0^1 \vec{\alpha} L d\xi$$

Equivalence of moments about node j:

$$(L\vec{t})\,x\,\vec{f}_{\alpha i} = \int_0^1 L(1-\xi)\,\vec{t}x\vec{\alpha}L\,d\xi = (L\vec{t})\;x\;\int_0^1 (1-\xi)\,\vec{\alpha}L\,d\xi$$

Provided the integral is different from 0 and $\vec{t}x\vec{\alpha}\neq 0$, we must have

$$\vec{f}_{\alpha i} = L\int_0^1 \vec{\alpha}\cdot(1-\xi)\,d\xi$$

The other expression in (2.3.1) can be derived similarly by taking moments about node i.

This static reasoning cannot be applied to forces $\vec{\alpha}$ parallel to the element direction.

To derive expressions for the equivalent nodal forces, we use the expressions derived in Sec. 2.2. We assume that the element properties are homogeneous over its length. We follow the classification of Sec. 2.2, distinguishing between static and dynamic forces.

We assume that the water current velocity and acceleration are given by their nodal values $\vec{v}_{wi}, \vec{v}_{wj}, \vec{a}_{wi}, \vec{a}_{wj}$ and interpolated linearly to interior points.

2.3.1 Static Forces.

i) Tangential friction force.

The tangential velocity component of the relative water velocity at ξ is:

$$\vec{V}_t(\xi) = (\vec{V}_i \cdot \vec{t})(1-\xi)\vec{t} + (\vec{V}_j \cdot \vec{t})\xi\vec{t} = (V_{ti}(1-\xi) + V_{tj}\xi)\vec{t}$$

Force on segment $ds = Ld\xi$:

$$\vec{\phi}_F(\xi)Ld\xi = \pm\frac{1}{2}\rho_W c_T \pi dL|\vec{V}_t|^2\vec{t}d\xi,$$

with + if $\vec{V}_t \cdot \vec{t} > 0$, - if $\vec{V}_t \cdot \vec{t} < 0$. Substitute for $\vec{V}_t$

$$\vec{\phi}_F = \pm\frac{1}{2}\rho_W c_T \pi dL(\vec{V}_{ti}^2(1-\xi)^2 + 2\vec{V}_{ti}\cdot\vec{V}_{tj}(1-\xi)\xi + \vec{V}_{tj}^2\xi^2)\vec{t}.$$

To compute the equivalent nodal forces, we must consider two cases, dependent on whether $\vec{\phi}_F$ change direction over the element or not.

Case I: direction of $\vec{\phi}_F$ is the same along the element. Direct integration according to (2.3.1) gives:

$$\vec{f}_{Fi} = L\int_0^1 \vec{\phi}_F(1-\xi)d\xi =$$

$$(2.3.2) \qquad \pm\frac{1}{2}\rho_W c_T \pi dL(\frac{1}{4}V_{ti}^2 + \frac{1}{6}V_{ti}V_{tj} + \frac{1}{12}V_{tj}^2)\vec{t}$$

$$\vec{f}_{Fj} = L\int \vec{\phi}_F \xi d\xi =$$

$$\pm\frac{1}{2}\rho_W c_T \pi dL\left(\frac{1}{12}V_{ti}^2 + \frac{1}{6}V_{ti}V_{tj} + \frac{1}{4}V_{tj}^2\right)\vec{t} \ ,$$

with + if $V_{ti}, V_{tj} > 0$, - if $V_{ti}, V_{tj} < 0$.

Case II: direction of $\vec{\phi}_F$ changes over the element.

This case occurs if the signs of V_{ti} and V_{tj} are different. $\vec{V}_t$ is zero at

$$\xi_o = \frac{|V_{ti}|}{|V_{ti}| + |V_{tj}|} \ .$$

We can now write the nodal forces in the form

$$\vec{f}_{Fi} = L\left[\int_0^{\xi_o} \vec{\phi}_F (1-\xi) d\xi + \int_{\xi_o}^{1} \vec{\phi}_F (1-\xi) d\xi\right],$$

where the sign of $\vec{\phi}_F$ is different in each integral. Carrying out the integrations, we get:

$$\vec{f}_{Fi} = \pm\frac{1}{2}\rho_W c_T \pi dL\left[\frac{1}{4}V_{ti}^2\left(1-2(1-\xi_o)^4\right)\right.$$

$$\left. + 2V_{ti}V_{tj}\left(\xi_o^2 - \frac{4}{3}\xi_o^3 + \frac{1}{2}\xi_o^4 - \frac{1}{12}\right) + V_{tj}^2\left(\frac{2}{3}\xi_o^3 - \frac{1}{2}\xi_o^4 - \frac{1}{12}\right)\right]\vec{t}$$

(2.3.3)

$$\vec{f}_{Fj} = \pm\frac{1}{2}\rho_W c_T \pi dL\left[V_{ti}^2\left(\xi_o^2 - \frac{4}{3}\xi_o^3 + \frac{1}{2}\xi_o^4 - \frac{1}{12}\right)\right.$$

$$\left. + 2V_{ti}V_{tj}\left(\frac{2}{3}\xi_o^3 - \frac{1}{12}\xi_o^4 - \frac{1}{12}\right) + \frac{1}{4}V_{tj}^2\left(2\xi_o^4 - 1\right)\right]\vec{t}.$$

Here we take the upper signs if $V_{ti}>0$, $V_{tj}<0$, lower signs if $V_{ti}<0$, $V_{tj}>0$.

ii) Normal drag force.

a. General case.

Normal relative water velocity component:

$$\vec{V}_n(\xi) = \vec{V}(\xi) - \vec{V}_t(\xi)$$

$$= (\vec{V}_i-\vec{V}_{ti})(1-\xi) + (\vec{V}_j-\vec{V}_{tj})\xi = \vec{V}_{ni}(1-\xi)+\vec{V}_{nj}\xi.$$

Force on segment $ds=Ld\xi$:

$$\vec{\phi}_N L d\xi = \frac{1}{2}\rho_W c_N dL |\vec{V}_n| \vec{V}_n d\xi$$

Since the direction of $\vec{V}_n$ may change along the element, we decompose into two directions defined as follows: construct a vertical plane through the element. Let normal direction $\vec{n}_1$ lie in this plane and normal to $\vec{t}$, while the normal direction $\vec{n}_2$ is defined by $\vec{n}_2=\vec{t}\times\vec{n}_1$. $\vec{n}_1$ and $\vec{n}_2$ are unit vectors, which can be expressed in terms of the cartesian unit vectors $\vec{i},\vec{j},\vec{k}$.

We now decompose $\vec{V}_n$, $\vec{V}_{ni}$, and $\vec{V}_{nj}$ along the directions $\vec{n}_1,\vec{n}_2$:

$$\vec{V}_n = V_{n1}\vec{n}_1 + V_{n2}\vec{n}_2$$

$$\vec{V}_{ni} = V_{ni1}\vec{n}_1 + V_{ni2}\vec{n}_2$$

$$\vec{V}_{nj} = V_{nj1}\vec{n}_1 + V_{nj2}\vec{n}_2 \ ,$$

where $V_{n1} = V_{ni1}(1-\xi)+V_{nj1}\xi$, $V_{n2} = V_{ni2}(1-\xi)+V_{nj2}\xi$

Also $\quad |\vec{V}_n| = (V_{n1}^2+V_{n2}^2)^{1/2}$

Decompose $\vec{\phi}_N$ into components $\vec{\phi}_N = \phi_{N1}\vec{n}_1+\phi_{N2}\vec{n}_2$.

Hence

$$\phi_{N1}Ld\xi\vec{n}_1 = \tfrac{1}{2}\rho_W c_N dL|\vec{V}_n|V_{n1}d\xi\vec{n}_1 = \vec{\phi}_{N1}Ld\xi$$

$$\phi_{N2}Ld\xi\vec{n}_2 = \tfrac{1}{2}\rho_W c_N dL|\vec{V}_n|V_{n2}d\xi\vec{n}_2 = \vec{\phi}_{N2}Ld\xi$$

We hence find the expressions for the nodal forces:

$$\vec{f}_{Ni} = L\int_0^1 \vec{\phi}_N(1-\xi)d\xi = L[(\int_0^1 \phi_{N1}(1-\xi)d\xi)\vec{n}_1+(\int_0^1 \phi_{N2}(1-\xi)d\xi)\vec{n}_2]$$

$$\vec{f}_{Nj} = L\int_0^1 \vec{\phi}_N\xi d\xi = L[(\int_0^1 \phi_{N1}\xi d\xi)\vec{n}_1+(\int_0^1 \phi_{N2}\xi d\xi)\vec{n}_2]$$

In the general three-dimensional case, where $V_{ni1}, V_{ni2}, V_{nj1}, V_{nj2}$ may have arbitrary values, the expressions for $\vec{\phi}_{N1}$ and $\vec{\phi}_{N2}$ become complicated and not explicitly integrable. One method to avoid this is to use numerical integration, the other is to simplify by assuming that $\vec{\phi}_N$ has a linear distribution

along the element. The latter approach is not completely consistent with our approach of assuming a linear distribution of velocity along the element, but may still be sufficiently accurate for practical purposes. In a two-dimensional formulation the expressions are simplified and can be explicitly integrated.

We assume a linear distribution of $\vec{\phi}_N$ along the element. At the nodes k=i,j we have

$$\vec{\phi}_{Nk} = \frac{1}{2}\rho_W c_N d|\vec{v}_{nk}|^2 \vec{e}_k,$$

where $\vec{e}_k$ is a unit vector in the direction of $\vec{v}_{nk}$. Then at ξ:

$$\vec{\phi}_N(\xi) = \vec{\phi}_{Ni}(1-\xi)+\vec{\phi}_{Nj}\cdot\xi.$$

The equivalent nodal forces become:

$$\vec{f}_{Ni} = L\int_0^1 [(1-\xi)^2\vec{\phi}_{Ni}+(1-\xi)\xi\vec{\phi}_{Nj}]d\xi$$

$$= \frac{L}{6}(2\vec{\phi}_{Ni}+\vec{\phi}_{Nj})$$

(2.3.4)

$$\vec{f}_{Nj} = L\int_0^1 [\xi(1-\xi)\vec{\phi}_{N1}+\xi^2\vec{\phi}_{Nj}]d\xi$$

$$= \frac{L}{6}(\vec{\phi}_{Ni}+2\vec{\phi}_{Nj})$$

For a two-dimensional cable in a vertical plane, there are no forces in the direction of $\vec{n}_2$, so $\vec{\phi}_N=\vec{\phi}_{N1}$. Then we

can integrate the force distribution for $\vec{\phi}_N$ based on the linear velocity distribution. We use $V_{ni}=\vec{V}_{ni}\cdot\vec{n}_1$, $V_{nj}=\vec{V}_{nj}\cdot\vec{n}_1$

$$\vec{\phi}_N = \pm\frac{1}{2}\rho_W C_N d|\vec{V}_n|^2\vec{n}_1 = \pm\frac{1}{2}\rho_W C_N d(V_{ni}(1-\xi)+V_{nj}\xi)^2\vec{n}_1,$$

with + sign if $\vec{V}_n\cdot\vec{n}_1>0$, - sign if $\vec{V}_n\cdot\vec{n}_1<0$. We must consider two separate cases, dependent on whether $\vec{\phi}_N$ changes direction over the element or not.

Case I: the direction of $\vec{\phi}_N$ is the same along the element.

$$\vec{f}_{Ni} = L\int_0^1 \vec{\phi}_N(1-\xi)d\xi$$

$$= \pm\frac{1}{2}\rho C_N dL(\frac{1}{4}V_{ni}^2 + \frac{1}{6}V_{ni}V_{nj} + \frac{1}{12}V_{nj}^2)\vec{n}_1$$

(2.3.5)
$$\vec{f}_{Nj} = L\int_0^1 \vec{\phi}_N\xi d\xi$$

$$= \pm\frac{1}{2}\rho C_N dL(\frac{1}{12}V_{ni}^2 + \frac{1}{6}V_{ni}V_{nj} + \frac{1}{4}V_{nj}^2)\vec{n}_1,$$

with + if $\vec{V}_{ni}\cdot\vec{n}_1 = V_{ni}>0$, - if $\vec{V}_{ni}\cdot\vec{n}_1<0$.

Case II; the direction of $\vec{\phi}_N$ changes along the element. We have $\vec{V}_n = \vec{V}_{ni}(1-\xi)+\vec{V}_{nj}\xi = 0$ when

$$\xi = \xi_o = \frac{|V_{ni}|}{|V_{ni}|+|V_{nj}|} .$$

$$\vec{f}_{Ni} = \frac{1}{2}\rho_W C_N dL \left\{\int_0^{\xi_o} \vec{\phi}_N(1-\xi)d\xi + \int_{\xi_o}^{1} \vec{\phi}_N(1-\xi)d\xi\right\}$$

$$\vec{f}_{Nj} = \frac{1}{2}\rho_W C_N dL \left\{\int_0^{\xi_o} \vec{\phi}_N \xi d\xi + \int_{\xi_o}^{1} \vec{\phi}_N \xi d\xi\right\},$$

where different signs are valid for $\vec{\phi}_N$ in $[0,\xi_o>$ and $<\xi_o,1]$. Carrying out the integrations, we get:

$$(2.3.6a)\quad \vec{f}_{Ni} = \pm\frac{1}{2}\rho_W C_N dL \left\{\frac{1}{4}V_{ni}^2(1-2(1-\xi_o)^4)\right.$$

$$\left. + 2V_{ni}V_{nj}(\xi_o^2-\frac{4}{3}\xi_o^3+\frac{1}{2}\xi_o^4-\frac{1}{12}) + V_{nj}^2(\frac{2}{3}\xi_o^3-\frac{1}{2}\xi_o^4-\frac{1}{12})\right\}\vec{n}_1,$$

with + sign if $\vec{V}_{ni}\cdot\vec{n}_1>0$, $\vec{V}_{nj}\cdot\vec{n}_1<0$, - sign if $\vec{V}_{ni}\cdot\vec{n}_1<0$, $\vec{V}_{nj}\cdot\vec{n}_1>0$.

Correspondingly at node j

$$(2.3.6b)\quad \vec{f}_{Nj} = \mp\frac{1}{2}\rho_W C_N dL\left\{V_{ni}^2(\xi_o^2-\frac{4}{3}\xi_o^3+\frac{1}{2}\xi_o^4-\frac{1}{12})\right.$$

$$\left. + 2V_{ni}V_{nj}(\frac{2}{3}\xi_o^3-\frac{1}{2}\xi_o^4-\frac{1}{12}) + \frac{1}{4}V_{nj}^2(2\xi_o^4-1)\right\}\vec{n}_1,$$

with - sign if $\vec{V}_{ni}\cdot\vec{n}_1>0$, $\vec{V}_{nj}\cdot\vec{n}_1<0$, + sign if $\vec{V}_{ni}\cdot\vec{n}_1<0$, $\vec{V}_{nj}\cdot\vec{n}_1>0$.

b. Linear drag force for small cable velocities in current.

It will be useful to have an expression for the linear

deviation of the drag force, due to small velocities of the cable. $\vec{v}_w$ is the non-vanishing water velocity and $\vec{v}_c$ is the cable velocity. The relative water velocity $\vec{V}=\vec{v}_w-\vec{v}_c$ has normal component $\vec{V}_n=\vec{v}_{wn}-\vec{v}_{cn}$. We assume $|\vec{v}_{cn}|<<|\vec{v}_{wn}|$. For simplicity we also assume that $\vec{v}_{cn}$ and $\vec{v}_{wn}$ lie in one plane through the element, i.e. we consider a plane configuration.

The normal drag force on a small segment $ds=Ld\xi$ is:

$$\vec{\phi}_N(\xi)Ld\xi = \frac{1}{2}\rho_W C_N dL|\vec{v}_{wn}-\vec{v}_{cn}|^2 d\xi\vec{e},$$

where $\vec{e}$ is a unit vector in the direction of $\vec{V}_n$. In equilibrium $\vec{v}_c=0$, so the corresponding force is:

$$\vec{\phi}_N^{\,o}(\xi)Ld\xi = \frac{1}{2}\rho_W C_N dL|\vec{V}_{wn}|^2 d\xi\vec{e}.$$

We look for the deviation of the drag force due to $\vec{v}_{cn}$, $\vec{\phi}_N-\vec{\phi}_N^{\,o}$. This may be expressed as

$$(\phi_N-\phi_N^o)Ld\xi = \rho_W C_N dL(-\vec{v}_{wn}\cdot\vec{v}_{cn}+\frac{1}{2}|\vec{v}_{cn}|^2)\vec{e}$$

Neglecting the term $|\vec{v}_{cn}|^2$, we have the linear deviation force

$$\vec{\eta}(\xi)Ld\xi = -\rho_W C_N dL(\vec{v}_{wn}\cdot\vec{v}_{cn})\vec{e}$$

This equation shows that $\vec{\eta}$ is always in the opposite direction of $\vec{v}_{cn}$. By linear interpolation we have

$$\vec{v}_{wn} = \vec{v}_{wni}(1-\xi)+\vec{v}_{wnj}\xi \ ,$$

$$\vec{v}_{cn} = \vec{v}_{cni}(1-\xi)+\vec{v}_{cnj}\xi \ .$$

Hence

$$\vec{\eta}(\xi)=-\rho_W C_N dL[\vec{v}_{wni}\cdot\vec{v}_{cni}(1-\xi)^2+(\vec{v}_{wni}\cdot\vec{v}_{cnj}+\vec{v}_{wnj}\cdot\vec{v}_{cni})(1-\xi)\xi$$

$$+ \vec{v}_{wnj}\cdot\vec{v}_{cnj}\xi^2]\vec{e} \ .$$

The nodal forces are then, assuming unchanged direction of $\vec{e}$:

$$\vec{f}_{Li} = L\int_0^1 \vec{\eta}(1-\xi)d\xi =$$

$$= -\rho_W C_N dL[\tfrac{1}{4}\vec{v}_{wni}\cdot\vec{v}_{cni}+\tfrac{1}{12}(\vec{v}_{wni}\cdot\vec{v}_{cnj}+\vec{v}_{wnj}\cdot\vec{v}_{cni})+\tfrac{1}{12}\vec{v}_{wnj}\cdot\vec{v}_{cnj}]\vec{e}$$

$$\vec{f}_{Lj} = L\int_0^1 \vec{\eta}\xi d\xi$$

$$= -\rho_W C_N dL[\tfrac{1}{12}\vec{v}_{wni}\cdot\vec{v}_{cni}+\tfrac{1}{12}(\vec{v}_{wni}\cdot\vec{v}_{cnj}+\vec{v}_{wnj}\cdot\vec{v}_{cni})+\tfrac{1}{4}\vec{v}_{wnj}\cdot\vec{v}_{cnj}]\vec{e}.$$

iii) Buoyancy force.

Since the element is assumed straight, we get directly from (2.2.3), with $\kappa = 0$, the buoyancy force on the small segment $Ld\xi$,

$$\vec{\phi}_B L d\xi = -\rho_W A \vec{t} x (\vec{g} x \vec{t}) L d\xi,$$

and the nodal forces:

$$(2.3.8) \qquad \vec{f}_{Bi} = \vec{f}_{Bj} = -\frac{1}{2} \rho_W A L \vec{t} x (\vec{g} x \vec{t})$$

iv) Gravity force

We have for the segment $Ld\xi$ from (2.2.4)

$$\vec{\phi}_w L d\xi = \rho_c A \vec{g} L d\xi,$$

and the nodal forces

$$(2.3.9) \qquad \vec{f}_{wi} = \vec{f}_{wj} = \frac{1}{2} \rho_c A L \vec{g}$$

v) Tension force

Different assumptions can be made about the tension force. It may be assumed to be constant, R, in each element. In this case there will be a tension discontinuity at nodes between adjoining elements in a total model. Alternatively, the tension may be assumed to have nodal values R_i and R_j.

Since we are considering forces as they act on the nodes, we have the nodal forces

$$(2.3.10) \qquad \vec{f}_{Ri} = R_i \vec{t}, \quad \vec{f}_{Rj} = -R_j \vec{t},$$

where $R_i=R_j=R$ if the tension is taken as constant in the element.

2.3.2 Dynamic Forces.

We use the notations:

$\vec{v}_{wi},\vec{v}_{wj}$: water velocities at nodes i,j. The tangential components are $\vec{v}_{wit},\vec{v}_{wjt}$, normal components $\vec{v}_{win},\vec{v}_{wjn}$.

$\vec{v}_{ci},\vec{v}_{cj}$: cable nodal velocities, with tangential components $\vec{v}_{cit},\vec{v}_{cjt}$, normal components $\vec{v}_{cin},\vec{v}_{cjn}$.

$\vec{V}_i=\vec{v}_{wi}-\vec{v}_{ci}$, $\vec{V}_j=\vec{v}_{wj}-\vec{v}_{cj}$: relative water velocities at the nodes, with tangential components $\vec{V}_{it},\vec{V}_{jt}$, normal components $\vec{V}_{in},\vec{V}_{jn}$.

$\vec{a}_{wi},\vec{a}_{wj}$: water accelerations at the nodes, with tangential components $\vec{a}_{wit},\vec{a}_{wjt}$, normal components $\vec{a}_{win},\vec{a}_{wjn}$.

$\vec{a}_{ci},\vec{a}_{cj}$: cable nodal accelerations, with tangential components $\vec{a}_{cit},\vec{a}_{cjt}$, normal components $\vec{a}_{cin},\vec{a}_{cjn}$.

$\vec{a}_i,\vec{a}_j$: relative water acceleration at the nodes, with tangential components $\vec{a}_{it},\vec{a}_{jt}$, normal components $\vec{a}_{in},\vec{a}_{jn}$.

i) Inertia reaction of the cable.

At point ξ the cable acceleration is

$$\vec{a}_c(\xi) = \vec{a}_{ci}(1-\xi)+\vec{a}_{cj}\xi$$

For segment $Ld\xi$ we have from (2.2.6) the inertia force:

$$\vec{\phi}_I Ld\xi = -\rho_c ALd\xi\vec{a}_c$$

Hence the nodal forces are:

$$\vec{f}_{Ii} = L\int_0^1 (1-\xi)\vec{\phi}_I d\xi = -\frac{1}{6}\rho_c AL(2\vec{a}_{ci}+\vec{a}_{cj}),$$

(2.3.11)

$$\vec{f}_{Ij} = -\frac{1}{6}\rho_c AL(\vec{a}_{ci}+2\vec{a}_{cj}).$$

ii) Hydrodynamic inertia reaction.

At ξ the normal component of the relative water acceleration is

$$\vec{a}_n(\xi) = \vec{a}_{in}(1-\xi)+\vec{a}_{jn}\xi$$

From (2.2.7) we have the hydrodynamic inertia reaction on the segment $Ld\xi$

$$\vec{\phi}_H Ld\xi = C_M\rho_W ALd\xi\vec{a}_n \ .$$

Hence, the nodal forces are:

$$\vec{f}_{Hi} = \frac{1}{6}C_M\rho_W AL(2\vec{a}_{in}+\vec{a}_{jn})$$

(2.3.12)

$$\vec{f}_{Hj} = \frac{1}{6}C_M\rho_W AL(\vec{a}_{in}+2\vec{a}_{jn})$$

iii) Fictitious buoyancy force.

The normal component of the water acceleration at ξ is

$$\vec{a}_{wn} = \vec{a}_{win}(1-\xi)+\vec{a}_{wjn}\xi$$

According to (2.2.8) we have the fictitious buoyancy force on segment $Ld\xi$.

$$\vec{\phi}_A Ld\xi = \rho_w ALd\xi\vec{a}_{wn}$$

Hence, the nodal forces become

$$\vec{f}_{Ai} = \frac{1}{6}\rho_w AL(2\vec{a}_{win}+\vec{a}_{wjn})$$

(2.3.13)

$$\vec{f}_{Aj} = \frac{1}{6}\rho_w AL(\vec{a}_{win}+2\vec{a}_{wjn}).$$

iv) Internal friction forces.

The nodal tangential cable velocities are $\vec{v}_{cit}=v_{cit}\vec{t}$, $\vec{v}_{cjt}=v_{cjt}\vec{t}$. Hence the rate of change of strain is:

$$\dot{\varepsilon} = \frac{v_{cjt}-v_{cit}}{L}.$$

According to Sec. 2.2.2 iv, we have the nodal forces

$$\vec{f}_{vi} = A\, c_v \dot{\vec{\varepsilon}}_t = \frac{Ac_v}{L} (\vec{v}_{cjt} - \vec{v}_{cit})$$

(2.3.14)

$$\vec{f}_{vj} = -A\, c_v \dot{\vec{\varepsilon}}_t = -\frac{Ac_v}{L} (\vec{v}_{cjt} - \vec{v}_{cit}),$$

where c_v is the internal viscous coefficient per unit area.

CHAPTER 3. Static Equilibrium Configuration.

Before starting on a dynamic calculation, it is necessary to know the statical initial configuration. In many cases this can be approximately determined analytically. This is in particular the case with a heavy cable with a two-dimensional configuration in a vertical plane. If there is no current, the equilibrium is given approximately by the catenary. With current, a good approximation can be obtained from Pode's tables [10]. Several methods to estimate equilibrium configurations are described by Berteaux [11].

3.1 General Method.

Here we shall indicate an approach which is applicable in the general three-dimensional case, connecting directly with the finite element model described in Chapter 2. The method is iterative, since, in addition to satisfying equilibrium conditions at internal nodes, we must also satisfy certain boundary conditions at the upper and lower ends.

The solution then consists of assuming certain conditions at the upper end. Such conditions may be tension and direction of the cable. Then one proceeds down the cable by calculating the tension and direction of each element from equilibrium conditions at the internal nodes, until the bottom is reached. Then the computed conditions at the bottom are compared with the imposed restrictions. Restrictions at the

bottom may be a maximum tension at the anchor, a maximum angle of attack or a maximum horizontal distance (excursion) between the anchor and the float. In some technical applications the design of the anchor requires a horizontal pull force, which is achieved by having a certain length of cable (or chain) lying on the bottom up to the anchor. In particular applications, other restrictions may also apply.

If the restrictions at the bottom are not satisfied, it is necessary to make a new iteration by choosing new trial conditions at the upper end. A systematic method must be used to modify these conditions in a direction which tend to better satisfy all boundary conditions. A systematic approach for dealing with the static configuration of a multileg system is the method of imaginary reactions, developed by Skop and O'Hara [24].

3.2 Equilibrium Conditions at the Nodes.

The main analytical problem in this connection is to determine the configuration down the cable from the assumed upper end conditions. This can be done by a sequence of nodal equilibrium considerations. Consider the two adjoining

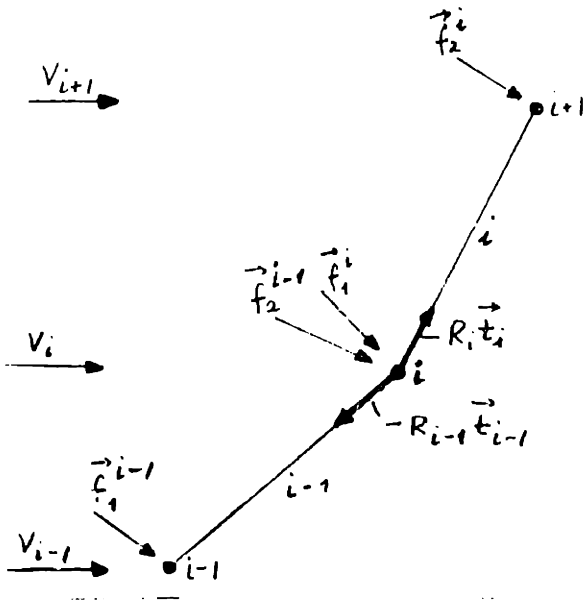

Fig. 3.2.1

Two Adjoining Finite Elements

elements i-1 and i in Fig. 3.2.1, with nodes i-1,i,i+1. The element tensions, assumed constant in each element, are R_{i-1} and R_i and the direction vectors are $\vec{t}_{i-1}$ and $\vec{t}_i$. The current velocities at the nodes are $\vec{v}_{i-1},\vec{v}_i,\vec{v}_{i+1}$. We can compute the total equivalent nodal forces for each element, according to Section 2.3, i.e. $\vec{f}_1^{\,i-1}$, $\vec{f}_2^{\,i-1}$, $\vec{f}_1^{\,i}$, $\vec{f}_2^{\,i}$. Hence we can write the equilibrium condition at node i

$$-R_{i-1}\vec{t}_{i-1} + R_i\vec{t}_i + \vec{f}_2^{\,i-1} + \vec{f}_1^{\,i} = 0,$$

which may be solved w.r.t. R_{i-1} or $\vec{t}_{i-1}$. In the former case we scalar multiply the equation by $\vec{t}_i$.

$$(3.2.1) \qquad R_{i-1} = \frac{R_i + (\vec{f}_2^{\,i-1} + \vec{f}_1^{\,i}) \cdot \vec{t}_i}{\vec{t}_{i-1} \cdot \vec{t}_i},$$

$$(3.2.2) \qquad \vec{t}_{i-1} = \frac{R_i \vec{t}_i + \vec{f}_2^{\,i-1} + \vec{f}_i^{\,i}}{R_{i-1}}$$

These equations are valid when all parameters are known. In progressing down the cable, the state of element i is known, and it is required to determine the state of element i-1. (3.2.1) and (3.2.2) can then be used as basis for iteratively determining the state of element i-1. We start by assuming $\vec{t}_{i-1}=\vec{t}_i$ and estimate R_{i-1} from (3.2.1). Next we use (3.2.2) to estimate $\vec{t}_{i-1}$. In this case the equation should be slightly modified

$$(3.2.2a) \qquad \vec{t}_{i-1} = \frac{R_i \vec{t}_i + \vec{f}_2^{\,i-1} + \vec{f}_1^{\,i}}{R_{i-1}\Phi},$$

where Φ is a factor to ensure that $\vec{t}_{n-1}$ is normalized, $|\vec{t}_{i-1}|=1$. For many practical purposes, this first approximation is sufficient, since the direction change between adjoining elements is small. Otherwise, the state of element i-1 can

be computed iteratively using (3.2.1) and (3.2.2a)

In this iteration process, properties of element i-1 must be known. In particular, the element length (e.g. in terms of the unstretched length L_o) and the elongation-tension properties $R(\varepsilon)$. Hence, when the tension has been estimated as R, the corresponding strain is ε and the length is $L=L_o(1+\varepsilon)$. If $\vec{r}_i$ is the known radius vector to node i, then the radius vector $\vec{r}_{i-1}$ to node i-1 is determined by

$$\vec{r}_{i-1} = \vec{r}_i - L\vec{t}_{i-1}.$$

CHAPTER 4. Forces Due to Deviations from Equilibrium.

In this chapter we make further developments of the tension and inertia forces, by expressing them in terms of the amount of deviation from equilibrium. In this manner the total forces can be expressed as an equilibrium value plus a contribution due to deviation from equilibrium. The deviation contributions can again be decomposed into a linear deviation term and a term expressing the effect of deviation from linearity. The linear deviations are expressed in terms of stiffness and mass matrices.

4.1 Tension Force Variations.

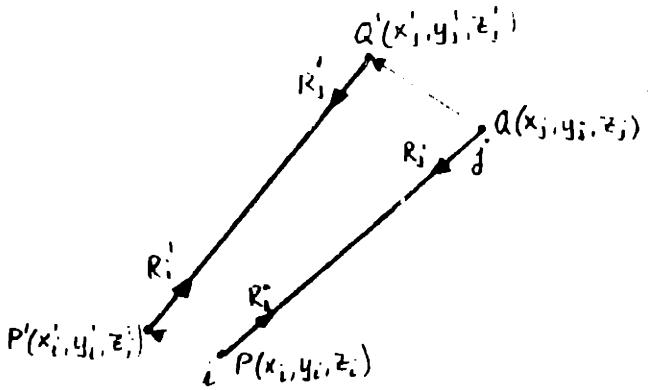

Fig. 4.1.1

Displaced State of Finite Element

Consider the element ij shown in Fig. 4.1.1. In equilibrium the nodal coordinates are $P(x_i,y_i,z_i)$ and $Q(x_j,y_j,z_j)$, and

the tensions are R_i, R_j. $R_i=R_j=R$ if the tension is assumed constant in the element.

We consider the situation when node i is moved to point $P'(x_i', y_i', z_i')$ and node j to $Q'(x_j', y_j', z_j')$. We write the nodal displacements

$$\vec{r}_i = r_{xi}\vec{i} + r_{yi}\vec{j} + r_{zi}\vec{k} = (x_i'-x_i)\vec{i} + (y_i'-y_i)\vec{j} + (z_i'-z_i)\vec{k}$$

$$\vec{r}_j = r_{xj}\vec{i} + r_{yi}\vec{j} + r_{zj}\vec{k} = (x_j'-x_j)\vec{i} + (y_i'-y_i)\vec{j} + (z_j'-z_j)\vec{k} \qquad (\alpha)$$

We also have the longitudinal unit vectors:

$$\vec{t} = t_x\vec{i} + t_y\vec{j} + t_z\vec{k} = \frac{1}{L}((x_j-x_i)\vec{i} + (y_j-y_i)\vec{j} + (z_j-z_i)\vec{k})$$

$$\vec{t}' = t_x'\vec{i} + t_y'\vec{j} + t_z'\vec{k} = \frac{1}{L'}((x_j'-x_i')\vec{i} + (y_j'-y_i')\vec{j} + (z_j'-z_i')\vec{k}, \qquad (\beta)$$

where

$$L = ((x_j-x_i)^2 + (y_j-y_i)^2 + (z_j-z_i)^2)^{1/2}$$

$$L' = ((x_j'-x_i')^2 + (y_j'-y_i')^2 + (z_j'-z_i')^2)^{1/2}. \qquad (\gamma)$$

Further, in the displaced position, the elastic tensions at the nodes are R_i' and R_j', which can be expressed by the linear elastic relations:

$$R_i'-R_i = R_j'-R_j = AE\,\frac{L'-L}{L} = AE\epsilon = \Delta R$$

We shall also use matrix notation to represent the displacements by the 6x1 matrix vector:

$$(\delta) \qquad \underline{r} = \begin{pmatrix} r_{xi} \\ r_{yi} \\ r_{zi} \\ r_{xj} \\ r_{yj} \\ r_{zj} \end{pmatrix}$$

In equilibrium the forces acting from the element on the nodes are

$$\vec{f}^{\,o}_{Ri} = R_i \vec{t}, \quad \vec{f}^{\,o}_{Rj} = -R_j \vec{t},$$

and in the displaced position

$$\vec{f}_{Ri} = R'_i \vec{t}', \quad \vec{f}_{Rj} = -R'_j \vec{t}'$$

We consider first the case of small displacements and thereafter make some remarks about large displacements.

4.1.1 Small Displacements. Stiffness Matrix of a Straight String Element.

We can express the element length in the displaced position, according to eqs. (α) and (γ)

$$L' = [(x_j - x_i + r_{xj} - r_{xi})^2 + (y_j - y_i + r_{yj} - r_{yi})^2 + (z_j - z_i + r_{zj} - r_{zi})^2]^{1/2}$$

$$= L[1 + 2t_x \frac{r_{xj} - r_{xi}}{L} + (\frac{r_{xj} - r_{xi}}{L})^2 + \text{terms in } y,z]^{1/2}$$

Under small displacements, we can neglect the terms $(\frac{r_{xj} - r_{xi}}{L})^2$, etc. and hence

$$L' \approx L(1 + t_x \frac{r_{xj} - r_{xi}}{L} + t_y \frac{r_{yj} - r_{yi}}{L} + t_z \frac{r_{zj} - r_{zi}}{L})$$

$$= L(1 + \frac{1}{L} \vec{t} \cdot (\vec{r}_j - \vec{r}_i)).$$

Hence we have the strain:

$$(\varepsilon) \quad \varepsilon = \frac{L' - L}{L} = \frac{1}{L} \vec{t} \cdot (\vec{r}_j - \vec{r}_i) ,$$

i.e. proportional to the tangential component of the relative displacement $\vec{r}_j - \vec{r}_i$.

Hence we can express the direction unit vector in the displaced position, according to eq. (β):

$$\vec{t}' = \frac{1}{L'}((x_j - x_i + r_{xj} - r_{xi})\vec{i} + (y_j - y_i + r_{yj} - r_{yi})\vec{j} + (z_j - z_i + r_{zj} - r_{zi})\vec{k})$$

$$= \frac{L}{L'}\vec{t} + \frac{1}{L'}(\vec{r}_j - \vec{r}_i)$$

We can decompose $\vec{r}_j - \vec{r}_i$ into components parallel and normal to $\vec{t}$. The parallel component is

$$\vec{r}_{jt}-\vec{r}_{it} = (r_j-r_i)\cdot\vec{t}\vec{t},$$

the normal component is

$$\vec{r}_{jn}-\vec{r}_{in} = \vec{r}_j-\vec{r}_i - (\vec{r}_{jt}-\vec{r}_{it}).$$

Hence we can write for $\vec{t}'$:

$$\vec{t}' = \frac{L}{L'}\vec{t} + \frac{1}{L'}[(\vec{r}_j-\vec{r}_i)\cdot\vec{t}\vec{t}+(\vec{r}_{jn}-\vec{r}_{in})]$$

$$= \vec{t} + \frac{1}{L'}(\vec{r}_{jn}-\vec{r}_{in})$$

For small displacements $\varepsilon<<1$ and we have $L'\approx L$. Hence we have to ε^2:

$$(\zeta)\quad \vec{t}' = \vec{t} + \frac{1}{L}(\vec{r}_{jn}-\vec{r}_{in}).$$

Thus $\vec{t}'-\vec{t}$ is essentially normal to $\vec{t}$.

Finally we express the nodal forces $\vec{f}_{Ri}$, $\vec{f}_{Rj}$:

$$\vec{f}_{Ri} = R_i'\vec{t}' = (R_i+\Delta R)(\vec{t}+\frac{1}{L}(\vec{r}_{jn}-\vec{r}_{in}))$$

$$= \vec{f}_{Ri}^{\,o} + \Delta R\vec{t} + R_i\cdot\frac{1}{L}(\vec{r}_{jn}-\vec{r}_{in}) + \Delta R\frac{1}{L}(\vec{r}_{jn}-\vec{r}_{in}).$$

For small displacements

$$\Delta R<<R,\ \frac{\vec{r}_{jn}-\vec{r}_{in}}{L}<<1$$

so that the last term can be neglected as small.

Correspondingly we have

$$\vec{f}_{Rj} \cong \vec{f}^{\,o}_{Rj} - \Delta R\vec{t} - R_j \frac{1}{L} (\vec{r}_{jn}-\vec{r}_{in}).$$

We now write the differences

$$\vec{f}_{Ri}-\vec{f}^{\,o}_{Ri} = U_i\vec{i} + V_i\vec{j} + W_i\vec{k} =$$

(η)

$$\vec{f}_{Rj}-\vec{f}_{Rj} = U_j\vec{i} + V_j\vec{j} + W_j\vec{k},$$

where U_i, U_j, etc. are the components of the force deviations. We also use the force matrix vector

(θ)
$$\underline{f} = \begin{pmatrix} U_i \\ V_i \\ W_i \\ U_j \\ V_j \\ W_j \end{pmatrix}$$

From the above we can write for the tension increase:

$$\Delta R = AE\varepsilon = \frac{AE}{L} [t_x(r_{xj}-r_{xi})+t_y(r_{yj}-r_{yi})+t_z(r_{zj}-r_{zi})],$$

and for the relative normal displacements

$$\vec{r}_{jn}-\vec{r}_{in} = (\vec{r}_j-\vec{r}_i) - (\vec{r}_j-\vec{r}_i)\cdot\vec{t}\vec{t} =$$

$$[r_{xj}-r_{xi} - ((r_{xj}-r_{xi})t_x+(r_{yj}-r_{yi})t_y+(r_{zj}-r_{zi})t_z)t_x]\vec{i}$$

$$+ [r_{yj}-r_{yi}-((r_{xj}-r_{xi})t_x+(r_{yj}-r_{yi})t_y+(r_{zj}-r_{zi})t_z)t_y]\vec{j}$$

$$+ [r_{zj}-r_{zi}-((r_{xj}-r_{xi})t_x+(r_{yj}-r_{yi})t_y+(r_{zj}-r_{zi})t_z)t_z]\vec{k}$$

Hence, we can write, according to eqs. (δ), (η) and (θ):

$$(4.1.1) \qquad \underline{f} = \begin{pmatrix} u_i \\ v_i \\ w_i \\ u_j \\ v_j \\ w_j \end{pmatrix} = (\underline{k}_E + \underline{k}_G) \begin{pmatrix} r_{xi} \\ r_{yi} \\ r_{zi} \\ r_{xj} \\ r_{yj} \\ r_{zj} \end{pmatrix} = (\underline{k}_E + \underline{k}_G)\underline{r} \ ,$$

where the elastic stiffness matrix is:

$$\underline{k}_E = \frac{EA}{L} \begin{pmatrix} t_x^2 & t_x t_y & t_x t_z & -t_x^2 & -t_x t_y & -t_x t_z \\ t_x t_y & t_y^2 & t_y t_z & -t_x t_y & -t_y^2 & -t_y t_z \\ t_x t_z & t_y t_z & t_z^2 & -t_x t_z & -t_y t_z & -t_z^2 \\ -t_x^2 & -t_x t_y & -t_x t_z & t_x^2 & t_x t_y & t_x t_z \\ -t_x t_y & -t_y^2 & -t_y t_z & t_x t_y & t_y^2 & t_y t_z \\ -t_x t_z & -t_y t_z & -t_z^2 & t_x t_z & t_y t_z & t_z^2 \end{pmatrix}$$

and the geometric stiffness matrix:

$$\underline{k}_G = \frac{1}{L} \begin{pmatrix} R_i \begin{pmatrix} t_y^2+t_z^2 & -t_x t_y & -t_x t_z \\ -t_x t_y & t_x^2+t_z^2 & -t_y t_z \\ -t_x t_z & -t_y t_z & t_x^2+t_y^2 \end{pmatrix}, & R_j \begin{pmatrix} -t_y^2-t_z^2 & t_x t_y & t_x t_z \\ t_x t_y & -t_x^2-t_z^2 & t_y t_z \\ t_x t_z & t_y t_z & -t_x^2-t_y^2 \end{pmatrix} \\ R_j \begin{pmatrix} -t_y^2-t_z^2 & t_x t_y & t_x t_z \\ t_x t_y & -t_x^2-t_z^2 & t_y t_z \\ t_x t_z & t_y t_z & -t_x^2-t_y^2 \end{pmatrix}, & R_i \begin{pmatrix} t_y^2+t_z^2 & -t_x t_y & -t_x t_z \\ -t_x t_y & t_x^2+t_z^2 & -t_y t_z \\ -t_x t_z & -t_y t_z & t_x^2+t_y^2 \end{pmatrix} \end{pmatrix}$$

The elastic stiffness matrix $\underline{k}_E$ represents the additional forces introduced by the elongation of the element, while the geometric stiffness matrix $\underline{k}_G$ represents the effects of changing the element direction. We see that $\underline{k}_E$ and $\underline{k}_G$ are symmetric.

From these relations, we can write the nodal forces in the displaced position under small displacements:

$$\begin{aligned} \vec{f}_{Ri} &= \vec{f}^{\,o}_{Ri} + U_i\vec{i} + V_i\vec{j} + W_i\vec{k} \\ \vec{f}_{Rj} &= \vec{f}^{\,o}_{Rj} + U_j\vec{i} + V_j\vec{j} + W_j\vec{k} \ . \end{aligned} \tag{4.1.2}$$

Writing $\vec{f}_{Ri} = f_{Rix}\vec{i} + f_{Riy}\vec{j} + f_{Riz}\vec{k}$,

$\vec{f}_{Rj} = f_{Rjx}\vec{i} + f_{Rjy}\vec{j} + f_{Rjz}\vec{k}$ and

$$\underline{f}_R = \begin{pmatrix} f_{Rix} \\ f_{Riy} \\ f_{Riz} \\ f_{Rjx} \\ f_{Rjy} \\ f_{Rjz} \end{pmatrix}$$

We can write briefly

$$\underline{f}_R = \underline{f}^{o}_R + (\underline{k}_E + \underline{k}_G)\underline{r}. \tag{4.1.3}$$

4.1.2 Large Displacements. Deviations from Linearity.

In the general case of large displacements, the force deviations are:

$$\vec{\phi}_i = \phi_{ix}\vec{i}+\phi_{iy}\vec{j}+\phi_{iz}\vec{k} = \vec{f}_{Ri}-\vec{f}^{\,o}_{Ri} = R'_i\vec{t}'-R_i\vec{t}$$

$$\vec{\phi}_j = \phi_{jx}\vec{i}+\phi_{jy}\vec{j}+\phi_{jz}\vec{k} = \vec{f}_{Rj}-\vec{f}^{\,o}_{Rj} = -R'_j\vec{t}'+R_j\vec{t}$$

Define the matrix vector

$$\underline{\phi}_R = \begin{pmatrix} \phi_{ix} \\ \phi_{iy} \\ \phi_{iz} \\ \phi_{jx} \\ \phi_{jy} \\ \phi_{jz} \end{pmatrix}$$

Then we can write

$$\underline{\phi}_R = (\underline{k}_E+\underline{k}_G)\underline{r} + \Delta\underline{f}_R \ ,$$

where $\Delta\underline{f}_R$ expresses the deviation of $\underline{\phi}_R$ from linearity. Hence we can finally write the nodal forces:

$$\underline{f}_R = \underline{f}^{o}_R + (\underline{k}_E+\underline{k}_G)\underline{r} + \Delta\underline{f}_R \quad . \tag{4.1.4}$$

4.2 Inertia Forces.

As mentioned in Sec. 2.3.2, we must account for two contributions to the inertia forces when the cable is accelerating: the inertia of the cable itself and the inertia of the surrounding water.

With given nodal velocities $\dot{\underline{r}}$ and accelerations $\ddot{\underline{r}}$, the velocity and acceleration distributions along the element are given by linear interpolation. We can use two methods to derive expressions for the inertia forces on the element:

i) Derive an expression for the kinetic energy T of the form $T = \frac{1}{2}\,\dot{\underline{r}}^T \underline{\underline{M}}\,\underline{r}$, where $\underline{\underline{M}}$ is a mass matrix. Considering the components i of $\underline{r}$ as generalized coordinates, the corresponding generalized momenta are

$$p_i = \frac{\partial T}{\partial \dot{r}_i} = (\underline{\underline{M}}\,\dot{\underline{r}})_i = \text{i'th component of } \underline{\underline{M}}\,\dot{\underline{r}} \ ,$$

provided $\underline{\underline{M}}$ is symmetric. Hence the matrix vector of momenta is:

$$\underline{p} = \underline{\underline{M}}\,\dot{\underline{r}}.$$

We then have the inertia reactions

$$\underline{f}_I = -\frac{d}{dt}\,\underline{p} = -\underline{\underline{M}}\,\ddot{\underline{r}} - \dot{\underline{\underline{M}}}\,\dot{\underline{r}}$$

ii) From the acceleration distribution $\vec{a}(\xi)$, we can determine the distribution of inertia force $\vec{\phi}_I(\xi)$, as in Sec. 2.2.2. Then the equivalent nodal forces are computed.

The first method assumes that it is possible to derive an expression for T. If the cable is assumed to be immersed in an infinite body of water with non-vanishing water velocity, a direct calculation will give an infinite value of the kinetic energy of the water. If we use the device of describing the motion in a coordinate system moving with the local current, we may still have difficulties if the current is non-uniform.

In the subsequent treatment the inertia forces of the cable itself is derived by method i), while the inertia forces of the surrounding is calculated with method ii).

The element is sketched in Fig. 4.2.1. The nodes have

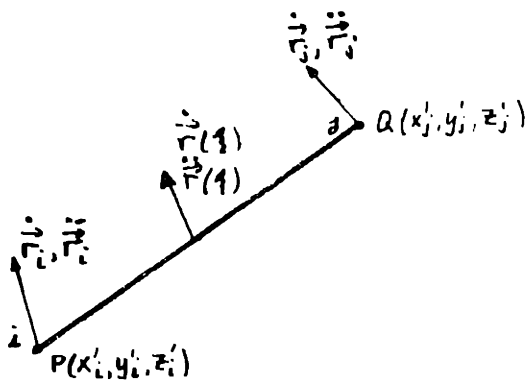

Fig. 4.2.1

Dynamic Variables

coordinates $P(x_i,y_i,z_i)$ and $Q(x_j,y_j,z_j)$. The velocities are $\dot{\vec{r}}_i$, $\dot{\vec{r}}_j$. The velocity at ξ is:

$$\dot{\vec{r}}(\xi) = \dot{\vec{r}}_i(1-\xi)+\dot{\vec{r}}_j\xi.$$

Hence the kinetic energy of segment $Ld\xi$ is

$$dT = \frac{1}{2}\rho_c A\dot{\vec{r}}^2 Ld\xi = \frac{1}{2}\rho_c A[\dot{\vec{r}}_i^{\,2}(1-\xi)^2+2\dot{\vec{r}}_i\cdot\dot{\vec{r}}_j\xi(1-\xi)+\dot{\vec{r}}_j^{\,2}\xi^2]Ld\xi.$$

Integrating over the element:

$$T = \frac{1}{6}\rho_c AL(\dot{\vec{r}}_i^{\,2}+\dot{\vec{r}}_i\cdot\dot{\vec{r}}_j+\dot{\vec{r}}_j^{\,2})$$

When we substitute for the components of $\dot{\vec{r}}_i,\dot{\vec{r}}_j$, according to eq. ($\delta$), we can write

$$T = \frac{1}{2}\dot{\underline{r}}^T\underline{\underline{m}}_c\dot{\underline{r}} \quad ,$$

where

$$\underline{\underline{m}}_c = \frac{m}{3}\begin{pmatrix} 1 & 0 & 0 & 1/2 & 0 & 0 \\ 0 & 1 & 0 & 0 & 1/2 & 0 \\ 0 & 0 & 1 & 0 & 0 & 1/2 \\ 1/2 & 0 & 0 & 1 & 0 & 0 \\ 0 & 1/2 & 0 & 0 & 1 & 0 \\ 0 & 0 & 1/2 & 0 & 0 & 1 \end{pmatrix}$$

is the cable element mass matrix and $m = \rho_c AL$ is the total element mass.

We get the nodal forces

$$\underline{f}_C = -\underline{m}_C\ddot{\underline{r}} \ .$$

To compute the hydrodynamic mass matrix, we use the expressions from eqs. (2.3.12), with zero water acceleration,

$$\vec{f}_{Hi} = -\frac{1}{6} C_M \rho_w AL(2\ddot{\vec{r}}_{in}+\ddot{\vec{r}}_{jn})$$

$$\vec{f}_{Hj} = -\frac{1}{6} C_M \rho_W AL(\ddot{\vec{r}}_{in}+2\ddot{\vec{r}}_{jn}) \ ,$$

where $\ddot{\vec{r}}_{in}, \ddot{\vec{r}}_{jn}$ are the normal components of the nodal accelerations. We can now write

$$\ddot{\vec{r}}_{in} = \ddot{\vec{r}}_i - \ddot{\vec{r}}_i \cdot \vec{t}\vec{t} = (\ddot{r}_{ix} - (\ddot{r}_{ix}t_x + \ddot{r}_{iy}t_y + \ddot{r}_{iz}t_z)t_x)\vec{L} +$$

$$(\ddot{r}_{iy} - (\ddot{r}_{ix}t_x + \ddot{r}_{iy}t_y + \ddot{r}_{iz}t_z)t_y)\vec{j} + (\ddot{r}_{iz} - (\ddot{r}_{ix}t_x + \ddot{r}_{iy}y_z + \ddot{r}_{iz}t_z))\vec{k},$$

where r_{ix}, r_{iy}, r_{iz} are the cartesian components of $\vec{r}_i$. We can write a similar expression for $\vec{r}_{jn}$. Substituting into the expressions for $\vec{f}_{Hi}$ and $\vec{f}_{Hj}$ and defining the matrix vector $\underline{f}_H$ from the components of $\vec{f}_{Hi}, \vec{f}_{Hj}$, we get

$$\underline{f}_H = -m_W \underline{m}_H \ddot{\underline{r}}$$

where

$$\underline{\underline{m}} = \frac{1}{3}C_M m_W \begin{pmatrix} 1-t_x^2 & -t_x t_y & -t_x t_z & \frac{1}{2}(1-t_x^2) & -\frac{1}{2}t_x t_y & -\frac{1}{2}t_x t_y \\ -t_x t_y & 1-t_y^2 & -t_y t_z & -\frac{1}{2}t_x t_y & \frac{1}{2}(1-t_y^2) & -\frac{1}{2}t_y t_z \\ -t_x t_z & -t_y t_z & 1-t_z^2 & -\frac{1}{2}t_x t_z & -\frac{1}{2}t_y t_z & \frac{1}{2}(1-t_z^2) \\ \frac{1}{2}(1-t_x^2) & -\frac{1}{2}t_x t_y & -\frac{1}{2}t_x t_z & 1-t_x^2 & -t_x t_y & -t_x t_z \\ -\frac{1}{2}t_x t_y & \frac{1}{2}(1-t_y^2) & -\frac{1}{2}t_y t_z & -t_x t_y & 1-t_y^2 & -t_y t_z \\ -\frac{1}{2}t_x t_z & -\frac{1}{2}t_y t_z & \frac{1}{2}(1-t_z^2) & -t_x t_z & -t_y t_z & 1-t_z^2 \end{pmatrix}$$

is the hydrodynamic mass matrix and $m_W = \rho_W AL$ is the water mass displaced by the element.

$\underline{\underline{m}}_C$ is independent of position, while $\underline{\underline{m}}_H$ depends on position via the components of $\vec{t}$. If we write $\underline{\underline{m}}_H^o$ for the hydrodynamic mass matrix in equilibrium, we write for a general position $\underline{\underline{m}}_H = \underline{\underline{m}}_H^o + \Delta\underline{\underline{m}}_H$.

For the total inertia force we have:

$$\underline{f}_I = \underline{f}_C + \underline{f}_H = -(\underline{\underline{m}}_C + \underline{\underline{m}}_H)\ddot{\underline{r}}$$

$$= -(\underline{\underline{m}}_C + \underline{\underline{m}}_H^o)\ddot{\underline{r}} + (\underline{\underline{m}}_H^o - \underline{\underline{m}}_H)\ddot{\underline{r}} = -\underline{\underline{m}}^o\ddot{\underline{r}} - \Delta\underline{\underline{m}}_H\ddot{\underline{r}},$$

where $\underline{\underline{m}}^o = \underline{\underline{m}}_C + \underline{\underline{m}}_H^o$. We have written $\underline{f}_I$ as the sum of a linear term, corresponding to the equilibrium configuration, and a term representing the effect of deviation from equilibrium.

4.3 Other Forces.

Consider an arbitrary situation, where the state of the element may be different from that of rest with the cable in the equilibrium configuration. Any of the force contributions in Sec. 2.3 can be computed from knowledge of the displacements $\underline{r}$, velocities $\dot{\underline{r}}$ and accelerations $\ddot{\underline{r}}$ and the water velocity $\vec{v}_w$. Let us call the corresponding force matrix $\underline{f}_x$ for any force contribution. At rest in the equilibrium configuration of the cable we have the corresponding equilibrium $\underline{f}_x^o$. Hence we can write

$$(4.3.1) \qquad \underline{f}_x = \underline{f}_x^o + \Delta\underline{f}_x \ ,$$

where $\Delta\underline{f}_x = \underline{f}_x - \underline{f}_x^o$ represents the effect of deviation from equilibrium.

Most of the forces will have $\Delta\underline{f}_x \neq 0$, except the gravity force on the cable. The tension force $\underline{f}_R$ and inertia forces $\underline{f}_C$ and $\underline{f}_H$ were given a special discussion in Secs. 4.1 and 4.2. For the other forces $\underline{f}_x$ can be computed from a given state and $\Delta\underline{f}_x$ found by subtracting $\underline{f}_x^o$.

Since the $\underline{f}_x$ are the real forces on the system, this way of separating the equilibrium and deviation forces allows us to include quite general relations between the dynamic state and the corresponding forces. E.g. if the elastic properties of the cable are non-linear, the deviation from linearity will contribute to $\Delta\underline{f}_R$ in (4.1.4).

CHAPTER 5. Finite Element Model for Total System

This chapter will describe the structure of a total model to represent a cable. Boundary conditions are discussed. Further the equations of motion for the free degrees of freedom are transformed to a normal mode formulation, where the normal modes are defined in terms of undamped, small amplitude oscillations of the cable about its equilibrium state.

5.1 The Total Cable System.

Fig. 5.1.1 shows a finite element model of a cable, modelled with 5 straight elements. Nodes and elements are identified by numbering systems. If we assume that all nodal

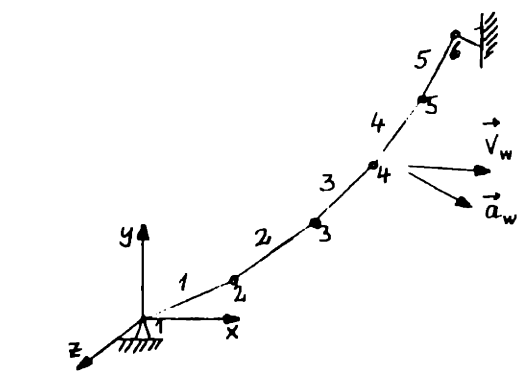

Fig. 5.1.1

Total Finite Element Model

coordinates (x_i, y_i, z_i) are known, then the cable geometry is defined. If we also know the nodal velocities $(\dot{x}_i, \dot{y}_i, \dot{z}_i)$, accelerations $(\ddot{x}_i, \ddot{y}_i, \ddot{z}_i)$ and the water velocity $\vec{v}_{wi}$ and

acceleration $\vec{a}_{wi}$ at all nodes, we can compute nodal forces for all elements by the results of Sec. 2.3.

At any node there are two adjoining elements, except at the upper and lower ends. The total forces at each node will be given by summation of contributions from each adjoining element.

We introduce column vectors, $\underline{R},\underline{F}$, to represent the totality of nodal displacements and forces for the total model, corresponding to the element column vectors $\underline{r},\underline{f}$ defined in Ch. 4. Hence if there are N nodes, each of 3 degrees of freedom, $\underline{R}$ and $\underline{F}$ have dimension 3Nx1. Reduced versions of $\underline{R},\underline{F}$ will be used later.

In an arbitrary dynamic state, we can write the nodal forces, $\underline{f}_F$, in the form indicated in eq. (4.3.1) as the sum of the equilibrium value $\underline{f}_F^o$ and a contribution due to deviation from equilibrium, $\Delta\underline{f}_F$. By summing all force contributions, we can write the total force matrix vectors:

Tangential friction force: $\underline{F}_T = \underline{F}_T^o + \Delta\underline{F}_T$

Normal drag force: $\underline{F}_N = \underline{F}_N^o + \Delta\underline{F}_N$,

Buoyancy force: $\underline{F}_B = \underline{F}_B^o + \Delta\underline{F}_B$

Gravity force: $\underline{F}_W = \underline{F}_W^o \quad ; \Delta\underline{F}_W = 0$

Tension force: $\underline{F}_R = \underline{F}_R^o - (\underline{K}_E+\underline{K}_G)\underline{R}+\Delta\underline{F}_R$

Cable inertia force: $\underline{F}_C = -\underline{M}_C^O \ddot{\underline{R}}$

Hydrodynamic inertia force: $\underline{F}_H = -(\underline{M}_H + \Delta\underline{M}_H)\ddot{\underline{R}}$

Fictitious buoyancy from water acceleration: $\underline{F}_A$

Viscoelastic internal force: $\underline{F}_V$

The total stiffness matrices $\underline{K}_E$, $\underline{K}_G$ and mass matrices $\underline{M}_C$, $\underline{M}_H$ are formed by a merge process from the corresponding element matrices $\underline{k}_E, \underline{k}_G, \underline{m}_C, \underline{m}_H$ in Ch. 4. The merge is essentially the result of expressing relations between tension forces, $\underline{F}$, and displacements, $\underline{R}$, similarly to sec. 4.1 to find $\underline{K}_E$, $\underline{K}_G$, and relations between inertia forces $\underline{F}$ and accelerations, $\ddot{\underline{R}}$, similarly to sec. 4.2, to find $\underline{M}_C, \underline{M}_H$. Details of the process are discussed in Zienkiewicz [11].

The components of $\underline{R}$ represent displacements measured from equilibrium. In Secs. 4.1 and 4.2 the stiffness and mass matrices were derived relative to cartesian x-,y-,z-displacements, and in the merge process this is also assumed to be the case. As indicated in Sec. 2.1, the displacements, and also the corresponding forces can be transformed to local, intensic coordinates $\vec{t},\vec{n},\vec{b}$ at each node, when nodal $\vec{t},\vec{n},\vec{b}$ have been defined. Corresponding to these displacement and force transformations, the stiffness and mass matrices must also be suitably transformed. There is no computational

gain in transforming to intrinsic coordinates, but the transformation may simplify the interpretation of final results. The subsequent treatment is independent of whether the degrees of freedom have been transformed or not, so long as there is consistency between $\underline{R}, \underline{F}, \underline{K}_E, \underline{K}_G, \underline{M}_C, \underline{M}_H$.

In addition to the forces listed above, it may for particular problems be necessary to include other forces. One particular example is the presence of concentrated masses on the cable, e.g. instrument packages. These must be assumed positioned at nodes in the model. The most convenient way to include these is to incorporate them directly into the finite element model. By specifying their mass and hydrodynamic mass properties, these can be incorporated directly into the mass matrices $\underline{M}_C$ and $\underline{M}_H$. The weight can be included into $\underline{F}_W$, the buoyancy into $\underline{F}_B$ and the fictitious buoyancy due to water acceleration into $\underline{F}_A$. Such concentrated masses can be assumed to give no stiffness contribution.

For completeness we shall also include among the forces a miscellaneous force $\underline{F}_M$, which is not among the forces described earlier, and whose nature will depend on the particular problem under study. In an arbitrary state we write $\underline{F}_M = \underline{F}_M^{\,o} + \Delta\underline{F}_M$.

5.2 Total Dynamic Equilibrium.

A total dynamic equilibrium relation for the system can be written:

$$\underline{F}_T+\underline{F}_N+\underline{F}_B+\underline{F}_W+\underline{F}_R+\underline{F}_C+\underline{F}_H+\underline{F}_A+\underline{F}_V+\underline{F}_M = 0.$$

Separating out the equilibrium forces and introducing the stiffness and mass matrices, we can write

$$\begin{aligned}(5.2.1)\quad \underline{\underline{M}}\ddot{\underline{R}}+\underline{\underline{K}}\underline{R} &= \underline{F}_T^{\,o}+\Delta\underline{F}_T+\underline{F}_N^{\,o}+\Delta\underline{F}_N+\underline{F}_B^{\,o}+\Delta\underline{F}_B+\underline{F}_W^{\,o}+\underline{F}_R^{\,o}+\Delta\underline{F}_R \\ &\quad - \Delta\underline{\underline{M}}_H\ddot{\underline{R}} +\underline{F}_A+\underline{F}_V+\underline{F}_M^{\,o}+\Delta\underline{F}_M \\ &= \Delta\underline{F}_T+\Delta\underline{F}_N+\Delta\underline{F}_B+\Delta\underline{F}_R-\Delta\underline{\underline{M}}_H\ddot{\underline{R}}+\underline{F}_A+\underline{F}_V+\Delta\underline{F}_M = \underline{F}\end{aligned}$$

since in equilibrium

$$\underline{F}_T^{\,o}+\underline{F}_N^{\,o}+\underline{F}_B^{\,o}+\underline{F}_W^{\,o}+\underline{F}_R^{\,o}+\underline{F}_M^{\,o} = 0.$$

We have written $\underline{\underline{M}} = \underline{\underline{M}}_C^{\,o}+\underline{\underline{M}}_H^{\,o}$ and $\underline{\underline{K}} = \underline{\underline{K}}_E+\underline{\underline{K}}_G$ for brevity.

Eq. (5.2.1) is the equation of motion, upon which the time integration will be based. If the state of the cable at time t, expressed as $\underline{R},\dot{\underline{R}},\ddot{\underline{R}}$, together with the state of the surrounding water, $\vec{v}_W,\vec{a}_W$ are known, all forces on the right hand side can be computed according to Sec. 2.3.

Before proceeding to the time integration, we have to

introduce boundary conditions into the problem. Further, we will simplify the mathematical problem by transforming the equations to normal coordinates. By doing this, the left hand sides of (5.2.1) can be decoupled.

5.3 Boundary Conditions.

Since $\underline{M}$ can be interpreted as a matrix of coefficients of a homogeneous quadratic form for the kinetic energy T, we conclude that $\underline{M}$ must be positive definite. However $\underline{K}$ is not generally positive definite, since we can make translational rigid body motions of the whole system, without disturbing the state of equilibrium.

To make the system determinate, we introduce boundary conditions. Normally these will specify the displacements of the bottom node to be zero, i.e. fixed, while the upper node has given displacements as a function of time, given by the motion of the moored vehicle. Other types of boundary conditions may also apply. These may be dynamic relating reaction forces to accelerations, or elastic, relating reaction forces to displacements.

Let us assume that we have specified a sufficient number of degrees of freedom. We identify these displacements as $\underline{R}_s$. The other degrees of freedom are considered as free in

the sense that they will take whatever values the laws of dynamics dictate. We identify these as $\underline{R}_f$.

If we call the right hand side of (5.2.1) $\underline{F}$, we can make a corresponding differentiation for the components of $\underline{F}$, by writing $\underline{F}_s$ and $\underline{F}_f$ for the forces corresponding to respectively the specified and the free degrees of freedom. $\underline{F}_s$ will represent the support reactions.

By rearranging the degrees of freedom, we can write for $\underline{R}$ and $\underline{F}$

$$\underline{R} = \begin{pmatrix} \underline{R}_s \\ \underline{R}_f \end{pmatrix} \quad , \quad \underline{F} = \begin{pmatrix} \underline{F}_s \\ \underline{F}_f \end{pmatrix}$$

By making corresponding changes in $\underline{K}$ and $\underline{M}$, we can write for (5.2.1)

$$(5.3.1) \quad \begin{pmatrix} \underline{M}_{ss} & \underline{M}_{sf} \\ \underline{M}_{fs} & \underline{M}_{ff} \end{pmatrix} \begin{pmatrix} \ddot{\underline{R}}_s \\ \ddot{\underline{R}}_f \end{pmatrix} + \begin{pmatrix} \underline{K}_{ss} & \underline{K}_{sf} \\ \underline{K}_{fs} & \underline{K}_{ff} \end{pmatrix} \begin{pmatrix} \underline{R}_s \\ \underline{R}_f \end{pmatrix} = \begin{pmatrix} \underline{F}_s \\ \underline{F}_f \end{pmatrix}$$

with the submatrices $\underline{M}_{ss}, \underline{M}_{sf}, \ldots$etc. If there are N_s specified degrees of freedom and N_f free degrees of freedom, where $N = N_s + N_f$ is the total number of degrees of freedom, $\underline{R}_s, \underline{F}_s$ have N_s components and $\underline{R}_f, \underline{F}_f$ have N_f components.

Eq. (5.3.1) can be considered as representing two sets of equations. In the first set, represented by the upper N_s specified degrees of freedom, we consider the displacements

$\underline{R}_s$ and accelerations $\ddot{\underline{R}}_s$ as known and the reaction forces $\underline{F}_s$ as unknown. In the second set, corresponding to the lower N_f free degrees of freedom, $\underline{F}_f$ are considered as known while $\underline{R}$ and $\ddot{\underline{R}}$ are unknwon. The two sets of equations can be explicitly written:

$$(5.3.2a)\quad \underline{\underline{M}}_{ss}\ddot{\underline{R}}_s+\underline{\underline{M}}_{sf}\ddot{\underline{R}}_f+\underline{\underline{K}}_{ss}\underline{R}_s+\underline{\underline{K}}_{sf}\underline{R}_f = \underline{F}_s$$

$$(5.3.2b)\quad \underline{\underline{M}}_{ff}\ddot{\underline{R}}_f+\underline{\underline{K}}_{ff}\underline{R}_f = \underline{F}_f-(\underline{\underline{M}}_{fs}\ddot{\underline{R}}_s+\underline{\underline{K}}_{fs}\underline{R}_s)$$

The term

$$\underline{F}_x = -(\underline{\underline{M}}_{fs}\ddot{\underline{R}}_s+\underline{\underline{K}}_{fs}\underline{R}_s)$$

represents the interaction from the specified on the free degrees of freedom. (5.3.2b) is the equation of motion for the free degrees of freedom.

The nature of the interaction term $\underline{F}_x$ can be compared to that of the simpler linear system of Fig. 5.3.1. The

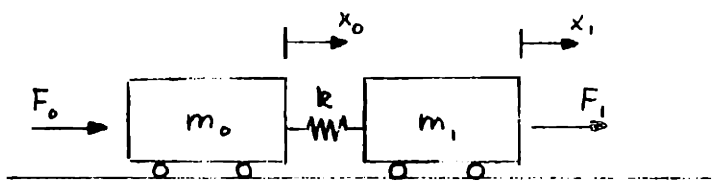

Fig. 5.3.1

Analogous Two-Mass System

equations of motion for this system can be written in the matrix form

$$\begin{pmatrix} m_o & o \\ o & m_1 \end{pmatrix} \begin{pmatrix} \ddot{x}_o \\ \ddot{x}_1 \end{pmatrix} + \begin{pmatrix} k & -k \\ -k & k \end{pmatrix} \begin{pmatrix} x_o \\ x_1 \end{pmatrix} = \begin{pmatrix} F_o \\ F_1 \end{pmatrix}$$

If we have specified $x_o(t)$ and consider x_1 as free, we have the equation for x_1:

$$m_1\ddot{x}_1+kx_1 = F_1+kx_o,$$

where kx_o is the interaction term. Since $k_{fs}=-k$, we have the interaction term $-k_{fs}x_o$, which is similar to $\underline{F}_x$, except that in this case there is no inertia coupling, $M_{fs}=0$.

5.4 Eigenfrequencies and Mode Shapes.

If we set the right hand side of (5.3.2b) equal to zero, we get the equation

$$(\alpha) \qquad \underline{\underline{M}}_{ff}\ddot{\underline{R}}+\underline{\underline{K}}_{ff}\underline{R} = 0$$

This equation is an equation of motion for free, undamped small amplitude oscillations of the cable about its equili-

brium configuration and with the end points fixed.

By determining the eigenfrequencies and corresponding mode shapes, we can achieve two goals:

1) the eigenfrequencies are usually important parameters for the dynamic behavior of a mechanical system,
2) we obtain transformation matrices to transform the dynamic problem to normal coordinates.

The latter is the most important here.

Assume $\underline{R}$ to be a harmonic function of time

$$\underline{R} = \underline{q}e^{i\omega t}$$

where ω is the frequency and $\underline{q}$ is a vector of amplitudes, describing the mode shapes. Substituting into eq. (α) and dropping the suffices of $\underline{\underline{M}}_{ff}, \underline{\underline{K}}_{ff}$, we get the eigenvalue problem

$$(\underline{\underline{K}}-\omega^2\underline{\underline{M}})\underline{q} = 0 \qquad (5.4.1)$$

with the eigenvalue $\lambda=\omega^2$ and eigenvector $\underline{q}$.

Here $\underline{\underline{M}}$ is positive definite and symmetric, $\underline{\underline{K}}$ is at least positive semidefinite and symmetric. The symmetry of $\underline{\underline{M}}$ and $\underline{\underline{K}}$ comes from the symmetry of the corresponding element matrices in Sec. 4.1 and 4.2.

The theory of this class of eigenvalue problem is discussed e.g. in Zurmühl [8] and Gantmacher [2]. From [8] we

get the following properties, when $n=N_f$ is the dimension of the problem.

1) All n eigenvalues $\lambda_i=\omega_i^2$ are real and positive.
2) There exist exactly n linearly independent eigenvectors $\underline{q}_i$.
3) The eigenvectors satisfy the generalized orthogonality relations:

$$\underline{q}_i^T \underline{\underline{M}} \underline{q}_j = 0 \quad \text{if } i \neq j$$
$$\neq 0 \quad \text{if } i = j.$$

By proper normalization of $\underline{q}_i$, we can satisfy

$$\text{(5.4.2a)} \quad \underline{q}_i^T \underline{\underline{M}} \underline{q}_j = \delta_{ij} = 0 \quad \text{if } i \neq j$$
$$= 1 \quad \text{if } i = j ,$$

where δ_{ij} is the Kronecker symbol. With this normalization we also have

$$\text{(5.4.2b)} \quad \underline{q}_i^T \underline{\underline{K}} \underline{q}_j = \lambda_i \delta_{ij} = 0 \quad \text{if } i \neq j$$
$$= \lambda_i \quad \text{if } i = j.$$

Let us collect all n eigenvectors into the square matrix $\underline{\underline{Q}}$:

$$\underline{\underline{Q}} = (\underline{q}_1, \underline{q}_2, \cdots \underline{q}_n).$$

Because of the linear independence of the $\underline{q}_i$, $\underline{\underline{Q}}$ is non-singular. Thus for a given $\underline{R}$, the equation

$$\underline{\underline{Q}}\underline{y} = \underline{R}$$

has a unique solution

$$(5.4.3) \qquad \underline{y} = \begin{pmatrix} y_1 \\ y_2 \\ \vdots \\ y_n \end{pmatrix} = \underline{\underline{Q}}^T \underline{\underline{M}}\underline{R}.$$

From this follows that we can write uniquely

$$(5.4.4) \qquad \underline{R} = \sum_{i=1}^{n} y_i \underline{q}_i,$$

as a linear combination of the eigenvectors $\underline{q}_i$, with the components y_i of $\underline{y}$ as coefficients. The coefficients y_i are the normal (or modal) coordinates of $\underline{R}$, relative to the eigenvectors $\underline{\underline{Q}}$. Hence there is a one-to-one correspondence between the normal coordinates $\underline{y}$ and the global coordinates $\underline{R}$.

If we use less than all normal coordinates, $y_1, y_2 \ldots y_m$, where $m<n$, and $\underline{q}_1 \ldots \underline{q}_m$, we can still use (5.4.3) to find $y_1, \ldots y_m$ for arbitrary $\underline{R}$. However, the correspondence between $\underline{y}$ and $\underline{R}$ is no longer one-to-one, since more than one $\underline{R}$ will give the same coefficients $y_1, \ldots y_m$. However, for given $y_1, \ldots y_m$, the corresponding $\underline{R}$ can be uniquely found

$$\underline{R}^m = \sum_{i=1}^{m} y_i \underline{q}_i \ .$$

5.5 Normal Form of the Equations of Motion.

Consider eq. (5.3.2b), writing $\underline{F}_f - \underline{F}_x = \underline{F}$ and dropping suffices

$$(5.5.1) \qquad \underline{\underline{M}}\ddot{\underline{R}} + \underline{\underline{K}}\underline{R} = \underline{F} \ ,$$

where $\underline{F}$ depends on the states of motion $\underline{R}, \dot{\underline{R}}, \ddot{\underline{R}}$ and the properties of the water. For the latter variables we use the symbol V. Hence

$$\underline{F} = \underline{F}(\underline{R}, \dot{\underline{R}}, \ddot{\underline{R}}, V) .$$

Premultiply (5.5.1) by $\underline{\underline{Q}}^T$ and substitute $\underline{R} = \underline{\underline{Q}}\underline{y}$. Further use (5.4.2):

$$(5.5.2a) \qquad \ddot{\underline{y}} + \underline{\underline{\lambda}}\underline{y} = \underline{\underline{Q}}^T\underline{F} = \underline{f} \ ,$$

where $\underline{\underline{\lambda}} = \mathrm{diag}(\lambda_i)$ is a diagonal matrix with the eigenvalues λ_i on the main diagonal. $\underline{f} = \underline{\underline{Q}}^T\underline{F}$ represents the transformed forces and can be interpreted as representing force components along each of the normal coordinates.

(5.5.2a) represents n equations of the form:

$$(5.5.2b) \qquad \ddot{y}_i + \lambda_i y_i = f_i \ ; \ i = 1,2,\ldots n.$$

Hence the transformation has separated the left hand sides of eqs. (5.5.2b), while the right hand sides normally remain coupled. (5.5.2b) are the normal equations of motion.

If we use only $m<n$ of the normal modes, we will get m of the equations (5.5.2b) from knowledge of m eigenvectors $\underline{q}_1,\ldots\underline{q}_m$.

5.6 A Linear Damping Term.

Inspection of eq. (5.5.2b) shows that the left hand sides have the same form as the equations of motion for an harmonic oscillator without damping. Since cables will have damping, the damping terms are contained in the right hand sides f_i in the form of drag and internal viscous damping.

However, it is possible to include linear damping terms into the left hand sides. This can be done approximately by the following reasoning. Consider the case of the cable moving in one of its normal modes, say the r'th. Then $y_r(t)\neq 0$ while all others $y_i\equiv 0$; $i\neq r$. If we consider the situation when $y_r=0$, $\dot{y}_r=1$, the cable is in the equilibrium configuration and moving with velocity $\dot{\underline{R}}=1\cdot\underline{q}_r$, where $\underline{q}_r$ is the r'th eigenvector. For this state we compute the linear drag force, $\underline{F}_L^r$, according to Sec. 2.3.1,iib, and the internal viscous force $\underline{F}_V^r$, according to Sec. 2.3.2,iv. We next transform $\underline{F}_L^r+\underline{F}_V^r$ to normal coordinates by

$$\underline{f}^r=\underline{Q}^T(\underline{F}_L^r+\underline{F}_V^r).$$

The r'th component of $\underline{f}^r, f_r^r$, gives the component of $\underline{F}_L+\underline{F}_V$ along the r'th mode. Since the modal velocity $\dot{y}_r=1$, we have a first approximation to the damping by writing $c_r=-f_r^r$ and setting the linearized modal damping force $c_r\dot{y}_r$. By adding the term $c_r\dot{y}_r$ to both sides of eq. (5.5.2b), we can write the equations of motion

$$\ddot{y}_r+c_r\dot{y}_r+\lambda_r y_r = f_r+c_r\dot{y}_r = f_r'. \tag{5.6.1}$$

The equations (5.6.1) are equivalent to (5.3.2b), since they have been deduced by mathematical manipulations.

CHAPTER 6. Integration of the Equations of Motion.

In this chapter, the integration over time of the normal mode equations of motion is discussed. In Ch. 5 we developed two equations of motion, eqs. (5.5.2b) and (5.6.1), which can both be integrated approximately.

We discuss first some general requirements to solutions $y_i(t)$ of the equations of motion. Then some methods in current use for integration of this type of equations are discussed briefly. Finally the method adopted in the present work is described.

6.1 General Requirements to Integrals.

Since eqs (5.5.2b) and (5.6.1) are deterministic, there will exist functions $y_i(t)$ satisfying these equations. If we knew these functions, we could substitute into the right hand sides to determine the forces f_i or f_i' as functions of time only. Then the equations would separate into n independent equations.

A solution $y_i(t)$ must satisfy the following relations of dynamics and kinematics:

1) The equations of motion (5.5.2b) or (5.6.1) must be satisfied at any time.

2) The kinematic relations between acceleration, velocity, and displacement must be satisfied:

$$\dot{y}_i(t) = \dot{y}_i(t_1) + \int_{t_1}^{t} \ddot{y}_i(\tau)d\tau$$

$$y_i(t) = y_i(t_1) + \int_{t_1}^{t} \dot{y}_i(\tau)d\tau$$

An approximate solution should satisfy these conditions as closely as possible.

6.2 Various Methods in Use.

Several techniques are possible for integrating approximately the equations of motion (5.5.2b) or (5.6.1). One method is to transform the equations to the form

$$(6.2.1) \qquad \ddot{y}_i = f_i'-c_i\dot{y}_i-\lambda_i y_i = f_i-\lambda_i y_i \; ; \quad i=1,2,\ldots n,$$

in which case there is no use of the linear damping coefficients c_i. This is used in the method by Newmark [29]. Argyris and Chan [27] and Argyris et al. [28] utilize similar transformations on the global equations of motion (5.3.2b). Newmark's method has gained some recognition and some discussion should be made of this method.

Let us consider the system at some time t_1, which is considered as the initial time. We suppose known the force $f_i(t_1)$, the displacement $y_i(t_1)$ and the velocity $\dot{y}_i(t_1)$, and we want

to determine the state at some later time $t_2=t_1+h$, where h is the time step. Since the force $f_i(t)$ is not known in the interval t_1 to t_2, it is not possible to integrate the equation by elementary methods. Newmark's method now makes the following reasoning: at time t_1, we can directly compute the acceleration $\ddot{y}_i(t_1)$ from (6.2.1). If a_2 is the value of the acceleration $\ddot{y}_i(t_2)$ at time t_2, the following formulas are adopted to estimate the velocity, v_2, and displacement, u_2, at t_2:

$$v_2 = \dot{y}_i(t_1)+(1-\gamma)\ddot{y}_i(t_1)\cdot h+\gamma a_2 h$$

(6.2.2)

$$u_2 = y_i(t_1)+\dot{y}_i(t_1)\cdot h+(\tfrac{1}{2}-\beta)\ddot{y}_i(t_1)h^2+\beta a_2 h^2,$$

where β and γ are constants. The notations a_2, v_2, u_2 are used for $\ddot{y}_i(t_2)$, $\dot{y}_i(t_2)$, $y_i(t_2)$ to indicate that these values are possibly only trial values in an iterative calculation. It is shown that if $\gamma \neq \frac{1}{2}$, a spurious damping is introduced, which may be negative and introduce a self-excited vibration from the numerical procedure. Thus one takes $\gamma = \frac{1}{2}$.

Provided $\beta \neq 0$, the following general procedure may be used to iteratively obtain the state at time t_2.

1) Assume values of the accelerations $a_{2i} \sim \ddot{y}_i(t_2)$ at t_2. (The symbol ~ is here used meaning "corresponding to".)

2) Compute the velocities $v_{2i} \sim \dot{y}_i(t_2)$ and displacements $u_{2i} \sim y_i(t_2)$ from (6.2.2), with a chosen value of β.

3) Transform a_{2i}, v_{2i}, u_{2i} to nodal accelerations $\underline{A}_2 \sim \ddot{\underline{R}}(t_2)$, velocities $\underline{V}_2 \sim \dot{\underline{R}}(t_2)$ and displacements $\underline{U}_2 \sim \underline{R}(t_2)$, as shown in eq. (5.4.4).

4) From $\underline{A}_2, \underline{V}_2, \underline{U}_2$ and the water properties V, we can compute forces $\underline{P}_2 \sim \underline{F}$, as in eq. (5.2.1). $\underline{P}_2$ can be transformed to normal coordinates by eq. (5.5.2a), giving the values $\underline{p}_2 \sim \underline{f}_2$ for the modal forces. We can now substitute in eq. (6.2.1) u_{2i} for $y_i(t_2)$ and f_{2i} for $f_i(t_o)$ to compute a new value $a'_{2i} \sim \ddot{y}_i(t_2)$.

5) Compare the derived accelerations a'_{2i} with the assumed a_{2i}. If they are sufficiently close for all modes i (or at least a representative selection) we can assume that we have found the best possible approximation. We then set as initial values for the next time step $\dot{y}_i(t_2)=v_2$, $y_i(t_2)=u_2$. If the values are not sufficiently close, the calculation must be repeated from step 1., using a new value of a_{2i}. It is usually best to set $a_{2i}=a'_{2i}$ for the next iteration.

A crucial point of this method seems to be the formulae (6.2.2), whose kinematical interpretation may be somewhat obscure. If $\beta = \frac{1}{8}$, it corresponds to assuming a constant acceleration equal to the initial $\ddot{y}_i(t_1)$ for the first half

interval and constant equal to the terminal value a_2 for the second half interval. If $\beta = \frac{1}{6}$, a linear variation of acceleration between $\ddot{y}_i(t_1)$ and a_{2i} is assumed. If $\beta = \frac{1}{4}$, a constant acceleration equal to the mean over the interval is assumed. In general, a simple kinematical interpretation is not possible for arbitrary values of β.

Two questions relating to this stepwise trial and error integration are the choice of the time step h and the question of convergence. If the variable y_i has a period T_i, h must certainly be less than T. With the special kinematic interpretations for $\beta = \frac{1}{8}, \frac{1}{6}, \frac{1}{4}$, one could expect that $h < \frac{T}{4}$, since it is difficult to approximate, e.g. a sine curve by a straight line over an angle larger than $\frac{\pi}{2}$. Newmark gives convergence limits, which depend on β, varying from $h < 0.551T$ for $\beta = \frac{1}{12}$ to $h < 0.381T$ for $\beta = \frac{1}{4}$. These values allow $h > \frac{T}{4}$.

The question of convergence has two aspects: whether the procedure will converge at all and, if it converges, whether it will converge to a correct result. The latter is not an obvious consequence of the former. Correct here means that the computed state at t_2 is the same as would be obtained by an exact integration of the equations of motion, if this were possible.

As an example, consider the equation for y(t):

$$y'' + y = 1; \quad y(0) = y'(0) = 0$$

The exact solution is y=1-cost. We compare this exact solution for the time interval 0 to $\pi/2$ with the result of using Newmark's procedure. The exact values are $y(\pi/2)=1$, $y'(\pi/2)=1$, $y''(\pi/2)=0$, $y''(0)=1$.

We take $\gamma=1/2$, $\beta=1/6$. Assume $a_2=y''(\pi/2)=0$. From (6.2.2) we get

$$v_2 = 0.875 \sim y'(\pi/2) = 1.0$$

$$u_2 = 0.822 \sim y(\pi/2) = 1.0$$

From the differential equation we get the derived acceleration.

$$a_2' = 1-u_2 = 0.178 \sim y''(\pi/2) = 0.$$

Thus, when the correct value $\ddot{y}(\pi/2)$ is taken for a_2, the derived state becomes different from the correct, when the step size is T/4. The process eventually converges to $v_2=0.884$, $u_2=0.874$, $a_2'=0.126$ after about six iterations.

This example points out a possible deficiency of Newmark's method, that convergence may be obtained, but to a wrong result if the step size becomes too large. The reason for this may be attributed to the nature of the kinematical relations (6.2.2), which attempts to approximate a curved acceleration curve by straight lines.

A slightly different approach is used by Argyris and Chan [27] and Argyris et al. [28]. They assume explicitly

that the acceleration can be approximated by a third degree polynomial in time and consequently the displacement becomes a fifth degree polynomial. A trial and error iteration process is employed to determine the state at the end of the time step. The kinematics here seems clearer than in Newmark's method.

6.3 The Present Method.

For problems of cable dynamics, like other dynamical systems, there is usually some characteristic period T_c for variations of the state. If the cable is being peridically excited, for example by the forced motion of its upper end, the excitation period will be the characteristic period when the system has reached a steady state of oscillation. If the cable is executing natural motion, in general all modes are excited. But each mode contributes different amounts to the total motion, and usually there will be one or more modes which dominate the motion. In this case the period of the lowest significant mode will represent the characteristic period.

In the previous finite element model for the cable, the tension variations are computed from the cable elongations,

which are again determined by the displacements of the longitudinal modes. These will normally have low natural periods compared to the transverse modes and the excitation periods. It was considered useful to have a method of integration, which allowed the use of time steps larger than some of the natural periods in the system. We hence tried to develop an integration method allowing this. It was intended that this method should be applicable under non-steady, i.e. transient, conditions.

The essential features of the method developed can be summarized as follows: It is assumed that there is some characteristic period T_c for variation of the significant contributions to the state of the system and hence also for the forces on the system. Choose a time step h much smaller than T_c, say $h<\frac{T_c}{16}$. h must be such that it is legitimate to assume that the forces on the system, i.e. $\underline{F}$ in (5.5.1), f_i in (5.5.2b) or f_i' in (5.6.1), have a linear variation in the interval. Based on a known initial condition at t_1, the solution is proceeded to $t_2=t_1+h$, by solving the differential equations (5.5.2b) or (5.6.1) exactly with linear right hand side, i.e. as a sum of a homogeneous and a particular solution. A systematic trial and error process is done for the final state, until a satisfactory agreement is found. This trial and error process is similar to Newmark's method. The present approach differs

from Newmark's in assuming a linear variation of forces instead of certain variations for the accelerations.

Assume known the dynamic state at t_1, i.e. displacements $y_i(t_1)$, velocities $\dot{y}_i(t_1)$ and accelerations $\ddot{y}_i(t_1)$. Together with knowledge of the water parameters V, we can compute the forces $f_i'(t_1)$ in (5.6.1). We now make a guess as to the forces on the system at t_2, i.e. $\phi_{i2} \sim f_i'(t_2)$. Then we assume the linear distribution

$$(\alpha) \qquad f_i'(t) = \alpha_i+\beta_i t; \quad t_1 \leq t \leq t_2$$

where $\alpha_i=f_i'(t_1)$, $\beta_i=(\phi_{i2}-f_i'(t_1))/h$. With these expressions for f_i', the eqs. (5.6.1) become decoupled. We solve each equation by writing $y_i(t)$ as a sum of a particular, $y_{ip}(t)$, and a homogeneous, $y_{ih}(t)$ solution:

$$y_i(t) = y_{ip}(t)+y_{ih}(t); \quad t_1 \leq t \leq t_2.$$

The general solutions of the homogeneous equations are

$$(6.3.1) \quad y_{ih}(t) = e^{-\frac{c_i}{2}\tau}(A_i\cos\omega_i\tau+B_i\sin\omega_i\tau) \quad \text{if } \lambda_i > \frac{c_i}{r}$$

$$= e^{-\frac{c_i}{2}\tau}(A_i+B_i\tau) \quad \text{if } \lambda_i = \frac{c_i}{4}$$

$$= e^{-\frac{c_i}{2}\tau}(A_i e^{\omega_i\tau}+B_i e^{-\omega_i\tau}) \quad \text{if } \lambda_i < \frac{c_i}{4}$$

where $\tau = t - t_1$,

$$\omega_i = (\lambda_i - \frac{c_i^2}{4})^{1/2} \quad \text{if } \lambda_i > \frac{c_i^2}{4}$$

$$= (\frac{c_i^2}{4} - \lambda_i)^{1/2} \quad \text{if } \lambda_i < \frac{c_i^2}{4} .$$

A_i, B_i are integration constants, determined by initial conditions at t_1.

The particular solutions are of the form:

$$y_{ip}(t) = a_i + b_i \tau$$

where $$a_i = \frac{1}{\lambda_i}(\alpha_i - c_i \frac{\beta_i}{\lambda_i}), \quad b_i = \frac{\beta_i}{\lambda_i} .$$

The constants A_i, B_i are determined from the initial conditions at t_1. With these relations we can estimate the state at t_2 and also the forces $\phi'_{i2} \sim f'_i(t_2)$. Comparing ϕ'_{i2} with the assumed ϕ_{i2}, we can determine if the approximation is sufficiently close. If not, we can repeat the calculation with the new $\phi_{i2} = \phi'_{i2}$, until sufficient agreement is reached.

An alternative approach is to repeat the calculation with $f'_i(t_2) = \phi_{i2}$ and then compare the new state with the previous calculation. When two successive calculations are sufficiently close, we can assume that the best accuracy has been obtained and terminate the calculation for the time step. This convergence must be obtained in all (or at least in some representative selection) modes. The final state

is the estimated state at time t_2 and the initial state for the next step.

Instead of using the linear interpolation (α) for $f_i'(t)$, it is possible to use higher degree interpolation polynomia's. E.g. if the time derivative of f_i' is known at t_1 and t_2, a third degree polynomial can be constructed. Some improvement in accuracy may be obtained by this.

CHAPTER 7. Computer Program.

A computer program based on the previous theory for dynamic analysis was made for the IBM360/168 computer of MIT's Information Processing Center. The program is experimental in the sense that it was designed to obtain a first assessment of what can be obtained by application of the finite element method, rather than trying to fully explore all possible applications.

The program was designed for analysis of a two-dimensional configuration. As boundary conditions, the cable was assumed to be fixed at the lower end, while the upper end was assumed to have a given displacement as function of time. The current may be given an arbitrary distribution in the vertical direction. The number of normal modes included is specified as input, but experience indicated that the best results were obtained when all modes were included. The elongation and tension changes are represented by the longitudinal modes, so at least some of the longitudinal modes must be included. Little advantage in computing time is gained by using less than all modes.

Fig. 7.1 shows a macro flow chart of the main computation steps and Fig. 7.2 is a flow-chart outlining the computations involved in the stepwise, iterative time integration. The time integration method is outlined in Sec. 6.3. In

Appendix A we give the listing of the FORTRAN MAIN program and the subroutine TIMINT, which controls the time integration. These two are the essential parts of the program. Other subroutines are concerned with reading data, performing matrix operations or calculating forces according to Sec. 2.3.

The program utilizes IBM library subroutines for the general eigenvalue problem (5.4.1). These routines use the method of triangular decomposition (Cholesky) together with Householder tri-diagonalisation to determine the eigenvalues and eigenvectors.

In constructing the program, it was found convenient to transform the global description of the displacements from cartesian x,y coordinates to local intrinsic t,n coordinates, according to Sec. 2.1. This facilitated the interpretation of output when results were referenced to the t,n directions. However, this feature is not essential to the method.

Input data consist of element properties, environment properties and specification of the displacement of the upper end as a function of time at discrete instants, t_i. The element properties are equilibrium nodal coordinates, cross sectional area, tension, elastic modulus, density, drag and mass coefficients and internal viscous coefficient.

The environmental data consist of water density and current distribution. For the upper end, displacement, velocity and acceleration are specified at instants t_i.

No parameters of the system are given a priori values in the program, and hence any consistent set of units can be used.

Certain simplifications were made in the program, compared to the previous theory. In particular, the variations of some force contributions from their equilibrium values were assumed of only minor significance and not taken into account. Referring to eq. (5.2.1), the forces $\Delta\underline{F}_T$ and $\Delta\underline{F}_B$ were not included. Further, the effects of water acceleration were not included, so $\underline{F}_A=\underline{0}$.

To estimate the consumption of computer time, a typical long run is reported. A cable with 10 elements and 18 degrees of freedom (Sec. 8.5) was analysed for a simulated real time of 70 sec, with a time step mostly of 0.25 sec. The total number of steps was 286. Total IBM 360/168 CPU time was 0.361 min and total cost was $9.86.

Average cost per step: 3.6 c/step.

CPU/real time ratio: 0.309

Average cost per real time second: 14.1 c/sec

Some features which were not included in the present version, can be recommended for expanding the program into a workable design program.

1) To incorporate a statical analysis prior to the dynamical analysis may be advantageous, particularly if there are strong currents.
2) To take into account the effect of waves in modifying the current distribution will give a more realistic representation of the interaction between cable and water.
3) It may be advantageous to allow a more complicated topology than the single cable assumed here, i.e. to be able to model cable nets or complete mooring systems involving several mooring lines.
4) The program does not take into account the variations of element parameters which occur in the real system, e.g. variations of cross section A with strain, of drag coefficients C_D with relative velocity or a non-linear elastic tension-strain relation. If laws for such variations are known, one can incorporate such features into the program.
5) It should be possible to include the effect of cable resting on the bottom. This may possibly be done by having a spring or spring/damper to represent the bottom boundary condition.

Macro flow chart program DYNLIN.

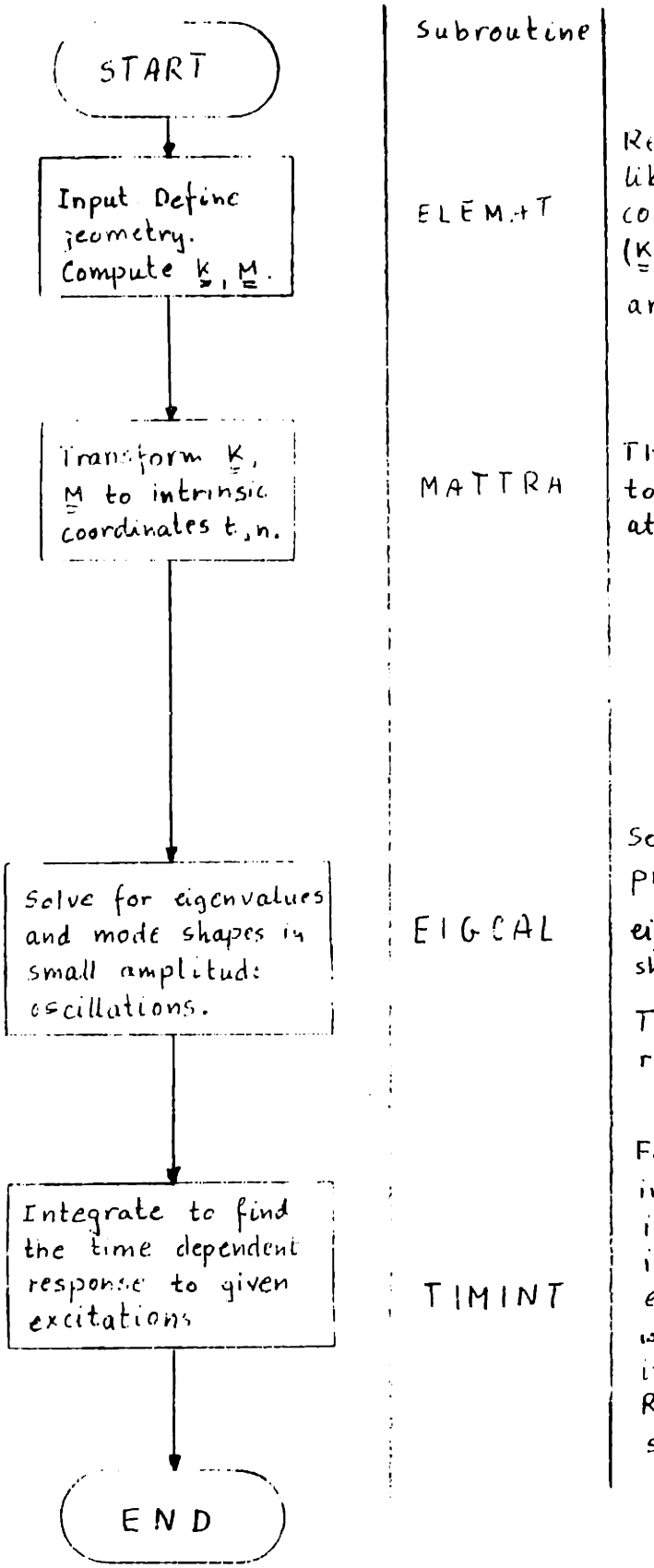

Subroutine	Comment.
ELEMAT	Reading data on the equilibrium configuration and computing the stiffness ($\underline{\underline{K}}$) and mass ($\underline{\underline{M}}$) matrices are done in one operation.
MATTRA	The system is transformed to local t, n coordinates at each node.
EIGCAL	Solving the eigenvalue problem $(\underline{\underline{K}} - \omega^2 \underline{\underline{M}})\underline{q} = 0$, the eigenvalues ω_i^2 and mode shapes $\underline{q}_i$ are determined. The $\underline{q}_i$ are expressed relative to t, n directions
TIMINT	For given excitation, specified in input, the dynamic response is calculated. At $t = 0$, the initial condition is rest in equilibrium. The calculation is stepwise in time and iterative for each step. Results are printed. See special flow chart for TIMINT.

Fig. 7.1.1

Macro Flow Chart Program DYNLIN

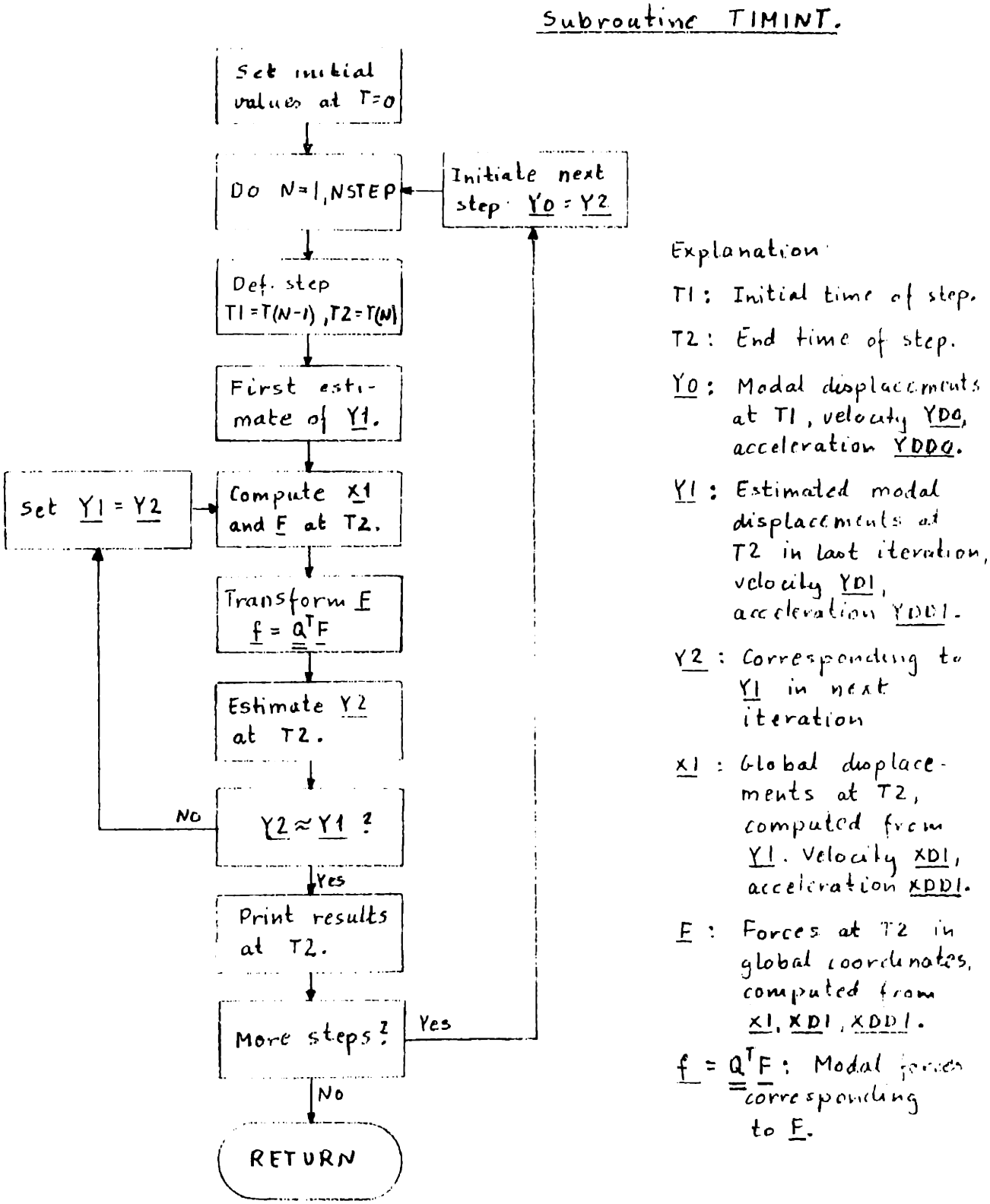

Fig. 7.1.2

Flow Chart Subroutine TIMINT

CHAPTER 8. Calculation Examples.

In this chapter, we give some calculation examples made with DYNLIN.

Sec. 8.1 Natural vibration of vertical cable in air suspended in one end.

Sec. 8.2 Propagation of an undamped, transverse wave on a straight string.

Sec. 8.3 Dynamic response of an initially straight cable, when a current is suddenly applied at t=0.

Sec. 8.4 Propagation of a transverse wave with damping.

Sec. 8.5 Analysis of mooring cables under forced excitation of the upper end.

The first four examples are of a theoretical nature, for which analytical solutions can be used for comparison. The last example simulates the case of mooring cable on a large vehicle.

8.1 Natural Vibrations of Cable Suspended in One End.

The case of a hanging chain or cable can be analyzed theoretically ([1],[5]), to compare with the finite element calculations. Consider a cable in air of weight density w per unit length. The cable length is L. Let coordinate s be measured vertically downwards, and let the transverse displacement be y(s,t), while the longitudinal displacements are assumed negligible. The tension at x is R(s)=w(L-s). For the transverse motion we can formulate the differential equation:

$$\frac{\partial^2 y}{\partial t^2} = \frac{1}{m}\frac{\partial}{\partial s}\left(R\,\frac{\partial y}{\partial s}\right),$$

where m=w/g is the mass per unit length. Expanding the right hand side gives

$$\frac{1}{m}\left[R\,\frac{\partial^2 y}{\partial s^2} + w\,\frac{\partial y}{\partial s}\right]$$

Introduce the new variable ξ by $\xi^2=L-s$. The differential equation is then transformed to:

$$\frac{\partial^2 y}{\partial t^2} = \frac{g}{4}\left(\frac{\partial^2 y}{\partial \xi^2} + \frac{1}{\xi}\,\frac{\partial y}{\partial \xi}\right)$$

Assume harmonic, free motion of angular frequency $\omega=pc$,

$$y(\xi,t) = u(\xi)\sin pct,$$

where $c^2=g/4$, p is the frequency factor.

Substitute

$$\frac{d^2u}{d\xi^2} + \frac{1}{\xi}\frac{du}{d\xi} + p^2u = 0$$

The solution of this Bessel equation which is finite at $\xi=0$ (s=L) is:

$$u(\xi)=CJ_o(p\xi)$$

where J_o is the zero order Bessel function. The frequency factor p is determined by $u|_{s=0} = 0$, i.e.

$$J_o(p\sqrt{L}) = 0$$

This gives the following expressions for the four lowest values of p [6]:

$$p\sqrt{L} = 2.4048,\ 5.5201,\ 8.6537,\ 11.7915,$$

where the right hand numbers are the zeroes at J_o.

The model analyzed has L=1000 m. Substituting this, we find for the four lowest natural modes, where the frequency is given by $f=pc/2\pi$:

$$f_1 = 1.895\cdot10^{-2}\ \text{Hz}$$

$$f_2 = 4.351\cdot10^{-2}\ \text{Hz}$$

$$f_3 = 6.821\cdot10^{-2}\ \text{Hz}$$

$$f_4 = 9.294\cdot10^{-2}\ \text{Hz}\ ,$$

For modes higher than the first, there are other zeroes than at s=0. These are given by

$$J_o(p_i \xi_o)=0 \qquad i=2,3,4,...$$

i.e.

$$p_i \xi_o = 2.4048,\ 5.5201,\ 8.6537,\ 11,7915,\ ....$$

To analyze the same system with the finite element method, several models were used, differing in element definition, as shown in Fig. 8.1.1. Models I, II and III have ten elements, model IV has five elements.

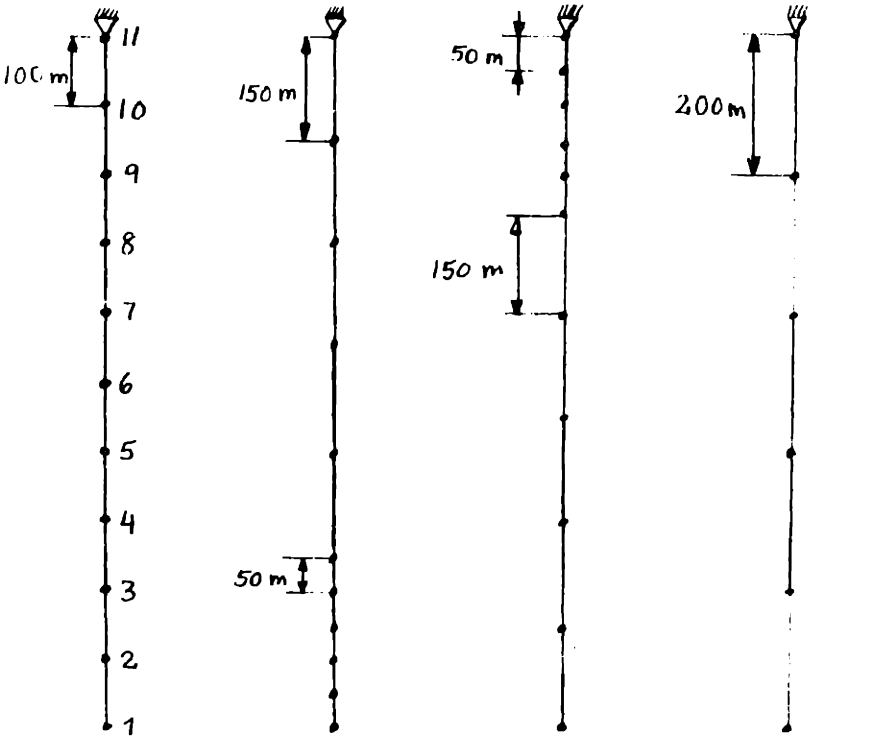

Fig. 8.1.1

Finite Element Models

The cable data are:

Cable length: $L=1000$ m

Cross section area: $A=1\ cm^2$

Density: $\rho_c = 7.8 \cdot 10^3 \frac{kp}{m^3}$

Weight per unit length: $w=1.78 \frac{kp}{m}$

Gravity acceleration: $g=9.81 \frac{m}{s^2}$

Table 8.1.1 compares the natural frequencies for the four lowest modes from the analytical solution and the four finite element models.

NATURAL FREQUENCIES IN HZ.

Mode	Analytical	Model I	Model II	Model III	Model IV
1	$1.895 \cdot 10^{-2}$	$1.896 \cdot 10^{-2}$	$1.897 \cdot 10^{-2}$	$1.896 \cdot 10^{-2}$	$1.898 \cdot 10^{-2}$
2	$4.351 \cdot 10^{-2}$	$4.393 \cdot 10^{-2}$	$4.404 \cdot 10^{-2}$	$4.441 \cdot 10^{-2}$	$4.504 \cdot 10^{-2}$
3	$6.821 \cdot 10^{-2}$	$7.069 \cdot 10^{-2}$	$6.976 \cdot 10^{-2}$	$7.313 \cdot 10^{-2}$	$7.644 \cdot 10^{-2}$
4	$9.294 \cdot 10^{-2}$	$10.03 \cdot 10^{-2}$	$9.865 \cdot 10^{-2}$	$10.67 \cdot 10^{-2}$	$11.76 \cdot 10^{-2}$

TABLE 8.1.1

It is seen that all models give good results for the first mode. Model I gives the best approximation to mode 2, while model II gives the best approximation to modes 3 and 4. The latter observation is as expected, since the shorter

elements in the lower part can better represent the larger curvatures which occur. Naturally, model IV is inferior to the three others.

In Fig. 8.1.2 are sketched the calculated mode shapes for model I. The analytical mode shapes are also shown for comparison. The difference becomes appreciable only for modes 3 and 4. In Table 8.1.2 is a comparison of the zeroes apart from S=0 in the analytical model and model I. S_o^i is the i'th zero measured from the upper end, measured in length unit meter.

POSITION OF ZEROES OF MODEL I AND ANALYTICAL SOLUTION

Mode	2		3		4	
	Analytic	Model I	Analytic	Model I	Analytic	Model I
S_o^1	810.2	809	593.1	581	461.4	439
S_o^2			922.8	917	780.8	755
S_o^3					958.4	942

TABLE 8.1.2

Natural mode shapes of hanging cable.

Finite element model I and analytic solution.

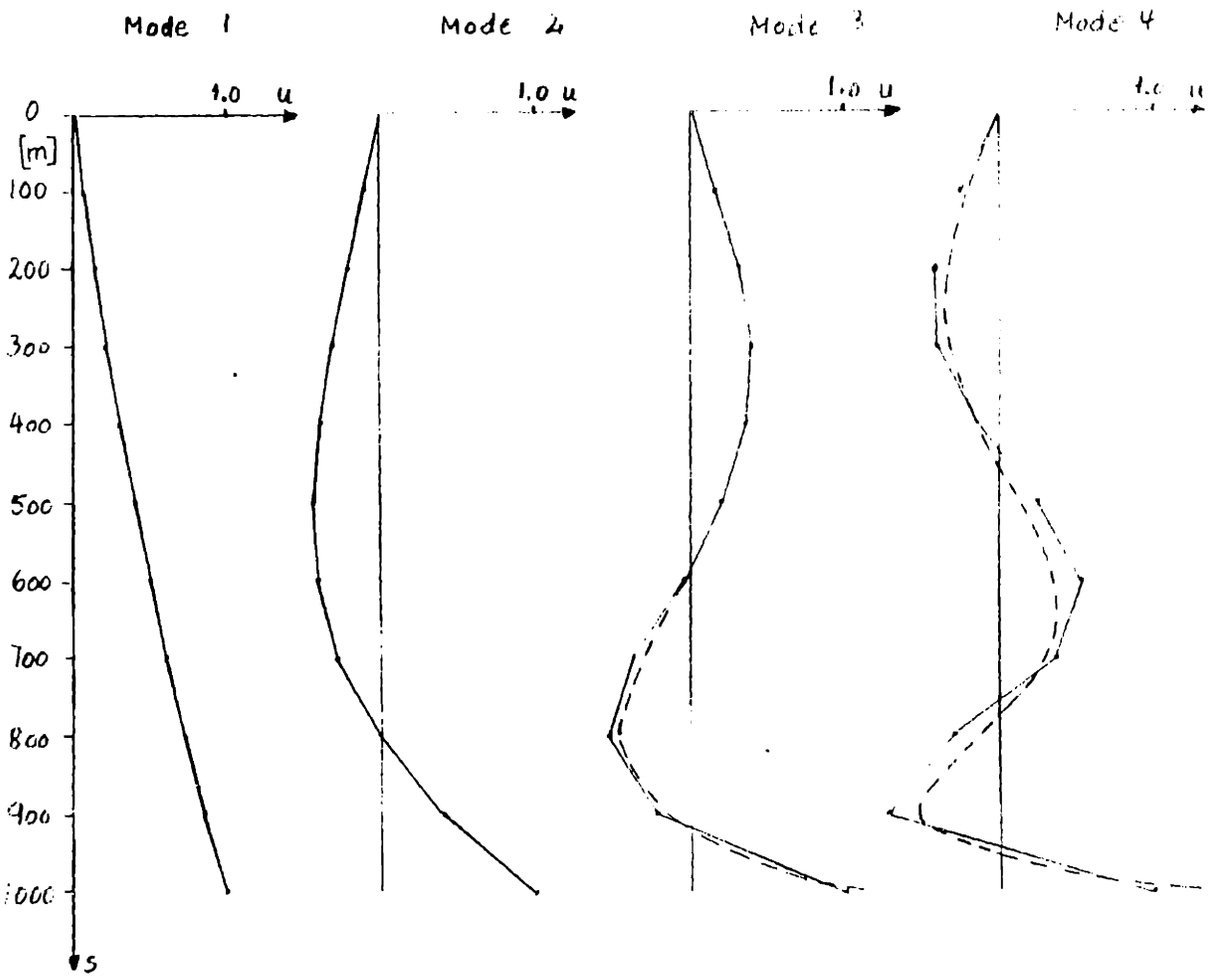

——— Model I

– – – – Analytic solution

Fig. 8.1.2

Natural Mode Shapes of Model I

and Analytic Solution

8.2 Transverse Waves on a Straight String.

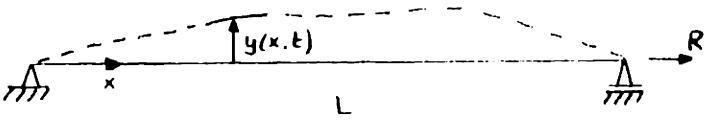

Fig. 8.2.1

Taut, Straight String

For a straight string of length L with constant tension R, the differential equation for small transverse displacements y(x,t) and no external force is the wave equation

$$\frac{\partial^2 y}{\partial x^2} - \frac{1}{c^2}\frac{\partial^2 y}{\partial t^2} = 0,$$

where $c = (\frac{R}{m})^{1/2}$ is the transverse wave velocity,

m is the mass per unit length.

It is here assumed for simplicity that the string is vibrating in air. A solution can be found by separation of variables; satisfying y(0,t)=y(L,t)=0:

$$y(x,t) = \sum_{n=1}^{\infty} \sin k_n x(A_n \cos \omega_n t + B_n \sin \omega_n t)$$

where $k_n = \frac{n\pi}{L}$, $\omega_n = ck_n$, A_n, B_n are constants to be determined from the initial conditions. The ω_n are the natural frequencies

of the string, with corresponding mode shapes $\sin k_n x$.

The initial conditions at t=0 are given displacements and velocities, $y(x,0)=u(x)$, $\frac{\partial y}{\partial t}(x,0)=v(x)$. Hence we find the coefficients A_n, B_n:

$$A_n = \frac{2}{L}\int_0^L u(x)\sin k_n x \, d_x$$

$$B_n = \frac{2}{\omega_n L}\int_0^L v(x)\sin k_n x \, dx$$

If initially the string is at rest, $v(x)=0$ and $B_n=0$. In this case we can write for $y(x,t)$:

$$(8.2.1) \qquad y(x,t) = \sum_{n=1}^{\infty} A_n \sin k_n x \cos \omega_n t$$

$$= \frac{1}{2}\sum_{n=1}^{\infty} A_n(\sin(k_n x+\omega_n t)+\sin(k_n x-\omega_n t))$$

This shows that the initial shape u(x) is separated into two waves of equal amplitude, moving in respectively negative and positive directions.

We choose as initial condition a half sine wave situated symmetrically about $x=\frac{L}{2}$ and of half wave length a:

$$u(x) = \beta \sin \frac{\pi}{a}(x-\frac{L-a}{a}); \quad \frac{L-a}{2} \leq x \leq \frac{L+a}{2}$$

$$= 0 \qquad ; \text{otherwise,}$$

where β is the amplitude. The coefficients A_n are:

$$A_n = -\frac{4\beta}{L}\frac{1}{\pi a}\frac{1}{(\frac{n}{L})^2-(\frac{1}{a})^2}\sin\frac{n\pi}{2}\cos\frac{n\pi a}{2L} \quad ; \text{ if } \frac{n}{L} \neq \frac{1}{a} .$$

A finite element model with 11 elements, L=1000 m, R=20000 kp was analyzed for comparison with the analytical solution. The model, with imposed initial displacement, is sketched in Fig. 8.2.2. The analytical initial condition

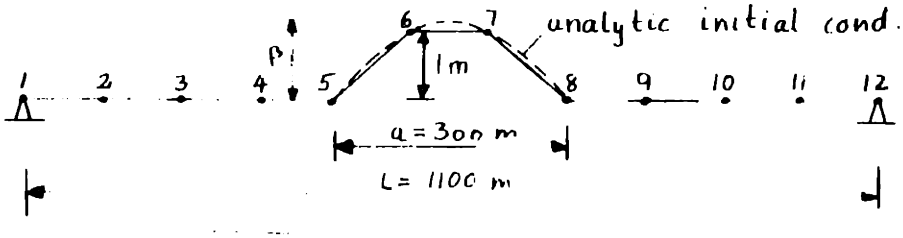

Fig. 8.2.2

Initial Conditions

is also shown for comparison. The half wave length of the sinusoidal initial condition is a=300 m, the initial transverse displacement of nodes 6 and 7 are 1 m, and the corresponding amplitude of the analytical initial condition is $\beta = (\sin\frac{\pi}{6})^{-1}$. The string has a weight per unit length $mg = 3.12\ kpm^{-1}$.

In Table 8.2.1 are listed the calculated eigenfrequencies ν_i [rad s^{-1}] for the finite element model and the analytical frequencies ω_i.

i	1	2	3	4	5	6	7	8	9	10
ν_i	0.719	1.452	2.215	3.022	3.886	4.818	5.807	6.813	7.743	8.429
ω_i	0.716	1.432	2.149	2.865	3.581	4.297	5.013	5.730	6.446	7.162

TABLE 8.2.1

It is seen that the ν_i are fairly close to ω_i for the lower modes but the differences become larger for the higher modes. The mode shapes fit fairly well the theoretical sinusiuds, and are not shown.

To transform the initial condition to normal coordinates, we use the results of Sec. 5.4. If the vector $\underline{v}(t)$ represents the transverse nodal displacements, we have $v_6(0)=v_7(0)=1$ and all other components of $\underline{v}(0)$ are zero.

If the matrix $\underline{\underline{Q}}$ is the matrix of eigenvectors, we have according to (5.4.3) for the initial modal displacements $\underline{y}(0)$:

$$\underline{y}(0) = \underline{\underline{MQ}}\underline{v}(0)$$

Since we have assumed the string is vibrating in air, there is no damping, so that the equations of motion (5.5.2b)

are homogeneous, uncoupled single degree of freedom equations. Hence for each transverse mode we may write

$$y_i(t) = y_i(0) \cos \nu_i t \quad ; \; i=1,2,\ldots 10,$$

and the total time evolution for the transverse displacement $v_j(t)$ of node j is:

$$(8.2.2) \qquad v_j(t) = \sum_{i=1}^{10} Q_{ji} y_i(0) \cos \nu_i t;$$

where Q_{ji} is the transverse displacement of node j in mode i. This equation is similar to (8.2.1) for the analytical solution, when it is taken into account that Q_{ji}, for fixed i and variable j, represents the i'th eigenvector, which is approximately of the form $\sin k_i x$. The frequencies ν_i are generally different from the ω_i, and there are finitely many modes for the finite element model but infinitely many for the analytical model.

Numerical calculations were done for three cases:

a) The finite element model, using the computer program

b) The analytical model (8.2.1) using 10 modes

c) The analytical mode, using 100 modes.

c) is assumed to represent the analytical solution with sufficient accuracy. The differences between b) and c) were usually small, so that only the results of c) are reported. The comparison between a) and c) is shown in

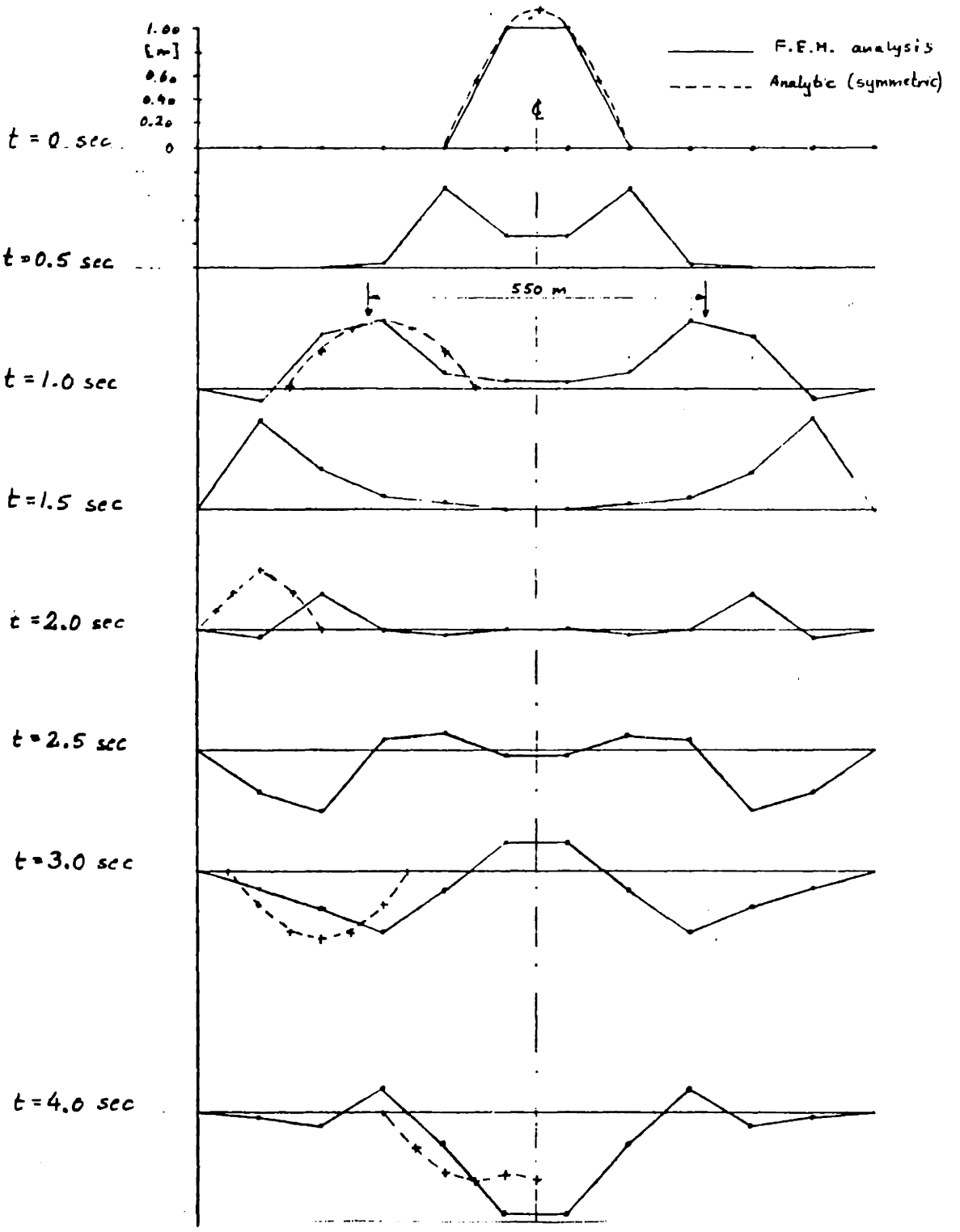

Fig. 8.2.3a

String Shape as Function of Time

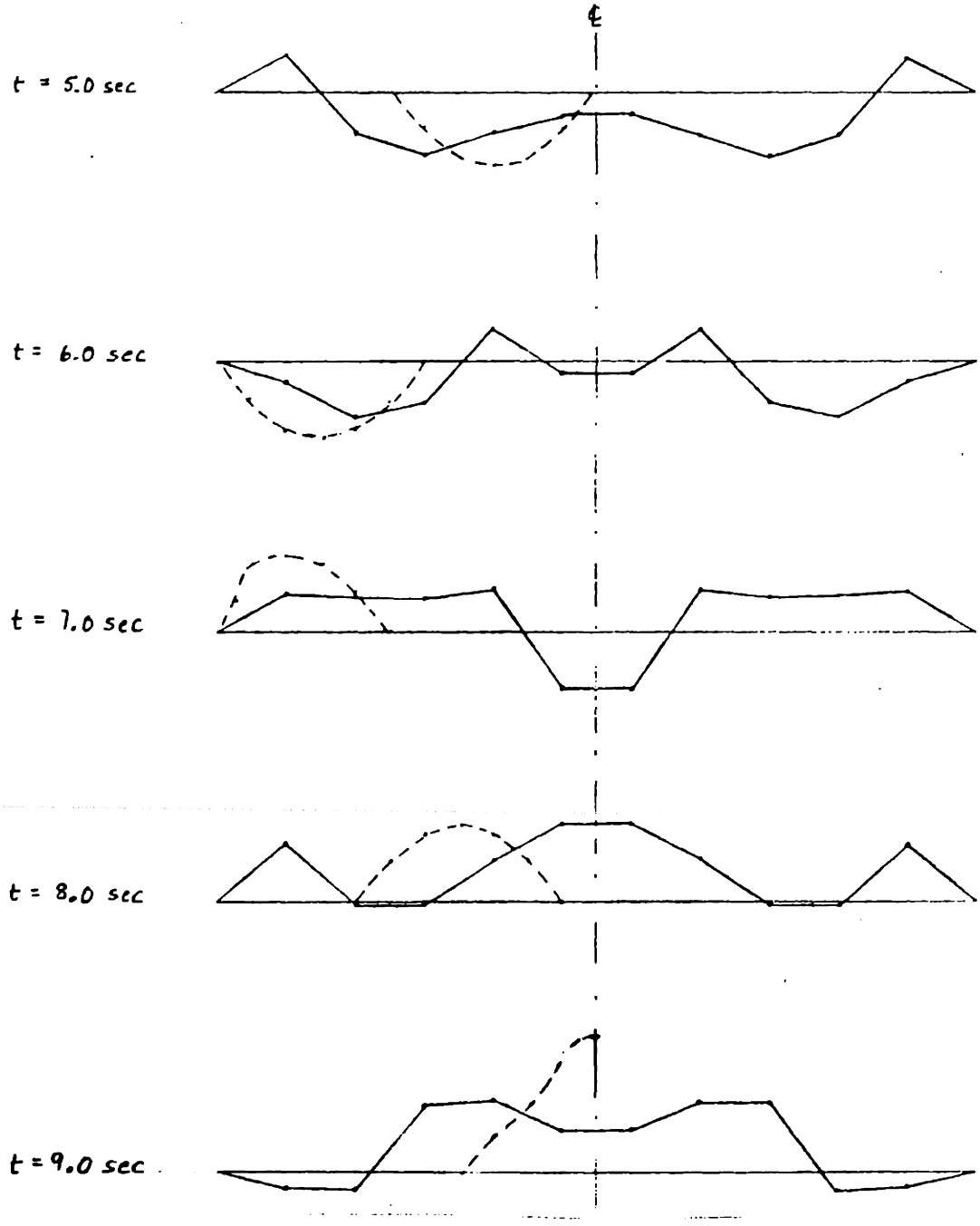

Fig. 8.2.3b

String Shape as Function of Time

Fig. 8.2.3. It is seen that, for the first 3-4 seconds, the analytical shape of the can be recognized in the finite element results, for longer times the f.e.m. results becomes diffused compared to the analytical solution.

From the shape at t=1.0 sec, we can estimate a distance between peaks of 550 m, corresponding to a wave velocity of 275 ms^{-1}. The analytical wave velocity is $c=(R/m)^{1/2}=250\ ms^{-1}$, i.e. a difference of 10%.

We believe that the basic reason for the difference between the analytical and f.e.m. results is the difference in eigenfrequencies ω_i and ν_i. Hence, if one used a finite element model with 110 elements instead of 11, one could expect the f.e.m. calculation to represent the 10 first eigenfrequencies with almost the same accuracy as the present model represents the first frequency. In that case a much better correspondence with the analytical solution would be expected, since by using 10 modes, we essentially repeat calculation b), which was found to correspond well with c).

8.3 Response of a Taut String with Current Suddenly Applied at t=0.

Consider a straight string of length L under constant tension R^o. The two ends are assumed fixed, Fig. 8.3.1a.

Fig. 8.2.3. It is seen that, for the first 3-4 seconds, the analytical shape of the can be recognized in the finite element results, for longer times the f.e.m. results become diffused compared to the analytical solution.

From the shape at t=1.0 sec, we can estimate a distance between peaks of 550 m, corresponding to a wave velocity of 275 ms^{-1}. The analytical wave velocity is $c=(R/m)^{1/2}=250\ ms^{-1}$, i.e. a difference of 10%.

We believe that the basic reason for the difference between the analytical and f.e.m. results is the difference in eigenfrequencies ω_i and ν_i. Hence, if one used a finite element model with 110 elements instead of 11, one could expect the f.e.m. calculation to represent the 10 first eigenfrequencies with almost the same accuracy as the present model represents the first. In that case a much better correspondence with the analytical solution would be expected, since by using 10 modes, we essentially repeat calculation b), which was found to correspond well with c).

8.3 Response of a Taut String with Current Suddenly Applied at t=0.

Consider a straight string of length L under constant tension R^o. The two ends are assumed fixed, Fig. 8.3.1a.

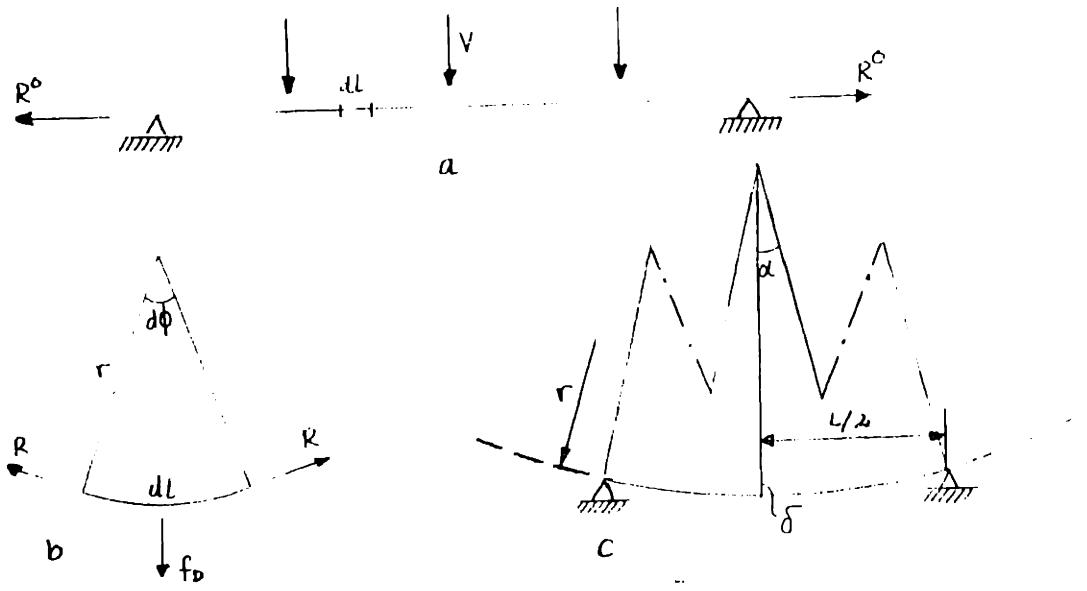

Fig. 8.3.1

String in Homogeneous Current

For times t<0, the current of the surrounding water is zero. At t=0 a homogeneous current of velocity V is suddenly applied normal to the string. It is required to analyze the subsequent motion of the string to a new equilibrium configuration under the drag force, see Fig. 8.3.1c.

When the string is essentially normal to the current, the drag force per unit length is given by

$$f_D = \frac{1}{2} \rho_W C_D d V^2,$$

where ρ_W is the water density, C_D is the drag coefficient, d is the diameter. For small displacements, we find from Fig. 8.3.1b in the new equilibrium:

$$r = \frac{d\ell}{d\phi} = \frac{R}{f_D} .$$

where r is the radius of curvature, which is assumed constant. Hence, from Fig. 8.3.1c, the angle α spanned by one half of the string length is

$$\sin\alpha = \frac{L}{2r}$$

and the transverse displacement of the midpoint m is:

$$\delta = r(1-\cos\alpha)$$

The elongation of the string from the first to the second equilibrium is

$$\Delta L = 2r(\alpha-\sin\alpha)$$

Following this elongation, we get an additional elastic tension:

$$\Delta R = \frac{\Delta L}{L} EA$$

where E is the elastic modulus, A is the cross section area.

A first approximation to δ can be found by assuming that R does not change, i.e. $R=R^{o}$. In this case δ can be computed directly from the above formulas. A better approximation is found by taking into account the change of tension R. In this case δ cannot be computed directly from the above formulae, so some iterations must be made to arrive at a consistent result.

The computer program was used to simulate dynamically the evolution from the first equilibrium to the second under both the above assumptions. The following data were used:

$$L = 1000 \text{ m}$$

$$V = 1 \text{ ms}^{-1}$$

$$C_D = 1.4$$

$$A = 4.54 \cdot 10^{-3} \text{m}^2$$

$$d = 7.60 \cdot 10^{-2} \text{m}$$

$$E = 5.12 \cdot 10^{9} \text{kpm}^{-2}$$

$$R^O = 100{,}000 \text{ kp}$$

Under constant tension the above formulae give the displacement $\delta_1 = 6.780$ m. Taking into account the variable tension, we get $\delta_2 = 6.602$ m and the additional tension is $\Delta R_2 = 2700$ kp.

The finite element model was constructed with 10 elements of equal length. In Fig. 8.3.2 are sketched the time evolution of the modal coordinates y_i; i=1,3,5,7,9 and the displacement of the string midpoint m(node 6), under the first calculation alternative ($R=R^O$). Due to the symmetry, the responses in modes 2,4,6,8 are vanishing. For the second calculation alternative the time evolution was similar, except for different limiting values.

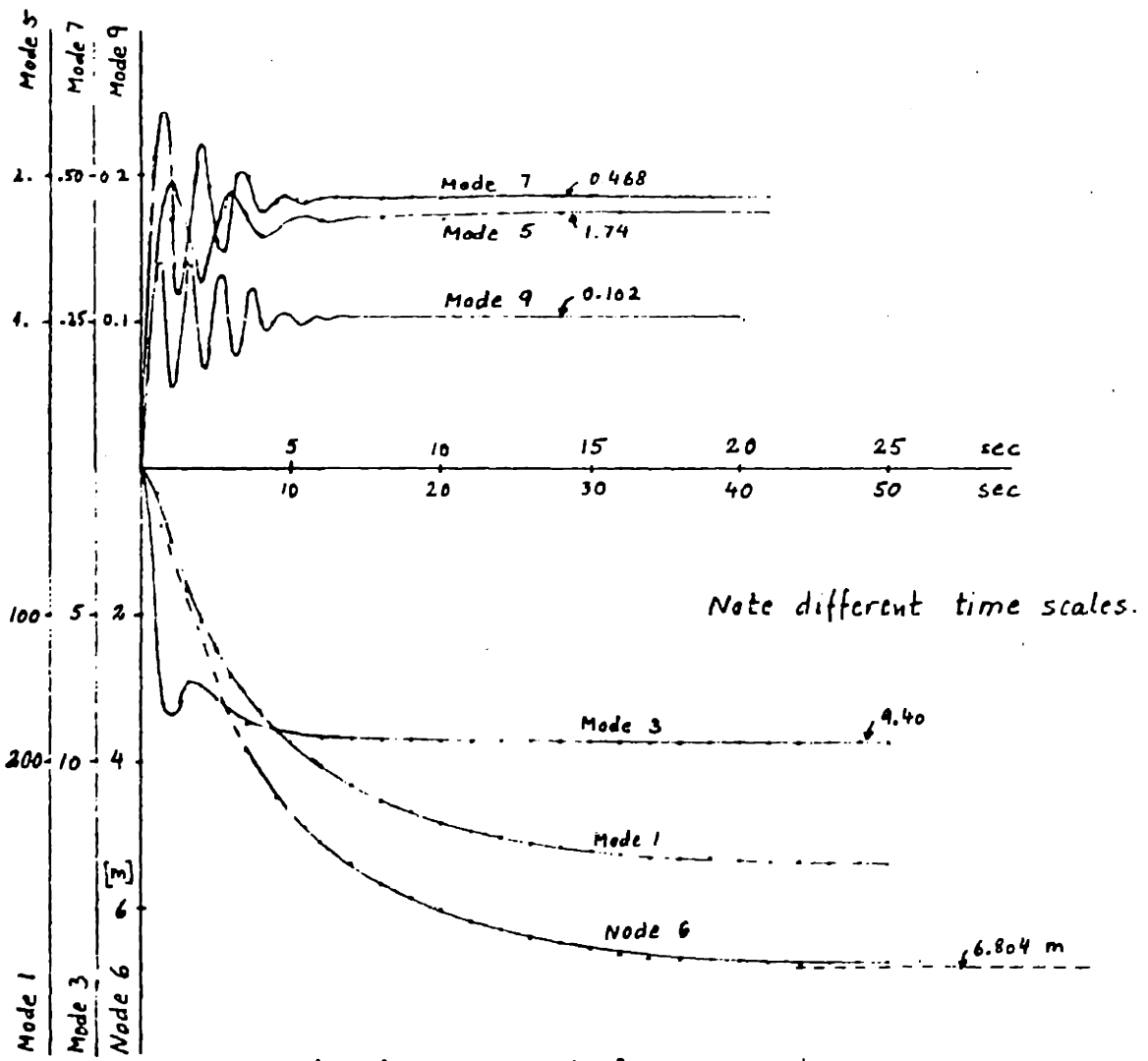

Fig. 8.3.2

Modal and Midpoint Response

It appears that mode 1 behaves like an overcritically damped degree of freedom, while the higher modes execute several oscillations before settling down to constant values. The midpoint displacement also behaves in an overcritical manner, which is a natural consequence of mode 1 giving the largest contribution to this displacement.

After the 50 second segment for which the calculation was carried out, the midpoint displacement had not completely reached an equilibrium state. Trying to extrapolate the computed results, we assume that the midpoint displacement δ follows the exponential law:

$$\delta = a(1-e^{-kt})$$

where a is the asymptotic displacement and k is a time factor. We estimated a and k from the calculated data at four times 35,40,45,50 sec.

For the first calculation ($R=R^{O}$=const.) the result was $k_1=0.09527s^{-1}$and $a_1 = 6.804$ m. This value of a_1 compares fairly well with the previously calculated value $\delta_1 = 6.780$ m. In the second case (R variable) $k_2=0.10330s^{-1}$ $a_2=6.618$ m. The value of a_2 corresponds fairly well with $\delta_2=6.602$ m.

In the first case only the transverse modes were used and consequently only transverse displacements were taken

into account. The computed additional tension in the final state varied from 7000 kp at the ends to 80 kp in the middle. In the second case both transverse and longitudinal modes were used in the calculation. In this case the additional tension had a fairly even distribution over the string length, e.g. at 50 sec, it varied between 2651 kp and 2655 kp, with an average of 2553 kp. Extrapolating the tension in the same manner as displacement, we estimate a terminal value 2668 kp, with fair correspondence with ΔR_2=2700 kp from the analytical solution.

8.4 Wave Propagation on String with Damping.

Consider a horizontal straight string of length L, mass per unit length m and tension R. We also assume that there is a transverse viscous damping force $-c\dot{y}$, where y is the transverse displacement. The right end (x=L) is assumed to have a forced harmonic motion Asin ωt in the transverse direction, while the left end (x=0) is fixed.

The differential equation for this string is

$$m \frac{\partial^2 y}{\partial t^2} + c \frac{\partial y}{\partial t} - R \frac{\partial^2 y}{\partial x^2} = 0.$$

Dividing through by m and writing c/m=2f, $R/m=v^2$ where v is the wave propagation velocity of the undamped string,

we have the differential equation

$$(8.4.1) \qquad \frac{\partial^2 y}{\partial t^2} + 2f \frac{\partial y}{\partial t} - v^2 \frac{\partial^2 y}{\partial x^2} = 0$$

The boundary conditions to be satisfied are

$$y(0,t) = 0$$

$$y(L,t) = A \sin \omega t$$

As we look for stationary solutions expressing the forced motion, we can assume solutions of the form (see e.g. Routh [5]):

$$y(x,t) = Me^{kx+\alpha t+\gamma}$$

where M, k and α are constants to be determined and γ represents a phase angle. To have the right time dependence at x=L, we must have $\alpha=\pm i\omega$. Substituting into (8.4.1) we get the condition

$$-\omega^2 \pm 2if\omega - v^2k^2 = 0$$

or

$$k^2 \equiv (a+ib)^2 = \frac{-\omega^2 \pm 2if\omega}{v^2} \quad .$$

For the real, a, and imaginary, b, parts of k we have

$$a^2-b^2 = -\frac{\omega^2}{v^2} \quad , \quad ab = \pm f\omega$$

Solving for a^2 and b^2 we find

$$(8.4.2a) \quad a^2 = \frac{\omega^2}{2v^2}\left(\sqrt{1+\frac{4f^2}{\omega^2}}-1\right)$$

$$(8.4.2b) \quad b^2 = \frac{\omega^2}{2v^2}\left(\sqrt{1+\frac{4f^2}{\omega^2}}+1\right)$$

Taking only $\alpha=+i\omega$, we find on substituting into the assumed expression for y:

$$y = Me^{(a+ib)x+i\omega t+i\gamma}$$

or taking only the real parts

$$(8.4.3) \quad y=M_1e^{ax}\cos(\omega t+bx+\gamma_1)+M_2e^{-ax}\cos(\omega t-bx+\gamma_2)$$

where M_1 and M_2 are constants and γ_1 and γ_2 are phase angles. To apply the boundary conditions:

At $x=0$, $y(0,t)=0$, i.e. $M_1+M_2=0$, $\gamma_1=\gamma_2$

At $x=L$, $y(L,t)=A\sin\omega t$.

$$A\sin\omega t = M_1(e^{aL}(\cos\omega t\cos(bL+\gamma_1)-\sin\omega t\sin(bL+\gamma_1)$$
$$- e^{-aL}(\cos\omega t\cos(-bL+\gamma_1)-\sin\omega t\sin(-bL+\gamma_1)))$$

From this it can be shown that M_1 and γ_1 must fulfill the relations (cf. Routh [5]):

$$\tan\gamma \cdot \tan bL = \frac{e^{aL}-e^{-aL}}{e^{aL}+e^{-aL}}$$

$$\left(\frac{A}{M_1}\right)^2 = e^{2aL}+e^{-2aL}-2\cos 2bL.$$

In (8.4.3) the term with $M_1 e^{ax}\cos(\omega t+bx+\gamma_1)$ represents a wave traveling in the negative x-direction and the amplitude $M_1 e^{ax}$ decreases in the propagation direction.

The term $M_1 e^{-ax}\cos(\omega t-bx+\gamma_1)$ is a wave traveling in the positive x-direction, again with decreasing amplitude $M_1 e^{-ax}$ in the propagation direction. With the excitation considered, the positive wave is the reflected wave at x=0 of the negative wave. If the damping is sufficiently large, the amplitude M_1 of the negative wave at x=0, is small compared to $A=e^{aL}M_1$. In this case practically speaking only the negative wave is being propagated while the positive wave becomes negligible.

This problem cannot be exactly simulated with our computer program, since it is based on velocity squared damping in the transverse direction. It would, of course, be possible to include a linear damping contribution in the program, but usually linear damping is not representative of a mooring line, so this feature would not be useful.

However, an approximate simulation can still be made, based on the following reasoning. Let a current V be

applied in the transverse direction. (Fig. 8.4.1). When the transverse velocity of the string is $\dot{y}$, the drag force is proportional to $(V-\dot{y})\,|V-\dot{y}|$. We assume that in equilibrium the string is straight under the current V. Referring to Sec. 8.3, this is not a true equilibrium where tension forces are in balance with the drag forces. However, we can think of some external constant force applied which exactly balances the drag force in equilibrium. This imagined force must be proportional to $-V^2$ and be assumed to act at all times. Then the deviation force due to drag is proportional to $(V-\dot{y})\,|V-\dot{y}|-V^2$. Further assume that $|\dot{y}|<|V|$. Then the forces $(V-\dot{y})\,|V-\dot{y}|$ and V^2 are positive in the direction of V and we may write the deviation force per unit length

$$F_D = \frac{1}{2}\rho_W C_C d((V-\dot{y})^2-V^2) = \frac{1}{2}\rho_W C_D d(-2V\dot{y}+\dot{y}^2),$$

where ρ_W is the water density, C_D is the drag coefficient and d is the string diameter. It is seen that F_D has two contributions, one proportional to $-V\dot{y}$, acting oppositely to $\dot{y}$, and one proportional to $\dot{y}^2$, always in the direction of V. The term proportional to $-V\dot{y}$ has the form of a viscous damping opposing the velocity $\dot{y}$ while the term proportional to $\dot{y}^2$ can be considered as a drift force in the direction of V with time average $\overline{\dot{y}^2}>0$.

The computer program was used to analyze the following problem. A taut cable (string) of length L=1100 m, density $m_o=0.318 kps^2m^{-2}$, tension R=60000 kp, cross section area $4\cdot10^{-4}m^2$, drag coefficient $C_D=1.2$ and immersed in a transverse water current of velocity $V=0.5ms^{-1}$was excited at the right end with displacement $A\sin\omega t$, where A=0.25 m, $\omega=1.257$ rad s^{-1}, i.e. period T=5 sec. The velocity amplitude at the right end was $A\omega=0.31ms^{-1}$, which is less than $V=0.5ms^{-1}$. The element model used 11 elements, each of length $\ell=100$ m. Only the transverse normal modes were used in the calculations. The parameters were adjusted so that the wave became practically completely dampened after traveling from the right end to the left, and hence the reflected wave at x=0 is negligible.

Starting from rest, the analysis was done for a period of 40 sec. The system seemed to reach a steady state after about 20 sec, after which time the displacements were exactly repeated to four digits with a period of 5 sec.

In the steady state the displacements were not exactly symmetrical about equilibrium, the displacements being larger in the direction of the current than in the opposite direction. This effect is ascribed to the drift force given by $\dot{y}^2$. At every point the velocity amplitude $y_m\omega$ was smaller than V, where y_m is the displacement amplitude about the mean position of the steady state vibration.

Table 8.4.1 summarizes the results of the steady state, where $+a_1$ denotes the maximum positive displacement (i.e. in the direction opposite the current, since the current was assumed in the negative y-direction, $-a_2$ is the maximum negative displacement, $y_m = \frac{1}{2}(a_1+a_2)$ is the oscillation amplitude and $d=a_1-a_2$ is the mean position. The results are given for each node, as they resulted from the calculations. y_m is plotted in Fig. 8.4.2.

If we consider only the damping term proportional to $-2V\dot{y}$, we can associate a viscous linear damping coefficient per unit length

$$C_L = \rho_W C_D dV = 1.380 \ \frac{kp \cdot s}{m^2}$$

The effective mass of the string must include the hydrodynamic mass $m_h=0.0408 kps^2m^{-2}$ of the surrounding water. The virtual mass per unit length is thus

$$m = m_o+m_h = 0.3588 \ kps^2m^{-2}$$

The undamped wave velocity is: $v_o = (\frac{60000}{0.3588})^{1/2}=408.9ms^{-1}$

The reduced linear damping coefficient is

$$2f = \frac{C_L}{m} = 3.847 \ s^{-1}$$

Then we can compute the coefficients a and b from the expressions (8.4.2)

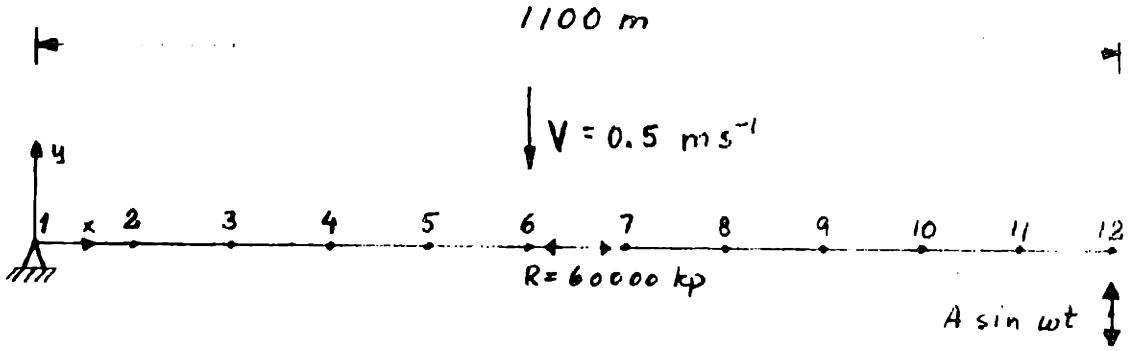

Fig. 8.4.1

Finite Element Model of String

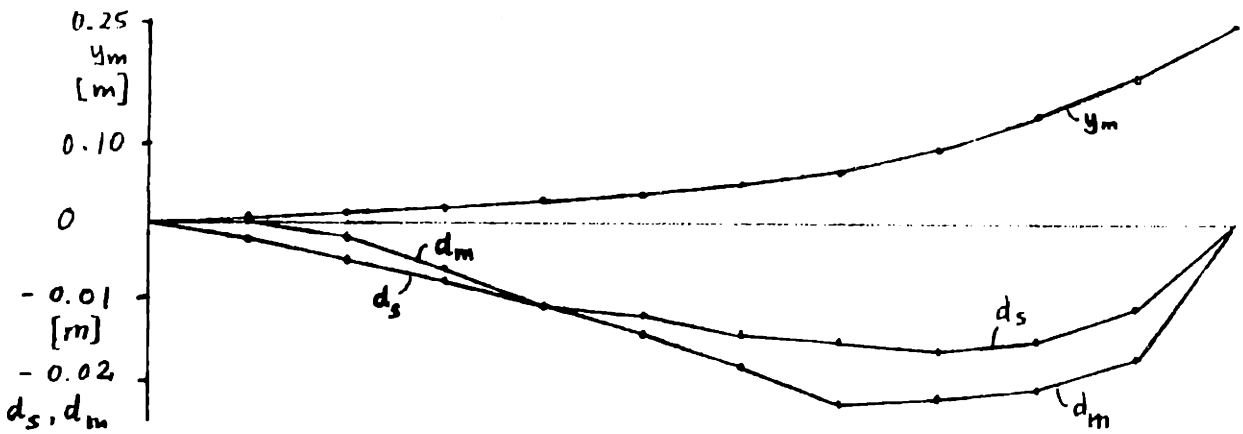

Fig. 8.4.2

Response Parameters of String

Node	$+a_1$ [m]	$-a_2$ [m]	y_m [m]	d_m [m]	β [m^{-1}]	V_s [ms^{-1}]	d_s [m]
1	0.	0.	0.	0.	---	0.	0.
2	$0.851 \cdot 10^{-2}$	$-0.787 \cdot 10^{-2}$	$0.819 \cdot 10^{-2}$	$0.064 \cdot 10^{-2}$	0.00342	$0.72 \cdot 10^{-2}$	$-0.22 \cdot 10^{-2}$
3	$0.147 \cdot 10^{-1}$	$-0.166 \cdot 10^{-1}$	$0.157 \cdot 10^{-1}$	$-0.019 \cdot 10^{-1}$	0.00308	$0.14 \cdot 10^{-1}$	$-0.046 \cdot 10^{-1}$
4	$0.195 \cdot 10^{-1}$	$-0.250 \cdot 10^{-1}$	$0.223 \cdot 10^{-1}$	$-0.055 \cdot 10^{-1}$	0.00302	$0.20 \cdot 10^{-1}$	$-0.070 \cdot 10^{-1}$
5	$0.236 \cdot 10^{-1}$	$-0.341 \cdot 10^{-1}$	$0.289 \cdot 10^{-1}$	$-0.105 \cdot 10^{-1}$	0.00308	$0.25 \cdot 10^{-1}$	$-0.094 \cdot 10^{-1}$
6	$0.305 \cdot 10^{-1}$	$-0.443 \cdot 10^{-1}$	$0.374 \cdot 10^{-1}$	$-0.138 \cdot 10^{-1}$	0.00317	$0.33 \cdot 10^{-1}$	$-0.116 \cdot 10^{-1}$
7	$0.413 \cdot 10^{-1}$	$-0.589 \cdot 10^{-1}$	$0.501 \cdot 10^{-1}$	$-0.176 \cdot 10^{-1}$	0.00321	$0.45 \cdot 10^{-1}$	$-0.137 \cdot 10^{-1}$
8	$0.578 \cdot 10^{-1}$	$-0.796 \cdot 10^{-1}$	$0.687 \cdot 10^{-1}$	$-0.209 \cdot 10^{-1}$	0.00323	$0.59 \cdot 10^{-1}$	$-0.152 \cdot 10^{-1}$
9	$0.839 \cdot 10^{-1}$	-0.1074	$0.956 \cdot 10^{-1}$	$-0.235 \cdot 10^{-1}$	0.00320	$0.83 \cdot 10^{-1}$	$-0.158 \cdot 10^{-1}$
10	0.1211	-0.1421	0.1316	$-0.210 \cdot 10^{-1}$	0.00319	0.12	$-0.148 \cdot 10^{-1}$
11	0.1728	-0.1884	0.1806	$-0.156 \cdot 10^{-1}$	0.00323	0.16	$-0.105 \cdot 10^{-1}$
12	0.25	-0.25	0.25	0	---	0.22	0.

TABLE 8.4.1

$$a = 3.238 \cdot 10^{-3} m^{-1}$$

$$b = 4.464 \cdot 10^{-3} m^{-1}$$

With b we can estimate the wavelength

$$\lambda = \frac{2\pi}{b} = 1407.6 \text{ m},$$

and the wave velocity:

$$v = \omega/b = 281.5 \text{ ms}^{-1}$$

From the results in Table 8.4.1 we can compare with theoretical predictions from the linear damping model. We assume a decay of the amplitudes y_m of the form

$$(8.4.4) \qquad y_m(x) = Ae^{\beta(x-L)} ,$$

where β is a factor corresponding to a in (8.4.3). Based on the amplitudes y_m at the nodes, we can compute values of β at the nodes.

$$\beta = \frac{1}{L-x} \ln \frac{A}{y_m} .$$

The results are shown in Table 8.4.1. The values β range between $3.02 \cdot 10^{-3} m^{-1}$ and $3.42 \cdot 10^{-3} m^{-1}$, which corresponds well with the analytical value $a=3.24 \cdot 10^{-3} m^{-1}$. This correspondence can be taken as confirming that the linear damping contribution $-V\dot{y}$ is dominant to the $\dot{y}^2$ contribution.

We can also try to test the hypothesis that the average displacements d_m can be ascribed to the forces given by $\dot{y}^2$. To some approximation this may be done by the following simulation: If we assume that the displacement y varies harmonically with amplitude y_m, the velocity will also have a harmonic variation of amplitude $y_m\omega$. The average value of $\dot{y}^2$ over one period is then $\frac{1}{2} y_m^2\omega^2$, which can be interpreted as giving rise to a drift force in the direction of V, with time averaged magnitude

$$F_d = \frac{1}{2} \rho_W C_D d \cdot (\frac{1}{2} y_m{}^2\omega^2)$$

Thus if we subject the string to a transverse current of velocity $V_s=y_m\omega/\sqrt{2}$, we have essentially a constant force equal to the average drift force F_d. This simulation was done by a calculation similar to Sec. 8.3, imposing the current V_s at each node according to the oscillation amplitude of the node, and starting the system from a straight configuration of rest with no current. The current was started at t=0 and the final equilibrium displacements d_s were computed dynamically. The distribution of V_s is shown in Table 8.4.1.

The resulting displacements of the nodes are given in Table 8.4.1 and a comparison between d_m and d_s is shown in Fig. 8.4.2. It is seen that d_s and d_m are of the same order of magnitude, but the relative differences are fairly large.

However, it should also be taken into account that the average displacements are of the order 1 cm, compared to the imposed displacements at the right end of 25 cm and the total cable length of 1100 m. We can compare the analytical wave velocity v=281.5 ms^{-1} and wave length λ=1407.7m with the computer calculations.

In Fig. 8.4.3 is drawn the string shape at ten times with a time difference of 0.5 sec, i.e. over one excitation period. If we follow the wave peak, which at 25.0 sec is located at x=877 m, it is seen to have displaced to x=370m at 27.0 sec. Hence we can estimate a wave velocity of 254 ms^{-1}. A similar analysis for the interval from 27.5 sec to 29.5 sec gives a wave velocity of 302 ms^{-1}. The average is 278 ms^{-1}, which corresponds well with the analytical 281.5 ms^{-1}.

From the distance between the peaks, which corresponds to one half wave length, at 25.0 sec, we estimate a wavelength of 1386 m. At 27.0 sec we get 1330 m, at 27.5 sec we get 1212 m and at 29.5 sec we get 1504 m. The average of these four values is 1358 m, which is a fair correspondence with the analytical 1408 m.

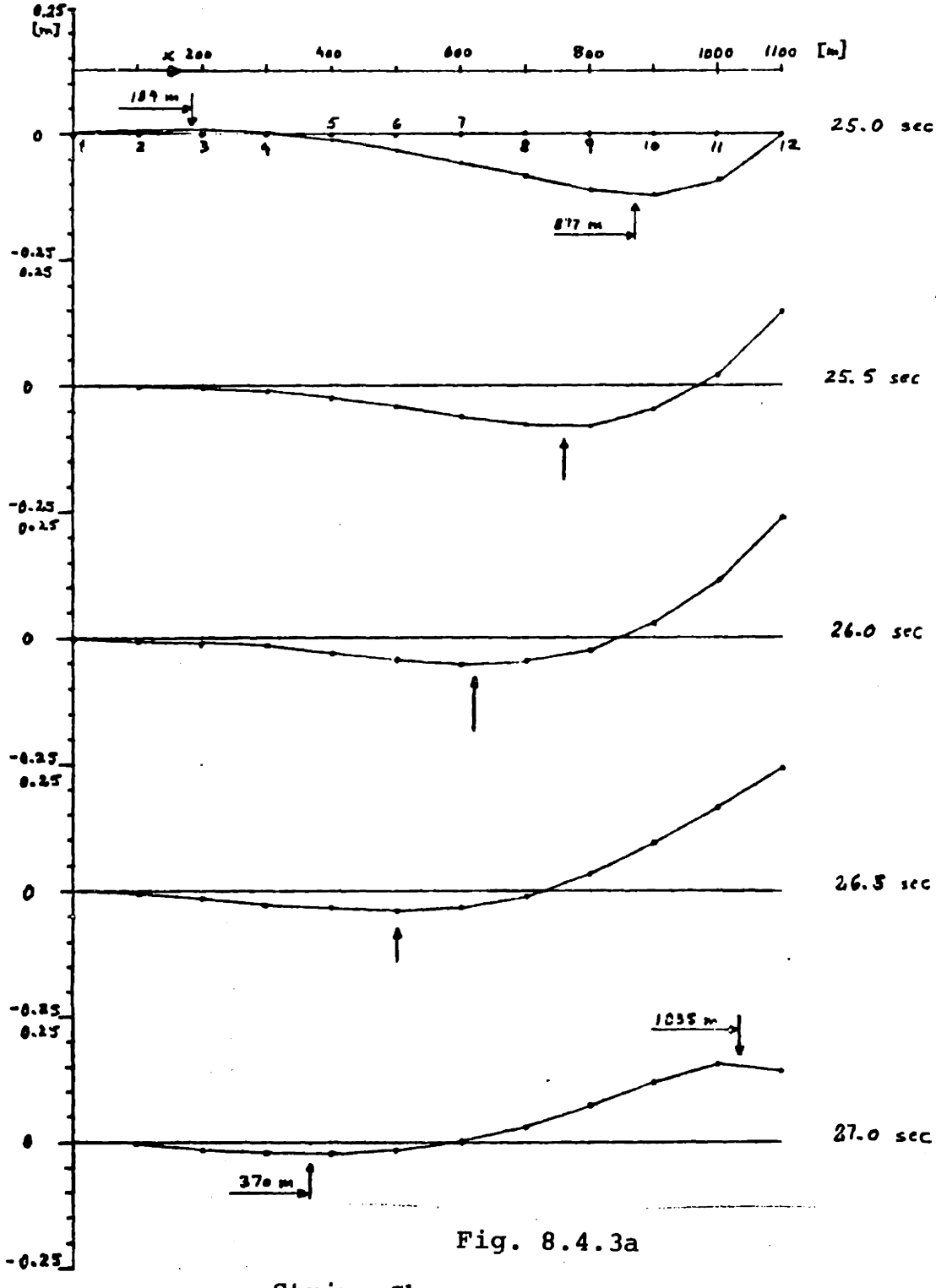

Fig. 8.4.3a

String Shape as a Function of Time

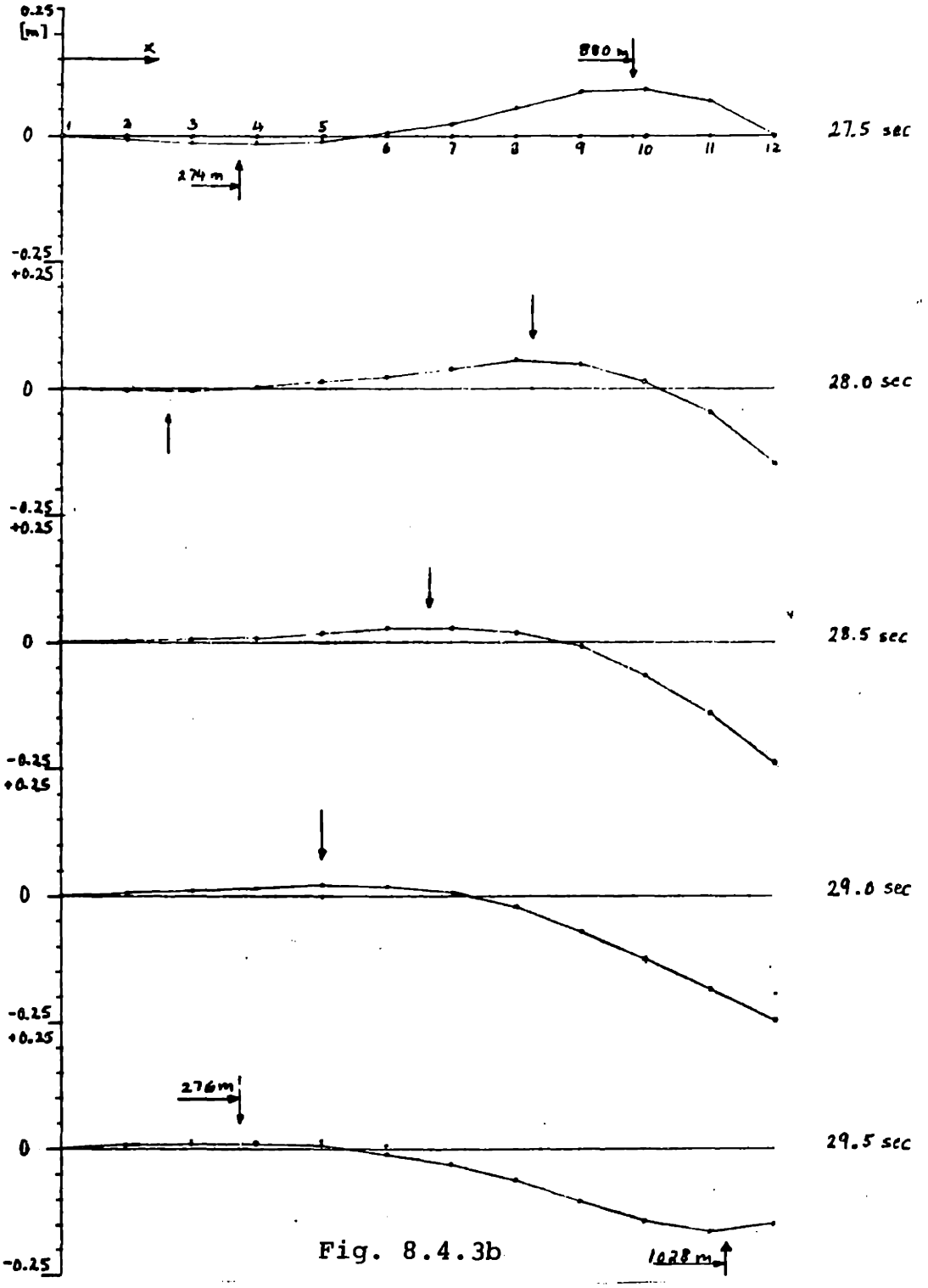

Fig. 8.4.3b

String Shape as a Function of Time

8.5 Analysis of Mooring Lines.

In this section an attempt to analyse two mooring lines is reported. The analysis aimed at computing the forced tension variations and displacements in the line as functions of time, when the upper end point is subjected to given displacement as function of time. A problem in this connection is the lack of experimental data relevant to the kind of analysis undertaken, i.e. measurement of the time dependent tension variations under known upper end displacement. One other analysis of the same scope was known. Some results were kindly furnished to the author by E. Furuholt of the Ship Research Institute of Norway. His analysis applied the finite element method. Other analyses and measurements often report their results in a statistical form, which make them difficult for comparison for the present analysis, which is nonlinear. In our view this kind (i.e. deterministic) of analysis is important for practical purposes, since it allows one to estimate the effect of transient loads, e.g. a single large wave, imposed on the vehicle.

Before starting the analysis, it is interesting to try to estimate qualitatively the kinds of results one will get and also single out those features which are essential, so that the main results do not get lost in details. Under steady harmonic excitation, one can expect there will exist

a harmonic response, of the same frequency as the excitation. If the system cannot be given an initial condition which corresponds exactly to this steady state, there will be some initial transient motions in the system which will die out with time, so that only the forced motion remains. As follows from the example in Sec. 8.4, one cannot always expect all points of the system to move in the same phase with respect to time, since there is a finite time for propagation of impulses within the system. However, in Sec. 8.4 the only mode of propagation in the cable was transverse displacements, but for a mooring cable the propagation mechanism is more complicated. Both longitudinal waves (stress waves) and transverse waves will exist at the same time, with the longitudinal wave velocity much larger than the transverse wave velocity. The longitudinal and transverse displacements are not independent due to the sag of the cable. If the tension is changed, there will be corresponding transverse displacements to change the sag.

The dampening of the initial transient is effected partly by the water drag, for the transverse modes, and partly by the internal friction of the cable, for the longitudinal modes. As the present analysis is concerned with a steel cable and data on viscous properties of steel cables were not known when doing the analyses, values for the internal viscous coefficient had to be assumed. When

the excitation is harmonic with periods corresponding to real sea states, i.e. 8-20 seconds, the responses in the longitudinal modes, with low natural periods, are effectively static in the steady state. Then the viscous forces will be small compared to the elastic tension forces and the internal friction is expected to have only little influence on the steady state response.

8.5.1 Description of the lines

A typical mooring for an off-shore platform is shown in Fig. 8.5.1. It is seen that a certain length of cable or chain is lying on the bottom from the anchor in order to give a horizontal force and to reduce possible shock loads on the anchor. This part is not included in our model.

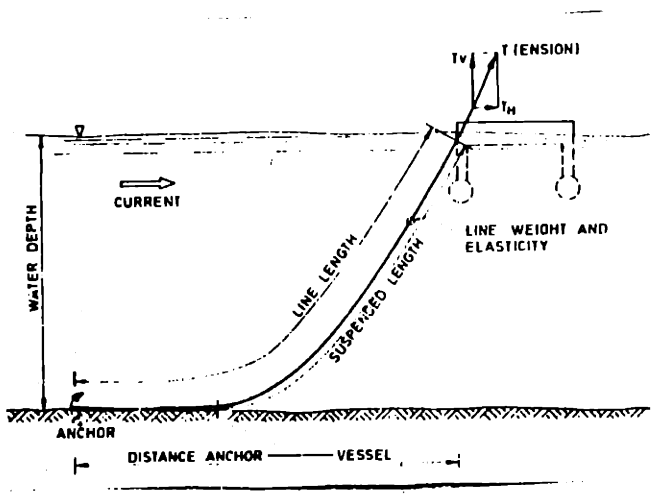

Fig. 8.5.1

Mooring Configuration

In our analysis we considered two examples of mooring lines. One represented a mooring in 500 m depth of water, the other in 200 m of water. The mooring cables were taken to be wire rope of the following characteristics:

Cross section: $A=4.54\cdot10^{-3}m^2$

Diameter: $d=0.076$ m

Weight density: $\gamma=5.44\cdot10^{3}kpm^{-3}$

Weight per unit length: $\gamma A=24.70\ kpm^{-1}$

Drag coefficient: $C_D=1.4$

Mass coefficient: $C_M=1.2$

Elastic modulus: $E=5.12\cdot10^{9}kpm^{-2}$

Internal friction (assumed values):

500 m depth: $C_V=4.72\cdot10^{8}kp\cdot s\cdot m^{-2}$

200 m depth: $C_V=2.30\cdot10^{7}kps\ m^{-2}$

Breaking strength: $B=294000$ kp

Equilibrium tension at upper end:

500 m depth: $R=98000$ kp

200 m depth: $R=57000$ kp

Equilibrium length:

500 m depth: $L=2145.0$ m

200 m depth: $L=1043.4$ m

Theoretical wave velocities:

Transverse waves:

500 m depth: $v_t=179\ ms^{-1}$

200 m depth: $v_t=136\ ms^{-1}$

Longitudinal waves: $v_\ell = 3039\ ms^{-1}$

The selection of these data is based on the communication with E. Furuholt, except for the internal friction coefficients, which are assumed values. The equilibrium configurations were assumed to be catenaries under a submerged weight of 20.2 kpm^{-1}.

It should be noted that the same equilibrium configuration was assumed with current and without current. Theoretically, this cannot be completely correct, since imposing a current would displace the equilibrium. To check the effect of imposing a current an analysis was made on the 500 m depth cable with current 1 ms^{-1}, similar to Sec. 8.2. This gave additional transverse displacements of 0.35 m in the upper part and a tension increase of 365 kp. These changes are small compared to the total values. Since our analysis is concerned with changes from equilibrium, we can assume that the effect of the difference in equilibrium state is not important.

In Figs. 8.5.2 and 8.5.3 are shown the equilibrium configurations for the two cables together with the tension variations. For both cables 10 finite elements of equal length were used. The figures also show the definition of tangential and normal directions on the cable.

Regarding the choice of internal friction coefficients

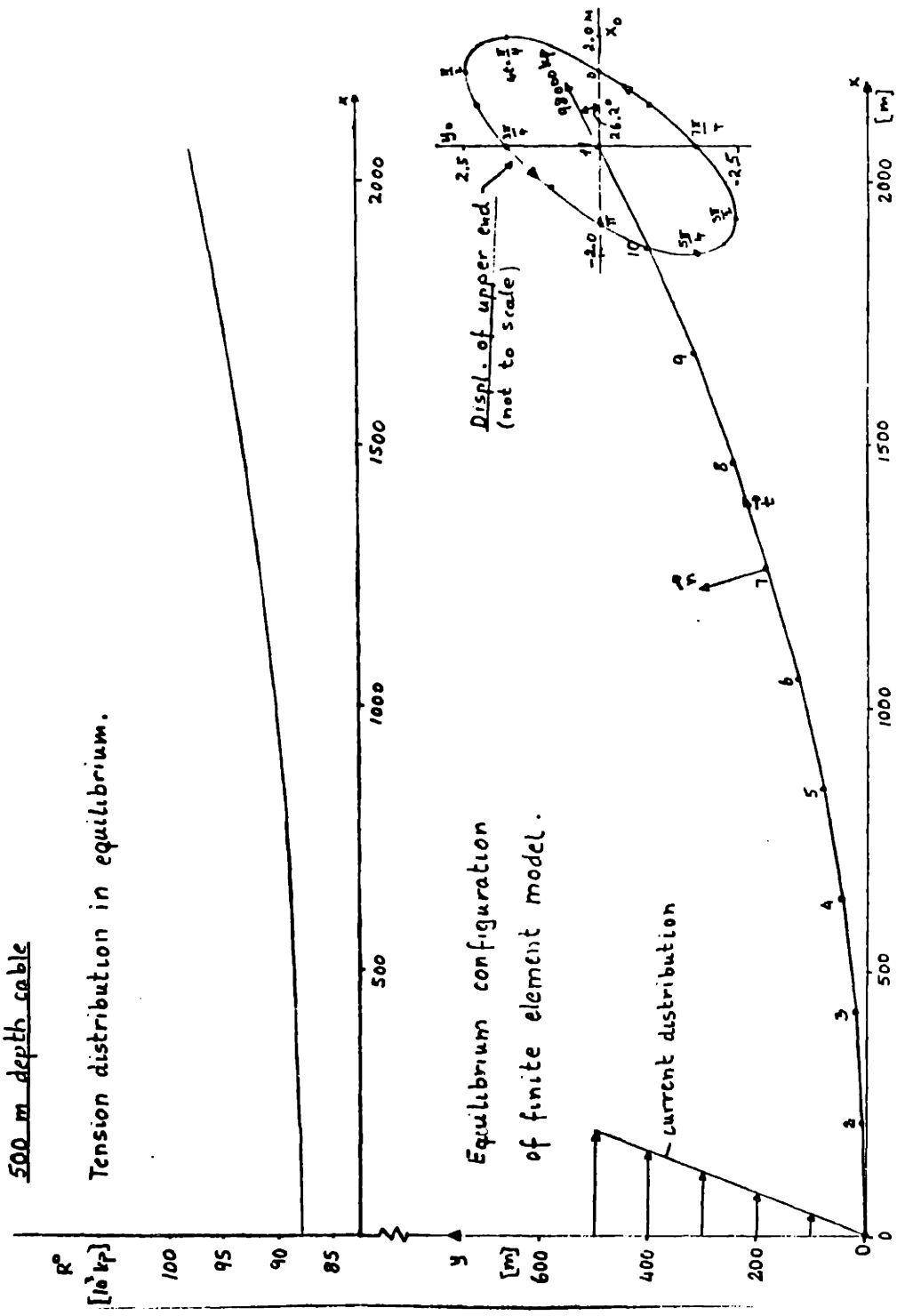

Fig. 8.5.2

Shape of Mooring Line at 500 m Depth

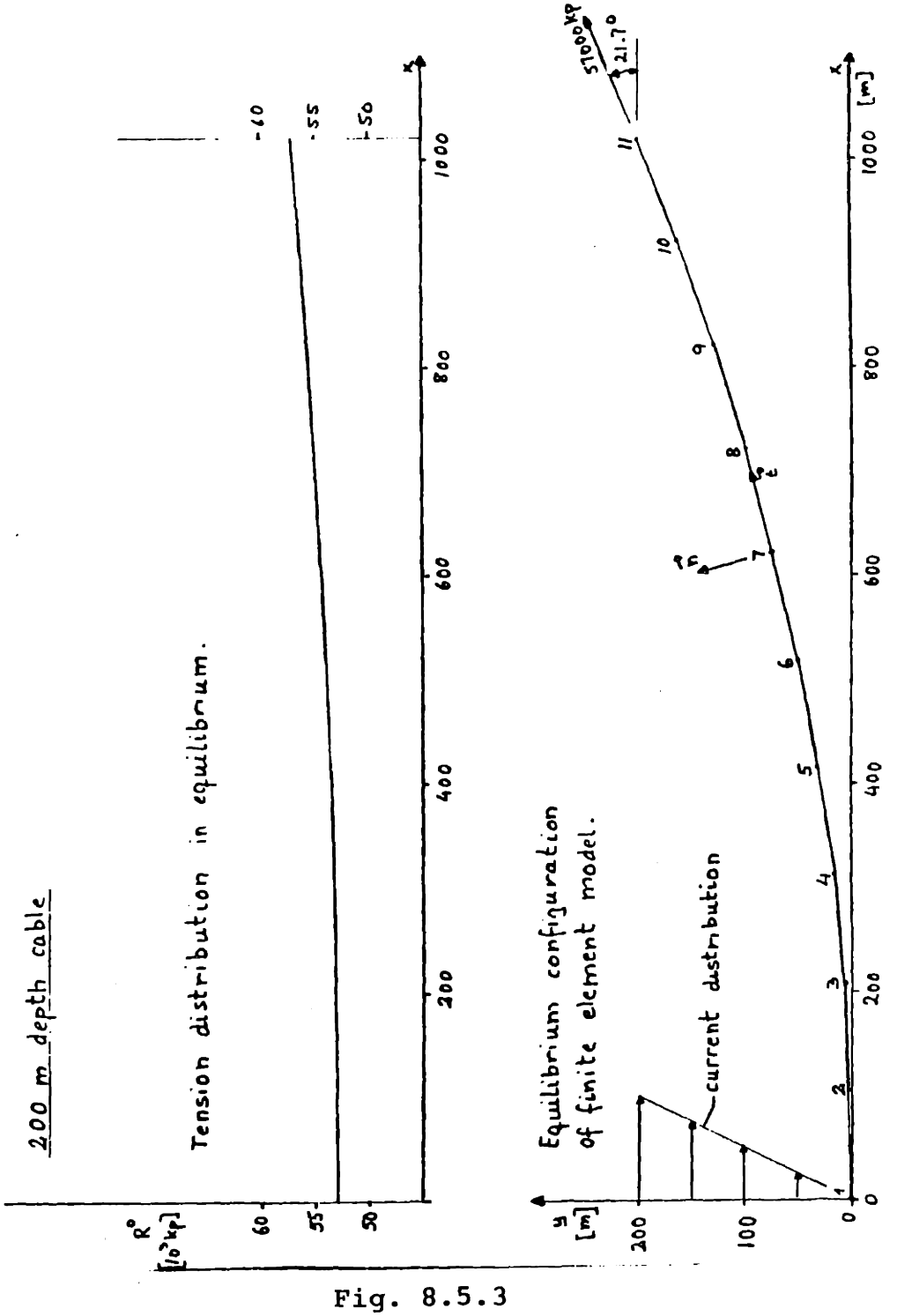

Fig. 8.5.3

Shape of Mooring Line at 200 m Depth

no data was known for steel wire cables when the calculations were done. In [21] is reported a value $c_v=2.79\cdot10^9$ kps m^{-2} for nylon. Hence our assumed values of $c_v=4.72\cdot10^8$ $kp\cdot s\cdot m^{-2}$ for the 500 m depth cable and $c_v=230\cdot10^7$ $kp\cdot s\cdot m^{-2}$ for the 200 m depth cable are smaller than the value for nylon. After the calculations had been done, values were found [23] for steel wire ropes of the order of magnitude $c_v\approx1.5\cdot10^6$ $kp\cdot s\cdot m^{-2}$. Hence our assumed values are larger than this. It was assumed that, for a steady state of vibration, the excitation periods would be much larger than the natural periods of longitudinal vibration, so that the longitudinal modes would be excited in an essentially quasi-static manner. In that case, the value chosen for the friction coefficient would have only a minor influence on the steady state response. Control calculations with lower values of the viscous coefficient seemed to confirm this assumption.

Technically, there is another damping mechanism in most real cables, which is not included in the model. That is the part of the cable resting on the sea floor up to the anchor. It is difficult to assess the effect of this in damping, but it can be assumed that in a real system longitudinal transients will be damped faster than predicted by internal friction alone.

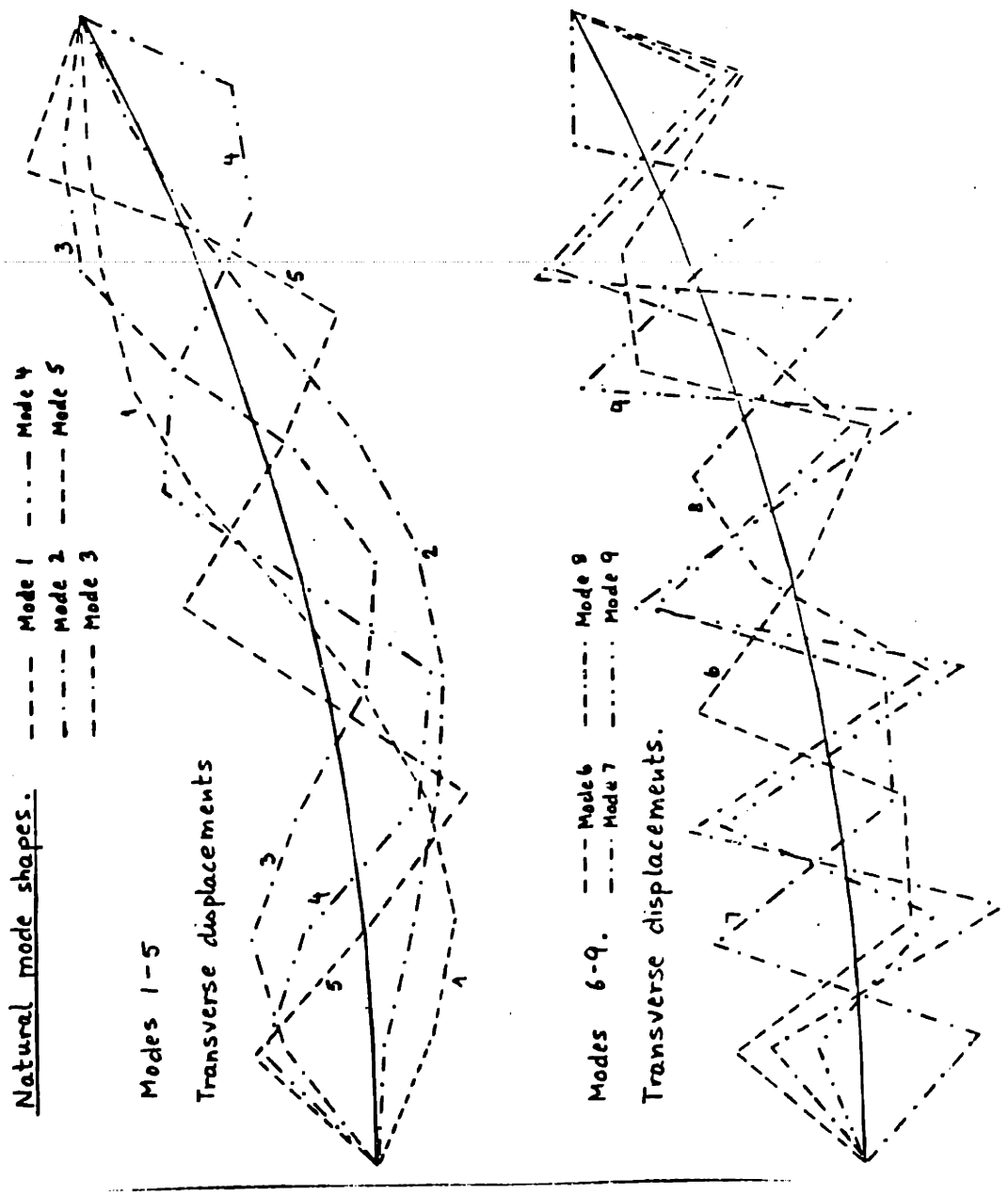

Fig. 8.5.4a

Natural Mode Shapes--Transverse Modes

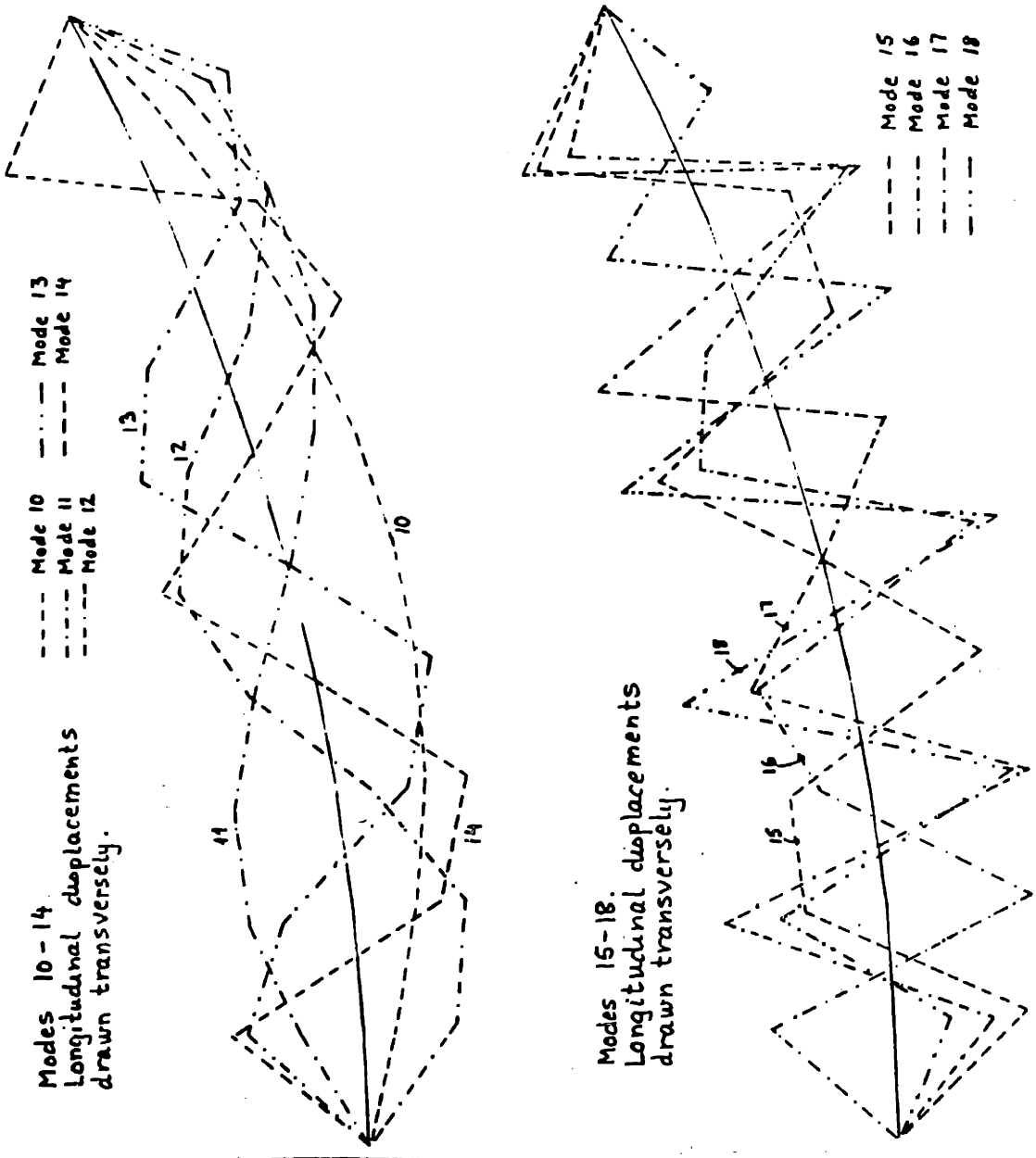

Fig. 8.5.4b

Natural Mode Shapes--Longitudinal Modes

Mode l	Natural periods [sec] 500 m depth cable	200 m depth cable
1	12.4	7.8
2	11.1	6.7
3	7.7	4.8
4	5.9	3.7
5	4.5	2.8
6	3.6	2.3
7	3.0	1.9
8	2.6	1.6
9	2.3	1.5
10	1.4	0.68
11	0.69	0.34
12	0.45	0.22
13	0.33	0.16
14	0.26	0.12
15	0.21	0.10
16	0.17	0.083
17	0.15	0.071
18	0.13	0.065

Modes 1-9 are essentially transverse, modes 10-18 are essentially longitudinal for both cables.

TABLE 8.5.1

8.5.3 Pull tests.

In order to get a first picture of the dynamic response of the cables, they were analysed in pull tests, in which the upper end was pulled a certain distance under constant velocity in 2 seconds and then held fixed in the extreme position. The extreme position had x-displacement x_1=1.414m, y-displacement y_1=2.5m, i.e. a total linear displacement z_1=2.87m.

The analyses were done with different current states. For the 500 m depth cable three states were used: one with no current, the two others with currents linearly varying from respectively 1 ms^{-1} and 2 ms^{-1} at the upper end to zero at bottom. For the 200 m depth cable, there was one state with no current and one linearly varying from 2 ms^{-1} at the upper end to zero at the bottom.

Since there were some transients present in the cable during the pull, element no. 6 seemed to be most representative of average values in the cable. Some results are shown in Figs. 8.5.5a,b, where the elastic tension deviation ΔR_6 in element 6 and the normal displacement v_6 of node 6 are drawn as functions of time for the 20 sec. periods for which the analyses were made. The diagrams show a rapid increase of tension in the pull period (0-2 sec). After 2 sec. the tension is relaxed towards equilibrium values.

500 m depth cable - pull tests

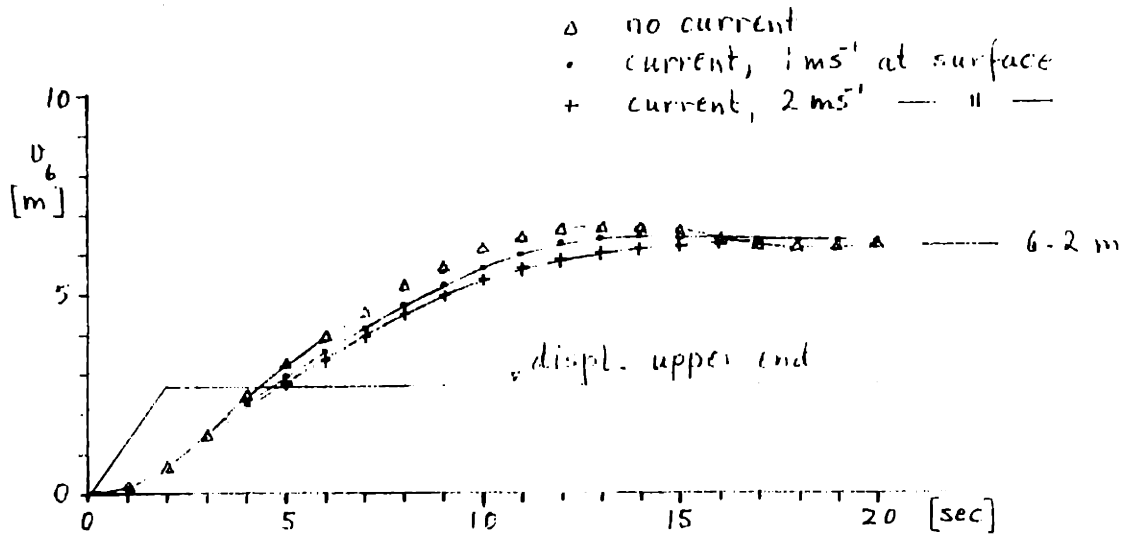

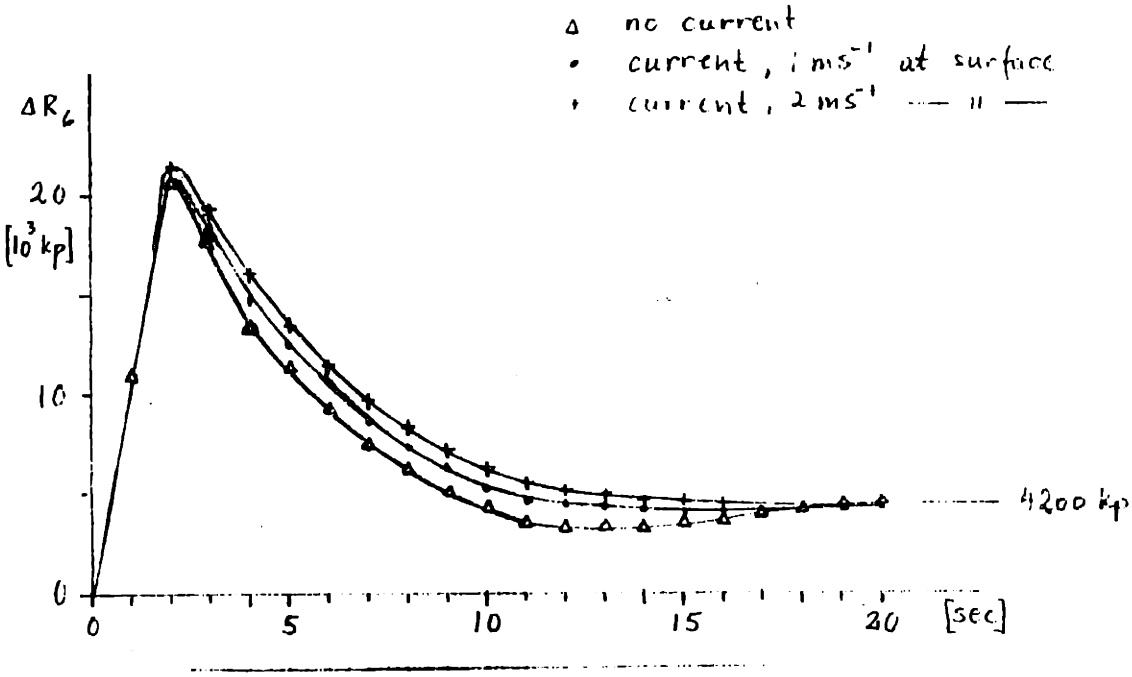

Fig. 8.5.5a

Pull Test Response--500 m Depth Cable

200 m depth cable : pull tests.

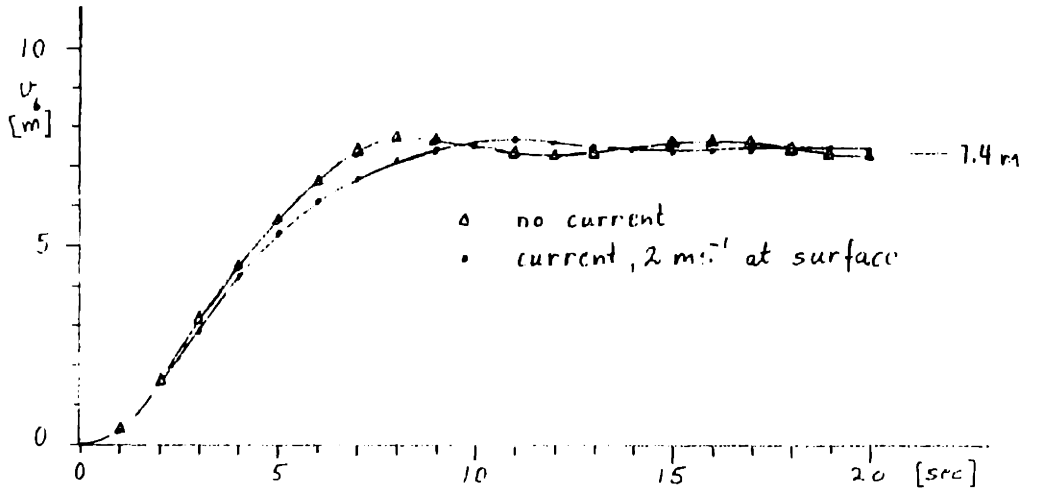

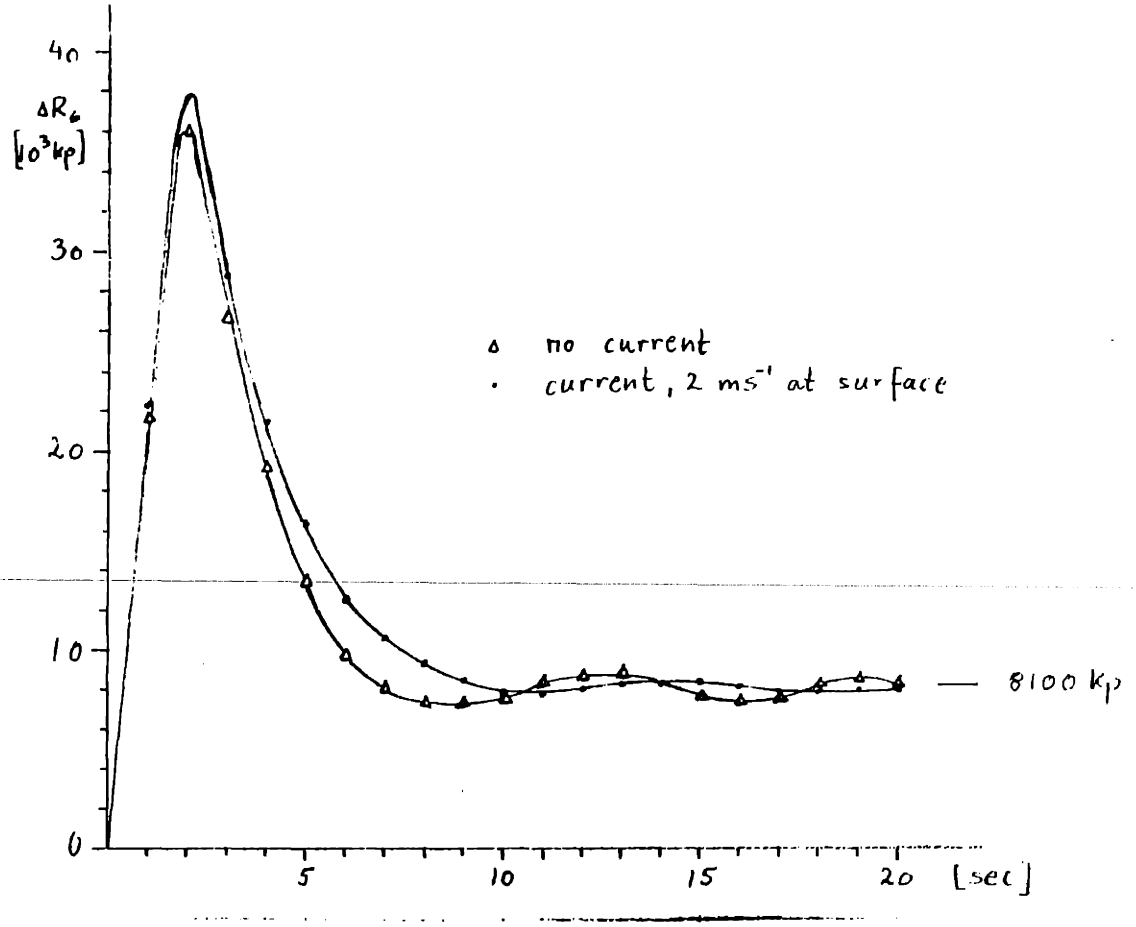

Fig. 8.5.5b

Pull Test Response--200 m Depth Cable

The peak tensions after 2 sec. seemed almost independent of the magnitude of the current, while the relaxation occurred somewhat more rapidly with no current than with current.

The equilibrium tensions can be estimated from the diagrams to about 4200 kp for the 500 m depth cable and about 8100 kp for the 200 m depth cable. Separate manual calculations with the catenary gave the results 4150 kp, respectively 8010 kp.

The limiting values of the normal displacements v_6 may be estimated from the diagrams as about 6.2 m for the 500 m depth cable and 7.4 m for the 200 m depth cable. The manual calculations gave respectively 6.4 m and 7.5 m. From the diagrams it also appears that the peak tension deviation for the 200 m depth cable (about 35000 kp) is larger than for the 500 m depth cable (about 21000 kp). This indicates that the shorter cable is more likely to get large transient tensions due to suddenly applied loads, but it should be noted that the static tension increase is also larger.

To check the effects of internal damping in the cable, the 500 m depth cable without current was subjected to the pull test with an internal damping 0.01 of that used previously. The results showed that the tension had an oscillatory, high frequency variation about the values in the diagram, while the normal displacement of node 6 was prac-

tically the same as in the diagram. From this one can infer, as would be expected, that the longitudinal transients are mainly influenced by internal damping, while the normal displacements, particularly in the relaxation phase, are guided by drag forces. It also indicates that the value chosen for the internal damping coefficient does influence the high frequency, transient longitudinal oscillations, but not, or at least only to a small extent, the average relaxation of the system towards equilibrium.

In this pull test of the 500 m depth cable with no current we also studied the initial motion in the period up to 3 sec in more detail. From the transverse displacements, v_6, of node 6, the velocity $\dot{v}_6$ and acceleration $\ddot{v}_6$ were estimated by computing first and second differences in time with a time interval h=0.2 sec. From the acceleration, the inertia force (I) was estimated and from velocity, the drag force (D) was estimated. Also the curvature could be estimated and the corresponding transverse tension force (A) was computed. All forces were estimated per unit length around node 6.

The results of this analysis are shown in Fig. 8.5.5c. It is seen that for the initial time up to about 1.2 sec, the transverse inertia force is larger than the drag force. After 1.2 sec the drag force dominates the inertia force and the latter becomes negative after about 2.5 sec. The

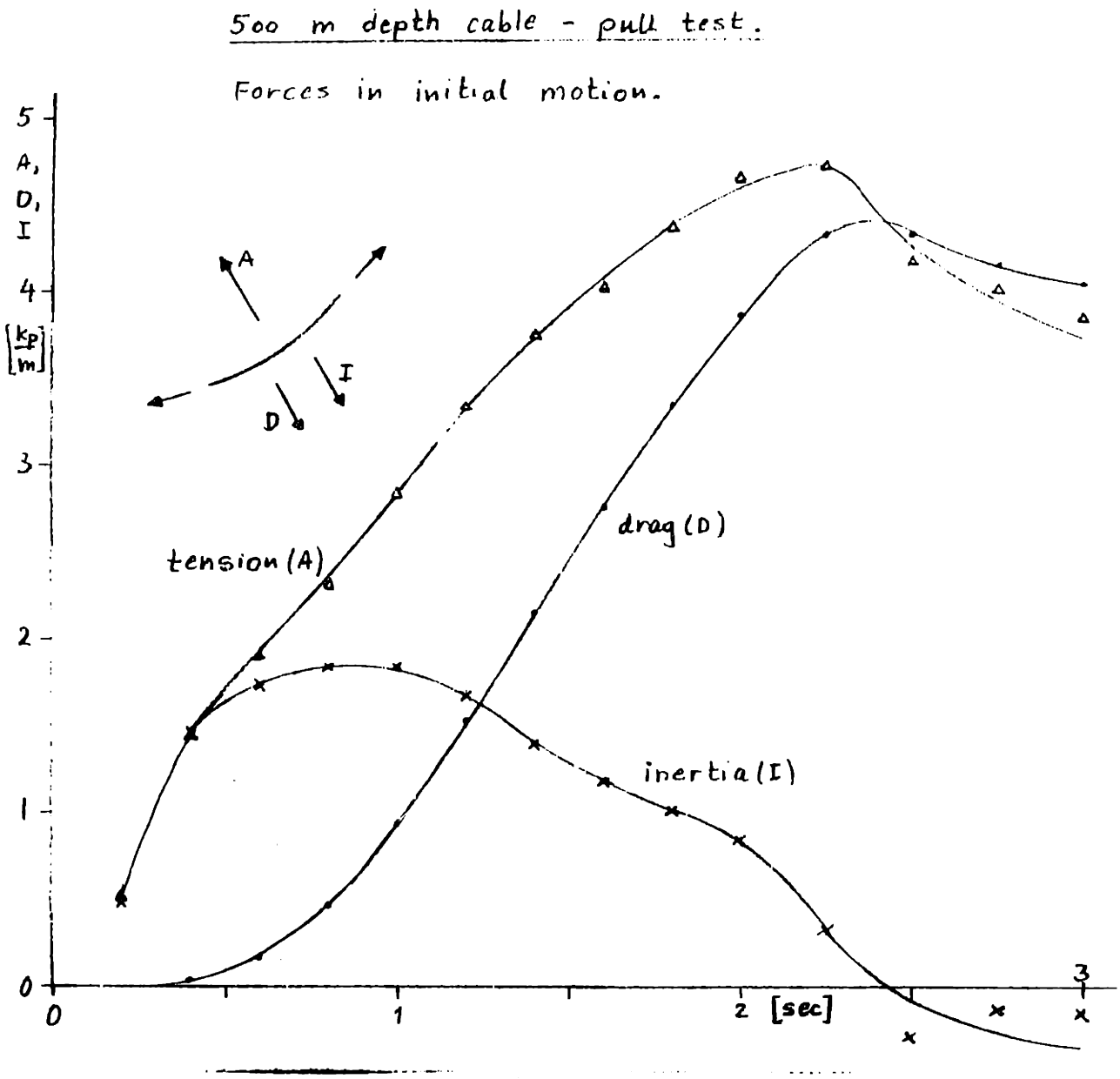

Fig. 8.5.5c

Force Balance in Initial Motion

tension force was corrected for the assumed strain rate dependence of the axial force, and in the diagram the transverse tension component is approximately equal to the sum of the inertia and drag forces.

Hence, we can conclude that the tension increase during the pull phase is caused initially by the inertia of the cable and later by the drag resistance to transverse motion. Part of the tension increase is also due to the change of equilibrium tension.

8.5.4 Response to forced harmonic excitation of the upper end.

The cables were excited at the upper end by given horizontal and vertical displacements:

$$x_o = a_x \sin(\omega t + \frac{\pi}{4})$$
$$y_o = a_y \sin \omega t,$$

with horizontal amplitude a_x=2.0 m, vertical amplitude a_y=2.5 m and with the horizontal displacement 45° before the vertical in phase, see Fig. 8.5.2. The excitation period $T_c = 2\pi/\omega$ was varied while the amplitudes were held fixed in the basic series of calculations. Other calculations were performed with variations of excitation amplitudes, current and internal damping of the cable material. The

time step used in the integration was normally 0.25 sec.

We present first some time dependent results for a specific calculation. Fig. 8.5.6 shows some features of the resulting response for the 500 m depth cable with excitation period T_c=10 sec and no water current. The first diagram shows the excitation displacements x_o, y_o. The second diagram shows the normal displacements v_i; i=3,6,9,11, for nodes 3,6,9,11 in the time segment from 20 to 35 seconds. The third diagram shows the elastic tension variations ΔR_6 for element 6.

The second diagram shows that the phase differences between the nodes 3,6,9 are small. Similar time functions were found for the other nodes except near the upper end, where the phase differences are somewhat larger. The differences cannot be accounted for as a result of transverse wave propagation, since the velocity of transverse waves, disregarding damping, is about 179 ms^{-1}, while the distance between nodes 3 and 9 is more than 1200 m. Further, node 3 is before nodes 6 and 9 in phase. We can interpret this result as transverse displacements being caused by the tension variations. The delay of displacements, compared to the tension variations in the third diagram, is then the result of hydrodynamic damping.

By comparing the tension variations in the third diagram with the excitation displacements x_o, y_o in the first

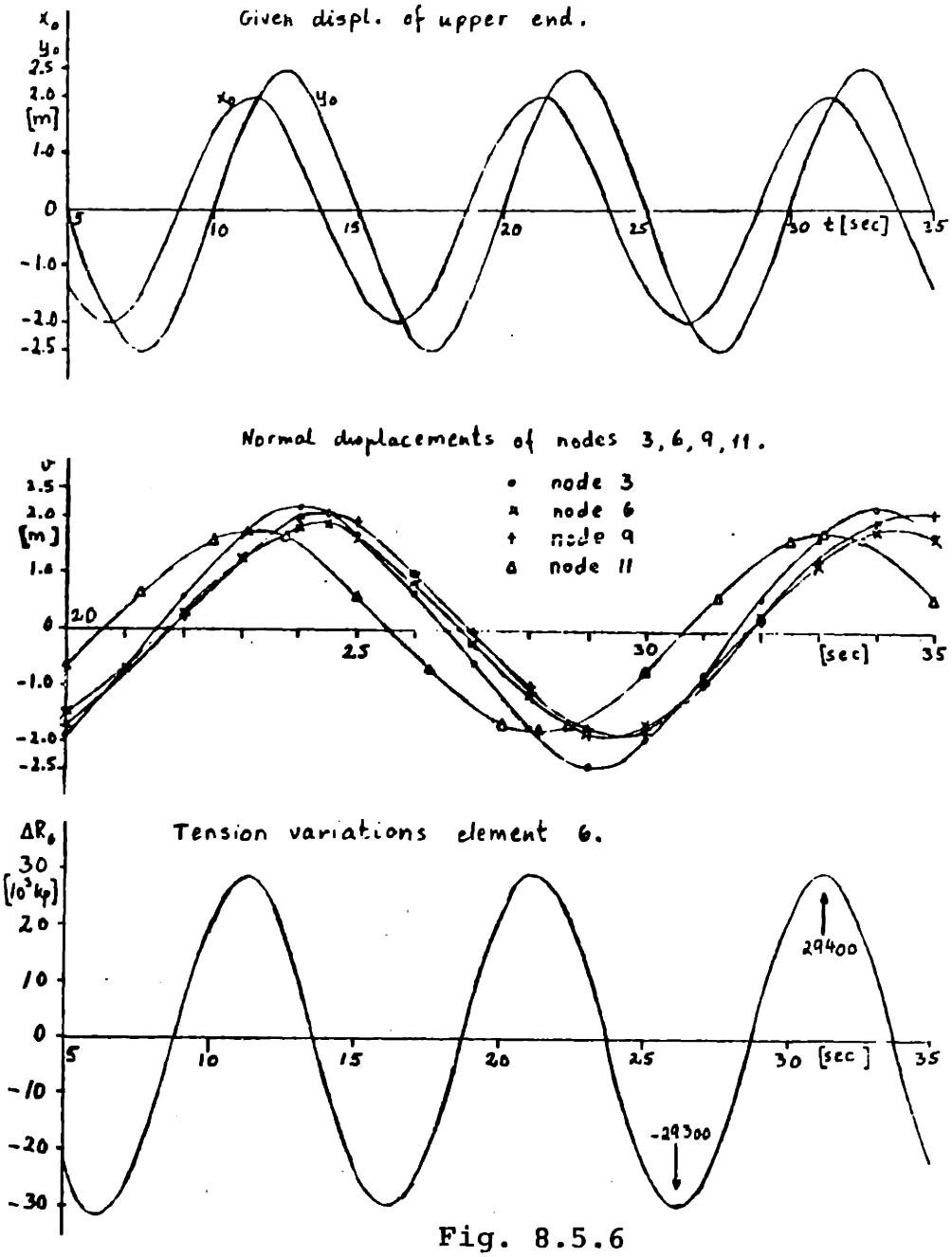

Fig. 8.5.6

Harmonic Time Dependent Response

diagram, we see that the tension variations are practically in phase with the horizontal displacements x_o. This might have been expected, since the angle between the cable and the horizontal is about 26° at the upper end.

In Figs. 8.5.7a-d are sketched the modal responses as functions of time. The ordinates are the modal coordinates $y_i(t)$ defined in Sec. 5.4. It appears that mode 1 has not completely reached a steady middle position after 35 sec. The other transverse modes (2-9) seem to have reached steady, periodic motions after at most 15 sec. The repetitive pattern with a period of 10 sec is good. For the higher modes (6-9) the deviations from sinusoidal shape become appreciable, but the amplitudes are small.

The longitudinal modes (10-18) are all practically in phase with the imposed x_o displacements and have no apparent distortion of the sinusoidal shape.

In Figs. 8.5.8 and 8.5.9 are shown the elastic tension amplitudes ΔR_6 in element 6 for various excitation periods T_c for the 500 m and 200 m depth cables respectively. The excitation amplitudes are kept constant. The analyses showed a tendency for the tension to increase with reduced T_c. The resonance periods showed merely as small deviations from the general trend, giving "hollows" in the diagrams. This indicates that the mass forces are insignificant compared to drag and tension forces for these cables with the excitation

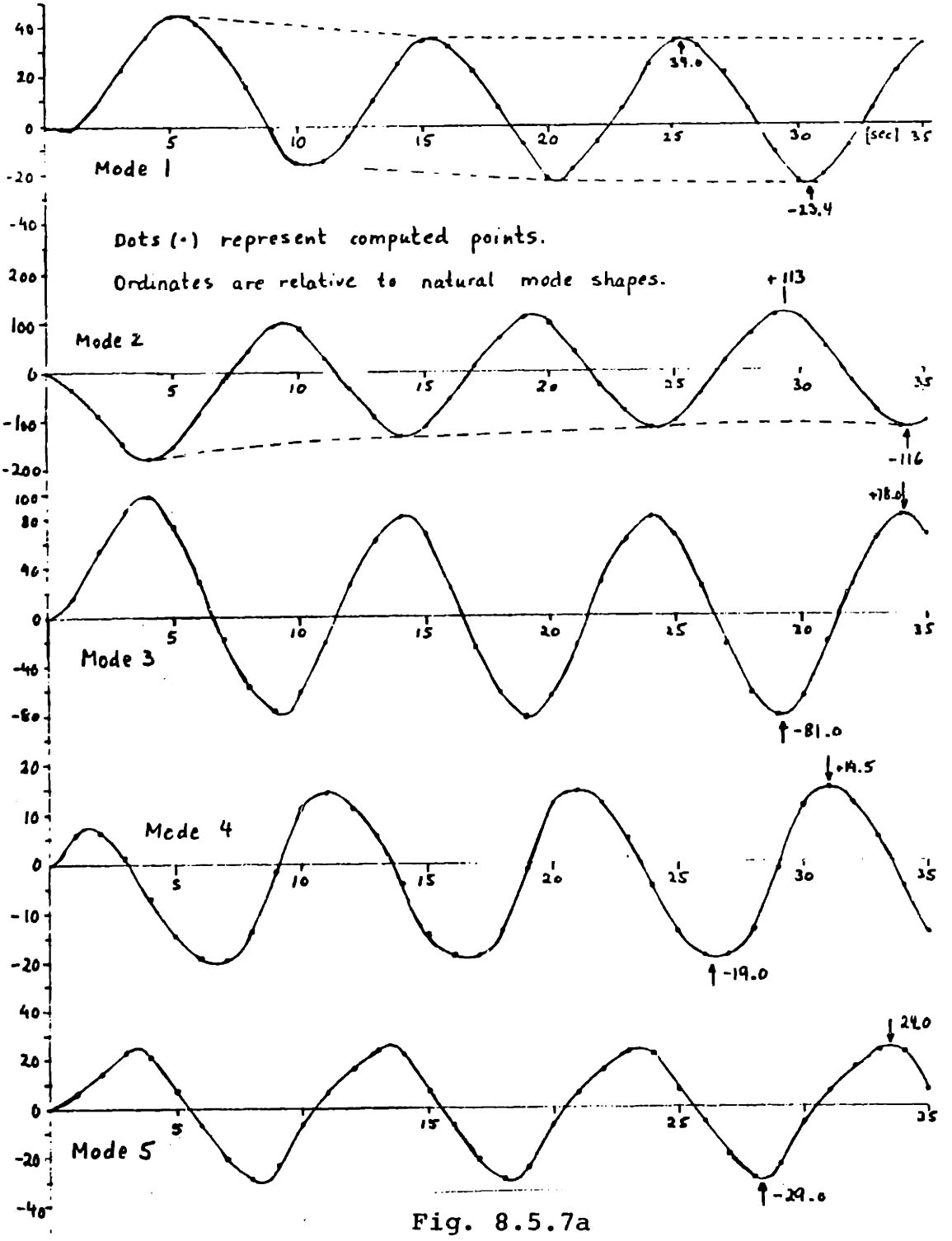

Fig. 8.5.7a

Harmonic Time Dependent Response--Mode 1-5

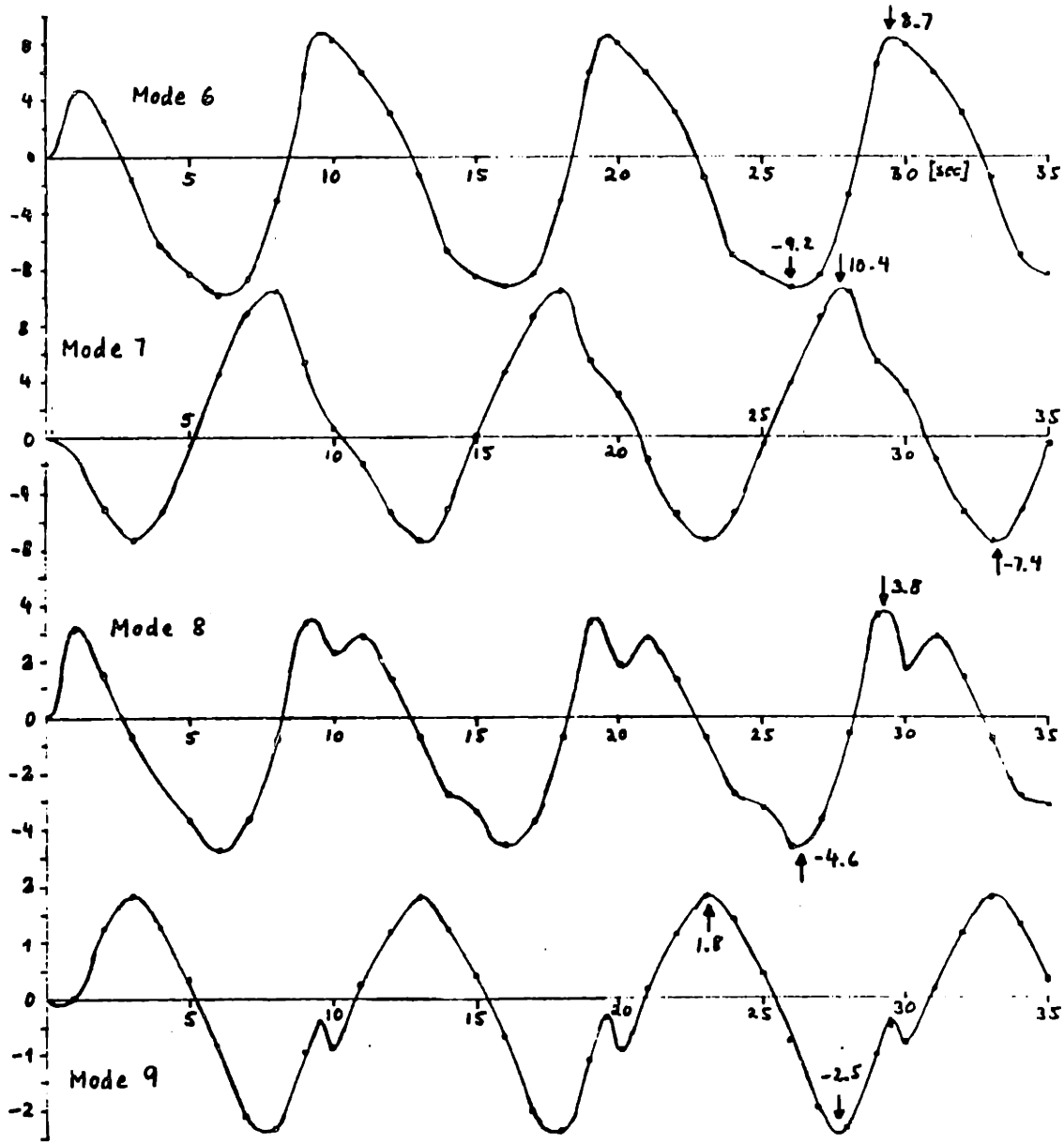

Fig. 8.5.7b

Harmonic Time Dependent Response--Mode 6-9

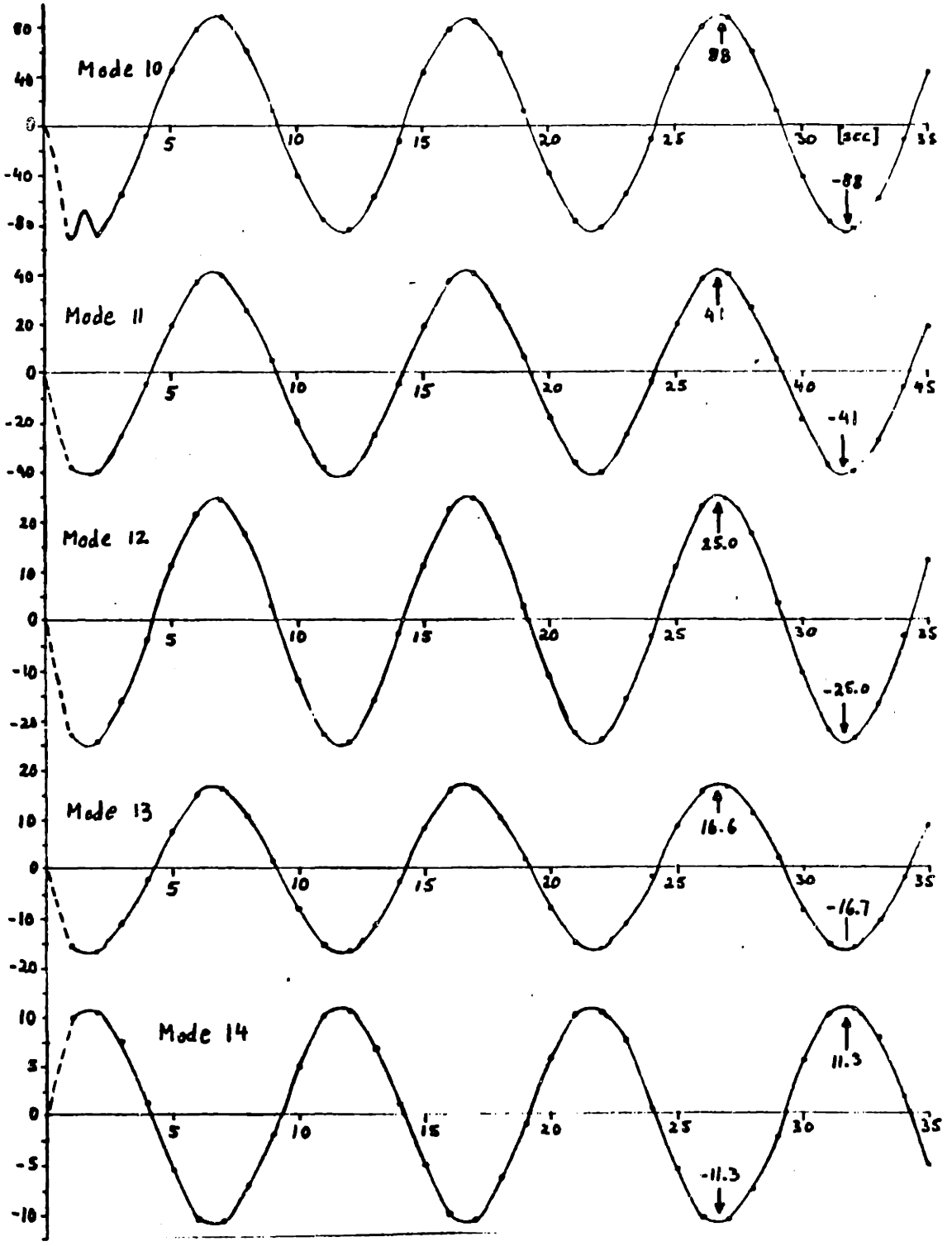

Fig. 8.5.7c

Harmonic Time Dependent Response--Mode 10-14

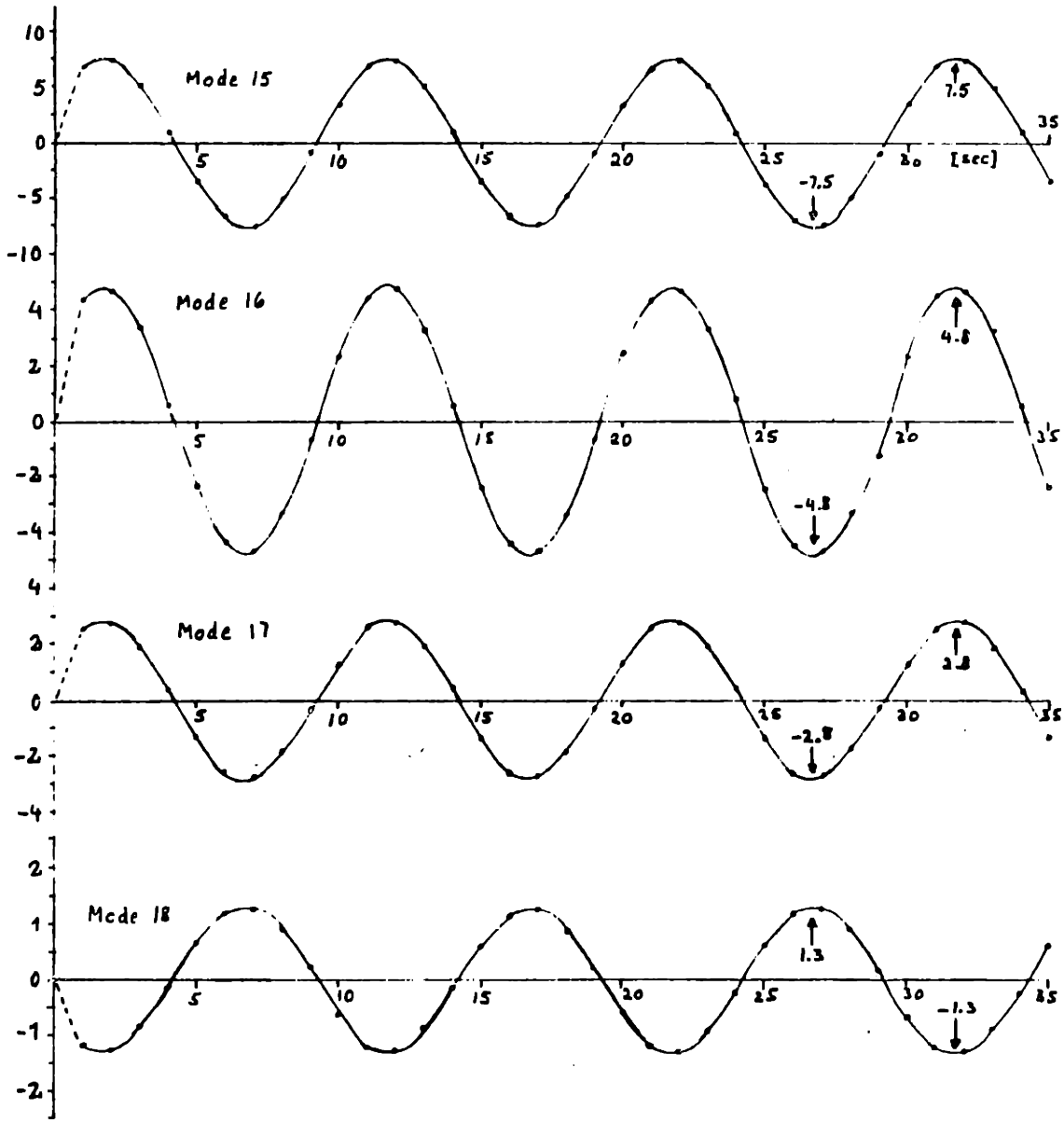

Fig. 8.5.7d

Harmonic Time Dependent Response--Mode 15-18

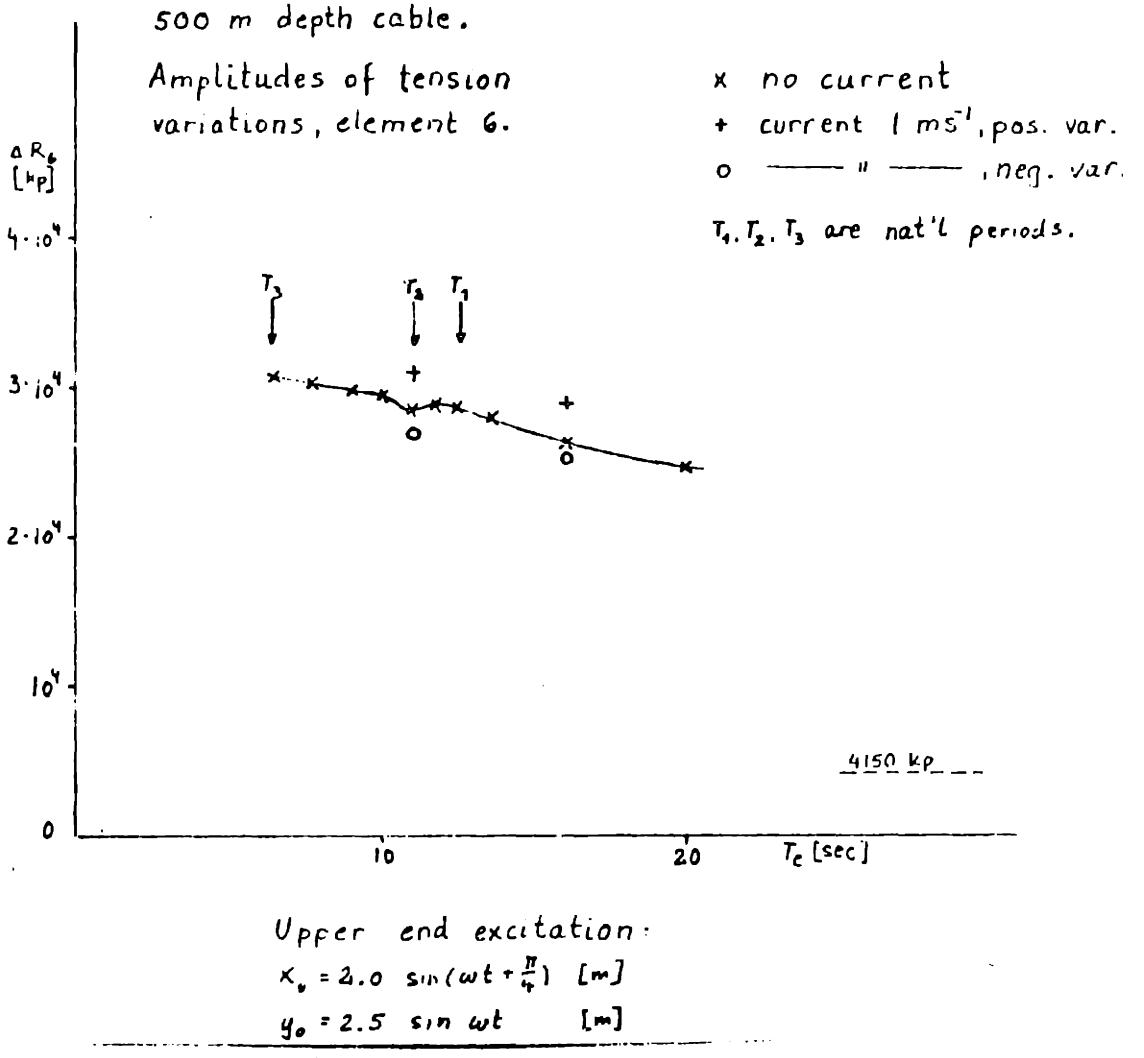

Upper end excitation:

$x_o = 2.0 \sin(\omega t + \frac{\pi}{4})$ [m]

$y_o = 2.5 \sin \omega t$ [m]

Fig. 8.5.8

Tension Variation Amplitudes as Function of T_e, 500 m Depth Cable

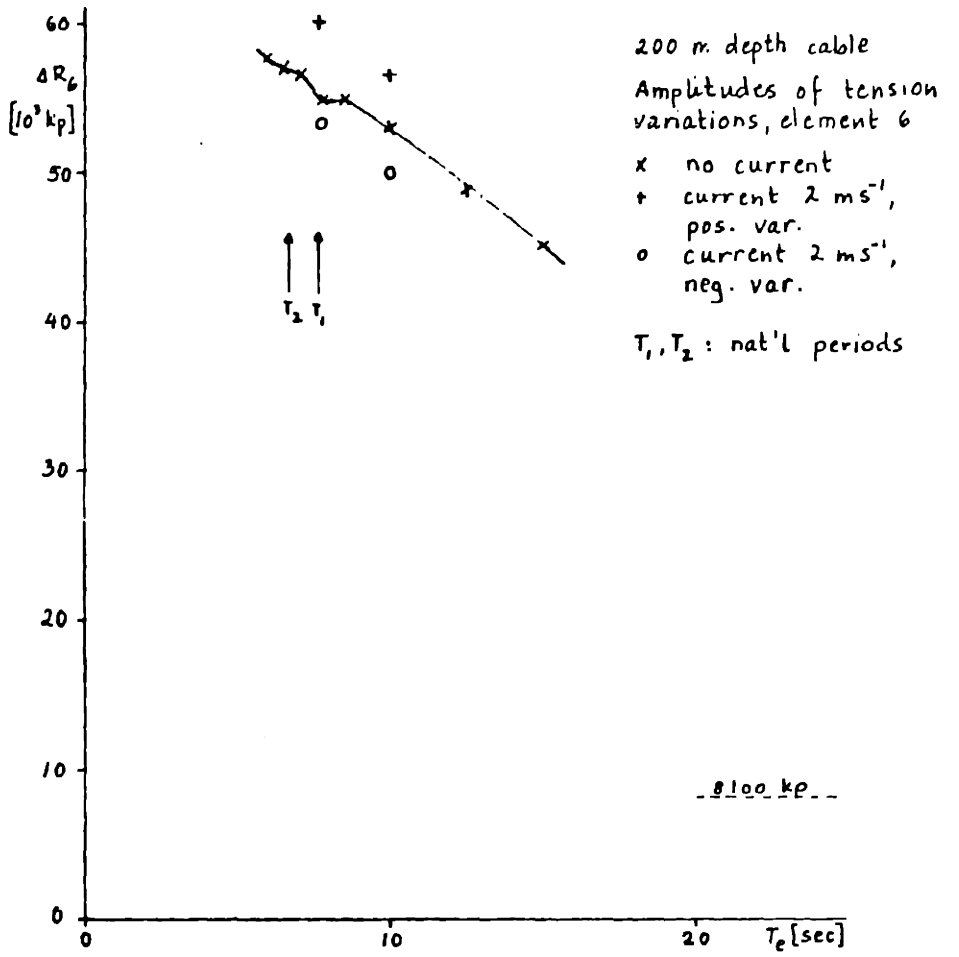

Upper end excitation

$x_0 = 2.0 \sin(\omega t + \frac{\pi}{4})$ [m]

$y_0 = 2.5 \sin \omega t$ [m]

Fig. 8.5.9

Tension Variation Amplitudes as Function of T_e, 200 m Depth Cable

periods and amplitudes used in the analyses. Because of the square dependence of drag forces on the velocities, one can expect the mass forces to be relatively more important with smaller excitation amplitudes.

For comparison, the mentioned communication from E. Furuholt showed a tension amplitude of 46300 kp for the 200 m depth cable at T_ℓ=9.3 sec. Our result from Fig. 8.5.9 is 54000 kp, which is 17% higher.

In the figures are also shown some results, reflecting the effect of currents. With zero current, the positive and negative variations of the tension were approximately equal. This was not the case with current. For the 500 m depth cable the current applied was linearly varying from 1 ms^{-1} at the upper node to zero at the bottom, for the 200 m depth cable the current was 2 ms^{-2} at the upper node. A positive current is moving in the positive x-direction, cf. Figs. 8.5.2 and 8.5.3. It is seen that the presence of the (positive) current will increase the positive tension variation and decrease (numerically) the negative tension variations. This is assumed to be caused by a non-linear effect, similar to the average drift force in Sec. 8.4, except in this case we have not always $|\dot{y}|<V$, especially near the bottom.

Fig. 8.5.9 indicates that for excitation periods of 9 sec. or lower and without current, the negative tension variation becomes numerically larger than the static tension,

which is 54000 kp for element 6. This predicts the possibility of a slack occuring in the cable under excitations of the assumed magnitude. In its present version, the computer program has no provision for realistically representing the occurrence of negative total tensions.

Variation of Excitation Amplitudes

An analysis was made to study the effect of varying the excitation amplitudes. Two cases of current were studied for the 500 m depth cable, one with zero current, the other with a current linearly varying from 2 ms^{-1} at the upper node to zero at the bottom.

Fig. 8.5.10 shows the results. The excitation amplitudes were varied by the factor α compared to the basic calculation, and the diagrams show the tension variation amplitude ΔR_6 in element 6 and the transverse displacement amplitude v_6 of node 6 as functions of α. In the case of zero current ΔR_6 and v_6 varied approximately symmetrically about zero. With current, the positive (ΔR_6^+, v_6^+) and negative (ΔR_6^-, v_6^-) amplitudes were different and the mean amplitudes of v_6 are shown in Fig. 8.5.10. The negative displacement amplitudes were larger than the positive.

It is seen that the tension variation is practically proportional to α, while the displacement varies less than

500 m depth cable - varying excitation amplitude.

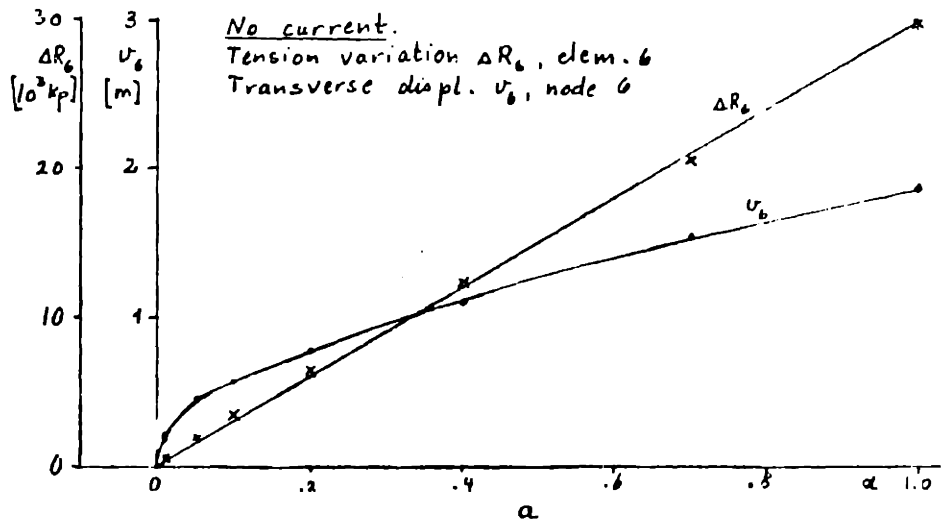

Parameter α defines excitation:

$x_0 = \alpha \cdot 2.0 \sin(\omega t + \frac{\pi}{4})$ [m],

$y_0 = \alpha \cdot 2.5 \sin \omega t$ [m]

of upper end point.

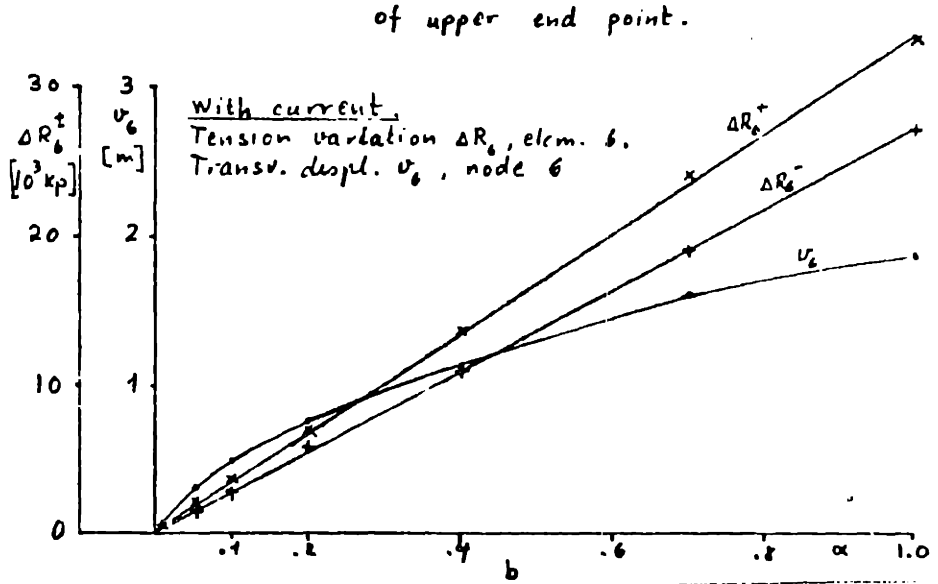

Fig. 8.5.10

Response as Function of Excitation Amplitude

proportional to α. This indicates that the tension variations are mainly determined by the upper end displacements. The transverse displacements are largely controlled by the drag forces, and hence varies less than proportional to α.

Some improvement of linear behavior of v_6 can be observed as a result of the presence of a current for $\alpha<0.1$. An explanation for this small range may be that over most of the cable is the local current velocity less than 2 ms^{-1}, and the component normal to the cable is still smaller, due to the decrease of current with depth.

Accuracy of Longitudinal Displacements

In order to get a good representation of the tension variations in the cable, it is necessary to have a good accuracy in the longitudinal displacements. In the steady state oscillation one can expect the tension variations to be almost evenly distributed along the cable, since an uneven distribution would set up longitudinal stress waves tending to equalize the tension variations. This would be a rapid process due to the large velocity of longitudinal waves of 3039 ms^{-1}.

The longitudinal stiffness of one element of the 500 m depth cable is $AE/L=1.08 \cdot 10^5$ kpm^{-1}. This indicates the sensitivity of the analysis to errors in longitudinal displacements.

An error in the relative longitudinal displacements of the two nodes in an element of 1 cm would result in an error in element tension of 1080 kp. For the 200 m depth cable the sensitivity of tension to errors in relative longitudinal displacementsof the nodes is $2.23 \cdot 10^5$ kpm^{-1}.

In the steady state the tension along the cable varied generally by less than ±5% of the maximum. In a typical case, the 500 m depth cable with excitation period 10 sec, the maximum tension deviationin element 6, 29380 kp, as recorded in Fig. 8.5.8, occurred at time 31.5 sec. At the same time, the distribution of tension over all elements varied between 30130 kp and 28310 kp. The following table shows this distribution.

Element	1	2	3	4	5	6	7	8	9	10
ΔR[kp]	30130	30080	29970	29820	29630	29380	29060	28690	28310	28440

TABLE 8.5

Effect of Internal Viscosity

Some calculations were repeated with lower internal viscous damping. The main effect of this was to increase the time required to reach a steady state of vibration, while the tensions and displacements in the steady state were only little

changed.

In a repeated calculation for the 500 m depth cable with internal friction reduced by a factor 0.1 and excitation period T_e=10 sec, the tension seemed to have approximately reached a steady state after about 20 sec. The calculated tension amplitude in element 6 was 30300 kp, compared to 29380 for the basic calculation. The transverse displacement amplitude of node 6 at 24.5 sec was 1.95, compared to 1.93 in Fig. 8.5.6.

With damping reduced by the factor 0.01 of the basic value, an attempt was made to "smooth" the transition from the initial state to the steady state excitation during a period of 2 sec. In this case an approximately steady response was reached after about 50 sec. The steady state tension amplitude was about 29950 kp and the maximum transverse displacement of node 6 was 1.90 m. There was no current with these calculations.

In view of the uncertainty associated with values of internal damping, it seems fortunate that the steady state results seem relatively insensitive to the value used.

We can estimate the maximum viscous force occurring during a cycle. For the 500 m depth cable with excitation period T_e=10 sec, the maximum strain is $\dot{\varepsilon}_{max}=1.2\cdot10^{-3}$, hence the maximum strain rate of change is $\dot{\dot{\varepsilon}}_{max}=0.7\cdot10^{-3}s^{-1}$. The maximum friction force is 1550 kp, with the basic viscous

coefficient $c_v = 4.72 \cdot 10^0$ kps m^{-2}. This force is about 5% of the maximum elastic tension, and there is a 90° phase difference in time between the friction force and the elastic tension.

In view of the finding of experimental data on internal damping of wire ropes after the calculations were done, it appears that it is not practical to calculate the transient response for a real time of up to maybe 100 seconds before a steady state is reached. A practical solution to this problem would be to design the computer program such that a steady state is reached in a relatively short time with a large coefficient of viscosity, after which a lower viscosity is used in the final calculation. This would be a method to approximately produce a realistic initial condition for the harmonic response.

Both for the pull tests and for the harmonic response, the use of large values of the internal damping coefficients tended to smoothen out the results, compared to using lower damping coefficients. The drawback of this is that transient tension peaks may not be sufficiently well described. On the other hand, by freeing the results of transients, one can describe the "dominant" response to the given excitations.

If one is interested in analyzing for possible transient peaks, a realistic value for the internal damping must be used. One must then also account for a possible dissipation at the lower end, due to cable resting on the sea floor.

8.5.5 Energy balance.

We can make an overall control of the analysis by computing the energy transport into and out of the system. The enrgy input is the work done by the reaction force at the upper end. The output is the energy lost due to the external drag force and the internal viscous forces in the cable.

The check was made for the 500 m depth cable with excitation period T_e=10 sec and no current. The data used are extracted from the computer output and some approximations are necessarily made in the manual analysis. It is assumed that in the steady state the transverse displacement of each node is varying harmonically between extreme values $+a_1$, $-a_2$ with amplitude $A= \frac{1}{2}(a_1+a_2)$ and with excitation period T_e=10 sec. The time interval from 25 to 35 sec was chosen for analysis. The vibrations were not completely symmetric about equilibrium, so that the extreme values a_1,a_2 are usually different, as also appears from Fig. 8.5.7. Typical values are a_1=+1.88m, $-a_2$=-1.74m (node 6).

The energy output from the system comes from the effects of drag resistance to the transverse motion (W_D) and the internal dissipation due to internal friction (W_I). The drag losses were computed from the calculated transverse oscillations of the nodes. These calculations were done for each element, and the effect of the phase differences between

neighboring nodes was disregarded. The energy loss from drag is proportional to the amplitudes to the third power.

The energy input is due to the work of the reaction force at the upper end. This reaction force is composed of contributions from the elastic tension and viscous force of the upper element and also the reaction force against the drag on the upper element. The drag forces of the other elements are transmitted to the reaction via the tension. $(R^{o}+\Delta R)\vec{t}$ is the elastic tension, $V\vec{t}$ is the viscous axial force, $N\vec{n}$ is the reaction force at the upper node from the drag force of the upper element, where $\vec{t},\vec{n}$ are directions tangential and normal to the upper element. Hence the total reaction force is $\vec{F}_R=(R^{o}+\Delta R)\vec{t}+V\vec{t}+N\vec{n}$. When $\vec{v}$ is the velocity of the upper node, the work of the reaction force is

$$W_F = \int_{T_1}^{T_2} \vec{F}_R\cdot\vec{v}\,dt = \int_{T_1}^{T_2}(R^{o}+\Delta R)\vec{t}\cdot\vec{v}dt+\int_{T_1}^{T_2} V\vec{t}\cdot\vec{v}dt+\int_{T_1}^{T_2} N\vec{n}\cdot\vec{v}dt\ .$$

where T_1=25 sec, T_2=35 sec.

Let $\vec{t}^{o},\vec{n}^{o}$ be the tangent and normal directions in equilibrium. Since $\vec{t}$ and $\vec{n}$ vary with time, we can write $\vec{t}=\vec{t}^{o}\cos\psi + \vec{n}^{o}\sin\psi$ and $\vec{n}=-\vec{t}^{o}\sin\psi +\vec{n}^{o}\cos\psi$, where $\psi(t)$ is the angle between $\vec{t}$ and $\vec{t}^{o}$. Hence we set:

$$\int_{T_1}^{T_2}(R^{o}+\Delta R)\vec{t}\cdot\vec{v}dt = \int_{T_1}^{T_2}(R^{o}+\Delta R)\cos\psi\vec{t}\cdot\vec{v}dt + \int(R^{o}+\Delta R)\sin\psi\vec{n}\cdot\vec{v}dt$$

As $\cos\psi \approx 1$ and $R^o = \text{const}$, $\int_{T_1}^{T_2} R^o \cos\psi \vec{v} dt = 0$. Then we have the work against R:

$$W_R = W_E + W_G ,$$

where

$$W_E \approx \int_{T_1}^{T_2} \Delta R \vec{t}^{\,o} \cdot \vec{v} dt$$

can be interpreted as work against the elastic stiffness forces, and

$$W_G = \int_{T_1}^{T_2} (R^o + \Delta R) \sin\psi \vec{n}^{\,o} \cdot \vec{v} dt$$

as work against the geometric stiffness forces.

The work against the viscous forces

$$W_V = \int_{T_1}^{T_2} V\vec{t} \cdot \vec{v} dt$$

can be treated similarly.

The drag force reaction work is

$$W_D' = \int_{T_1}^{T_2} N\vec{n} \cdot \vec{v} dt .$$

In carrying out the integrations to find W_E, W_G and W_V, Simpson's rule was used with time interval 0.5 sec. Values

for the integrand were taken from the computer output. The following results were obtained:

Energy input:

Work against elastic stiffness:	W_E = 76032 kpm
Work against geometric stiffness:	W_G = 2561 kpm
Work against viscous force:	W_V = 13077 kpm
Work against drag force reaction:	W_D' = 3496 kpm
Total input:	W_1 = 95166 kpm

Energy output:

External drag losses:	W_D = 87115 kpm
Internal viscous losses:	W_I = 13423 kpm
Total output:	W_2 =100583 kpm

The calculated difference between input and output is about 5%. Part of the difference may be explained as a result of disregarding phase differences in computing the external drag losses. Another possible error source is the assumption of harmonic variation of the transverse displacements. However, it is not easy to predict in which direction this error works, since the displacements recorded in Fig. 8.5.6 show no appreciable deviation from harmonic.

Due to the large value used to the internal damping, the contributions W_V and W_I have become artificially large. However, the two contributions are approximately of the same magnitude, and hence using different values for the internal damping would not be expected to change the balance between energy input and output.

CHAPTER 9. Summary and review.

9.1 Review of Calculation Model.

The present work is aimed at obtaining a numerical model for dynamic analysis of cables, with a special view to mooring systems. We have the view that the particular nature of the dynamic cable system makes it different in some respects from the classical linear, low damped vibration problem. Some established truths for such systems had to be reconsidered.

The method in itself has a large degree of flexibility in varying the cable parameters in dependence of the state of the system. For example, the cross sectional area may be considered as a function of the instantaneous tension (or strain), or the drag coefficient may be considered as a function of the instantaneous local velocity.

The cable is to a first approximation considered as a linear system, according to eq. (5.6.1), with corrections due to non-linearities included in the "force" term of the right hand side. Both transverse and longitudinal displacements are represented in a coupled system. The integration over time is done stepwise with a systematic trial and error iteration process to estimate the state at the end of each step. In this process displacements, velocities and accelerations are expressed first in terms of the normal coordinates. They are then transformed back to global coordinates for calculation of forces. The forces are again transformed to the normal coordinates for use in the equations of

motion. Thus there is a continuous transformation between global and normal coordinates during iteration.

The normal coordinates $\underline{y}$ in Ch. 5 were defined i terms of the normal modes of free oscillations of the undamped, linearized natural vibration problem. It is, however, important to note that because of the mathematical properties of the solutions of the eigenvalue problem (5.4.1), we can interpret the relation (5.4.4) as defining $\underline{y}$ as a new set of generalized coordinates for the n-dimensional vector space of displacements $\underline{R}$, relative to the eigenvectors $\underline{q}_i$ as basis. In this sense, the normal coordinates are independent of the eigenvalues $\lambda_i = \omega_i^2$. For numerically computed eigenvectors, the criterion of accuracy is the mass orthonormality relation (5.4.2a). These eigenvectors represent the best that can be obtained within the given finite element model. This normal coordinate description is mathematically equivalent to a description in terms of the global coordinates $\underline{R}$, provided a satisfactory accuracy has been obtained according to (5.4.2a). Naturally, the reason for choosing these generalized coordinates is the simple form obtained for the transformed equations of motion (5.5.2b) or (5.6.1).

For design purposes, it may be desirable to take into account the dependence of the drag coefficient on the instantaneous velocity. Such an improved hydrodynamic model may be obtained by assuming the drag coefficient to be a function of

Reynolds number, in a similar manner to the drag coefficient of a stationary body in a constant current, see e.g. Newman [30]. This approach was used by Webster [19] and also suggested by Williams [32]. However, most experimental data for the drag coefficient as function of Reynolds number are based on the assumption of a fixed body in a constant current or a body executing small amplitude oscillations in a constant current, i.e. steady conditions. This assumption is not satisfied for a cable executing large oscillations, since the cable velocity is continously varying. For a more refined analysis, one can also take into account vortex shedding effects (strumming), i.e. the dependence on the Strouhal number. Some efforts to treat these effects may be found in Griffin [31], but again considerations must be made of the unsteady conditions around a cable with varying velocity, as well as the different surface conditions of a relatively smooth wire rope and a chain. In the example shown in Fig. 8.5.6, Reynolds number varies between zero and 10^5 in a time interval of 2.5 sec.

For many real moorings is the boundary condition at the lower end more complicated than has been assumed here, as there is a length of cable (or chain) resting on the sea floor leading up to the anchor. During motion, part of the cable will be lifted from or laid down to rest on the sea floor. The detailed mechanics of this is complicated and some approximation may be necessary to represent it. One can either try to make a

dynamical model of this part, included in the cable model, or try to simplify by constructing an approximate spring-damper model to represent this lower end boundary condition.

The examples in Sec. 8.1-4 are intended to give an impression of the accuracy of results obtained by the model. In Sec. 8.1 and 8.2 it was found that the accuracy of the calculated natural frequencies decrease with the higher modes, the error in the highest transverse mode in Sec. 8.2 being about 18%. As a consequence of these frequency errors, the computed time evolution of the system in Sec. 8.2 deviates more and more from the analytical with time. On the other hand, in Sec. 8.4 all normal coordinates execute forced motion of the same period. In this case the periodic repetition of the motion is good, and the wave speed and wave length correspond well with linearized theory. The example in Sec. 8.3 shows that the effect of tension increase due to large transverse displacements is represented with good accuracy.

These results indicate the tentative conclusion that forced, steady motions are represented with better accuracy than free or transient motions, since the period of motion is determined by the excitation period and is independent of the eigenfrequencies, which may be erroneous for the higher modes.

In Sec. 6.3 the general rule about the selection of time step length was given that it should be small compared to the smallest dominant period T_c of the motion, say less than $T_c/16$. This rule seems fairly straightforward in a steady state forced

motion, when the system is oscillating with the excitation period and no transient, free motion remains. However, in situations where transient phenomena are involved, the concept of dominant period is not clear. In that case the time step length must to some extent be chosen on the basis of experience. If convergence is not obtained with one time step, one must try smaller steps until convergence is obtained.

The importance of choosing the time step lies in the convergence of the iteration process to determine the state at the end of the time step. Essentially, as outlined in Ch. 6, this iteration assumes a certain state at the end of the step, and, based on the displacements, velocities and accelerations in this state, the corresponding forces are computed. These forces then give the right hand sides of eqs. (5.5.2b) or (5.6.1). The assumed state is then checked for kinematical and dynamical compatibility with the known initial state of the time step. For the equations of motion the "force" terms are assumed to vary linearly in the time interval of the step. The equations of motion are integrated by finding the homogeneous solution, representing the free motion, and the particular solution, representing the forced motion. The constants of integration are determined from the known state at the beginning of the step. The criterion for compatibility is that the new derived state is sufficiently close to the assumed state, and this condition is to be satisfied simultaneously

for all normal coordinates used. If sufficient compatibility is not achieved, a new iteration must be made with a new assumed end state.

The easiest choice for the new assumed state is the last derived state. This was recommended by Newmark [29] , see Sec. 6.2. However, a modified method was also tried, where the new assumed state was taken as the average of the derived states of the two last iterations. This modification tended to improve the convergence of the iterations. The most important reason for slow convergence, or even divergence, was found to be the sensitivity of the tension force to errors in the longitudinal displacements.

It appears that the crucial point of the iteration is the determination of the new assumed state. Hence, if improved methods can be developed to find the new assumed state, this may allow the use of larger time steps.

For the cables analyzed in Sec. 8.5 the general time step was 0.25 sec, except for the starting phase, when steps down to 0.01 sec were used. A time step of 0.50 sec was also tried, but this resulted in divergence of the iterations. It was also tried to repeat a calculation with the shorter time step of 0.10 sec for some time period. This resulted only in small changes in the results. It was also experienced that the iterations converged more rapidly with the shorter time step. No systematic investigation into the effect of using different

time steps were made, so the conclusions made are only indicative.

The cables analyzed in Sec. 8.5 are fairly large by present-day technology and were selected because data were available for comparison. It can also be noted that these cables have a relatively small initial curvature. We find that the models used with ten elements and a general time step of 0.25 sec seem to give a satisfactory representation under the steady state conditions considered.

For other mooring cables the conditions will differ. The factors influencing the choice of finite element model are tension, length and initial curvature. The practical choice is a matter of experience, similarly to other applications of the finite element method. Since curvature is an important parameter, and the continuous curvature of the cable is represented by the discontinuous changes of direction between adjoining straight elements, it is reasonable to assume that a finer model, i.e. with more elements, should be used to represent a cable with larger initial curvature.

Also the form of excitation may influence the choice of model. In the ocean environment, the steady excitations considered typically contain periods from about 5 sec upwards to around 20 sec. Real mooring cables may have linearized natural periods in this range, as illustrated by the examples in Sec. 8.5. However, the longitudinal natural periods are usually below this range. Whether resonances occur, depends

on the amount of damping. For the examples in Sec. 8.5 it was found that the damping is sufficiently large to suppress resonances with excitation amplitudes of about 2 meters. We feel that under such steady, long period excitations should normally the excitation period not influence the choice of model, and the representation of geometry is the most important consideration.

Some cases of non-steady excitation may also be of interest. For example, one may be interested in the effect of a single, large wave in a train of smaller waves. The transient response of the moored vehicle will be given as input for calculation of the transient mooring cable response. The pull tests analyzed in Sec. 8.5 show crude examples of such transient analysis and indicate that the transient tension peak may be larger than would be predicted by a quasistatic analysis. If there are significant high frequency components in the transient excitation, the model should be such that natural periods of the cable close to such significant excitation periods have a reliable representation. In general, analysis of excitations with low period components can be expected to require a finer model than long period, steady excitations.

In the calculation examples of Ch. 8 a large number of normal coordinates were generally used. This may seem contrary to common practice for dynamic analysis, where it is assumed that a sufficiently accurate representation of the response can

be obtained in terms of a limited number of normal responses. This is usually a question of the accuracy required. It seems obvious that better accuracy is obtained by using more modes. This may be understood from the interpretation of the normal coordinates as new generalized coordinates, provided the mass orthonormality relation (5.4.2a) is satisfactorily fullfilled for all eigenvectors considered.

The particular case of the mooring cable of Sec. 8.5 also presents some additional particlular problems in this respect, because the tension variations are represented in terms of the relative longitudinal displacements between the nodes. Hence, it is necessary to include at least some of the longitudinal modes. Furthermore, since the forces in the system depend on the displacements, velocities and accelerations, it is necessary to have a good representation of the displacements, velocities and accelerations. This is especially the case with regard to the tension force, which is sensitive to errors in the longitudinal displacements. Also it should be considered that the normal coordinates are coupled, such that by excluding one coordinate the response of the others may be changed.

To compare the present method with other, similar analyses, one should have detailed information about the mathematical methods as well as the technical problems encountered in implementing and applying the method. The work most closely

related to the present is, to our knowledge, that carried out at the Ship Research Institute of Norway by E. Furuholt. That model takes given displacements of the upper end as boundary condition and calculates displacements and tension as functions of time. We repeated one of these analyses (Sec. 8.5) and got tension deviation amplitudes 17% larger. One reason for the difference may be that the work of Furuholt takes into account lifting of the bottom segment of the cable.

Websters [19] work is not in particular concerned with mooring problems, so a direct comparison of results is not possible. He uses a direct integration method. In our judgement his method is equivalent to ours. The differences may lie in technical details, like potential applications or the time step required by the integration technique. It should also be noted that the calculation examples given do not show the tension variations, which we believe to be the most difficult part of the analysis. More information for comparison will be obtained when more experience has been gained in using the methods.

9.2 Review of Calculation Results.

Some surprising results were obtained for the cables analyzed in Sec. 8.5. In particular the following points should be given some further discussion: 1) the ordering and mode shapes of the two lowest transverse mode shapes in

Fig. 8.5.4a, 2) the lack of resonance behaviour in Fig. 8.5.8 and 8.5.9, 3) the almost sinusoidal transverse motion of the cable in Fig. 8.5.6, in spite of the velocity squared dependence of the transverse drag force.

In Fig. 8.5.4a the lowest frequency mode shape has one node near the middle (S-shape), while the mode shape most similar to the lowest mode of a straight string under constant tension (U-shape) has the next lowest natural frequency. In order to estimate the influence of elasticity on the natural mode shapes, we made one calculation, where the elastic modulus was arbitrarily increased by a factor of 1000. In this case the U-shaped mode had its frequency increased by a factor of about 30, while the other transverse modes had much smaller changes. The U-shaped mode now had the highest frequency of all transverse modes. Hence we made the conclusion that the higher frequency of the U-shaped mode was caused by the initial curvature of the cable, necessitating extension of the cable, while all other transverse modes also have compensating longitudinal displacements and thus less extension and are consequently less influenced by the cable elasticity.

Compared to the simple, straight inelastic string under constant tension, the cable has at least three additional parameters which influence the mode shapes: initial curvature, variable tension and longitudinal elasticity. These factors make it difficult to anticipate the mode shapes.

According to Sec. 5.4 the mode shape matrix $\underline{\underline{Q}}$ should satisfy the mass orthonormality condition $\underline{\underline{Q}}^T \underline{\underline{M}}\ \underline{\underline{Q}} = \underline{\underline{I}}$ = unit matrix, when the eigenvectors are properly normalized. By normalizing the eigenvectors such that the diagonal terms of the triple matrix product were all 1, the off-diagonal components were of the order 10^{-12} or smaller in our calculation. This mass orthonormality check is taken as a verification of the correctness of the eigenvector calculation.

The lack of resonance appearance in the tension vs. excitation diagrams in Fig. 8.5.8 and 8.5.9 indicates a strong non-linear damping on the cable, such as to suppress resonance behaviour even close to the natural periods for the linearized system. This indicates that the motion is dominated by the tension and drag forces under these excitation amplitudes, while inertia forces only play a minor role. As a comparison Fig. 8.5.5c also shows a strong drag force compared to the inertia force after the system has been set into motion. It can also be noted that for a linear system does resonance amplification only occur for low damping.

As the drag force is assumed to have a square dependence on the cable transverse velocity, one may expect to obtain some degree of resonance behaviour with smaller excitation amplitudes, when the drag is less dominant over the inertia force. In testing the program we made some calculations on the 500 m depth cable with smaller excitation amplitudes.

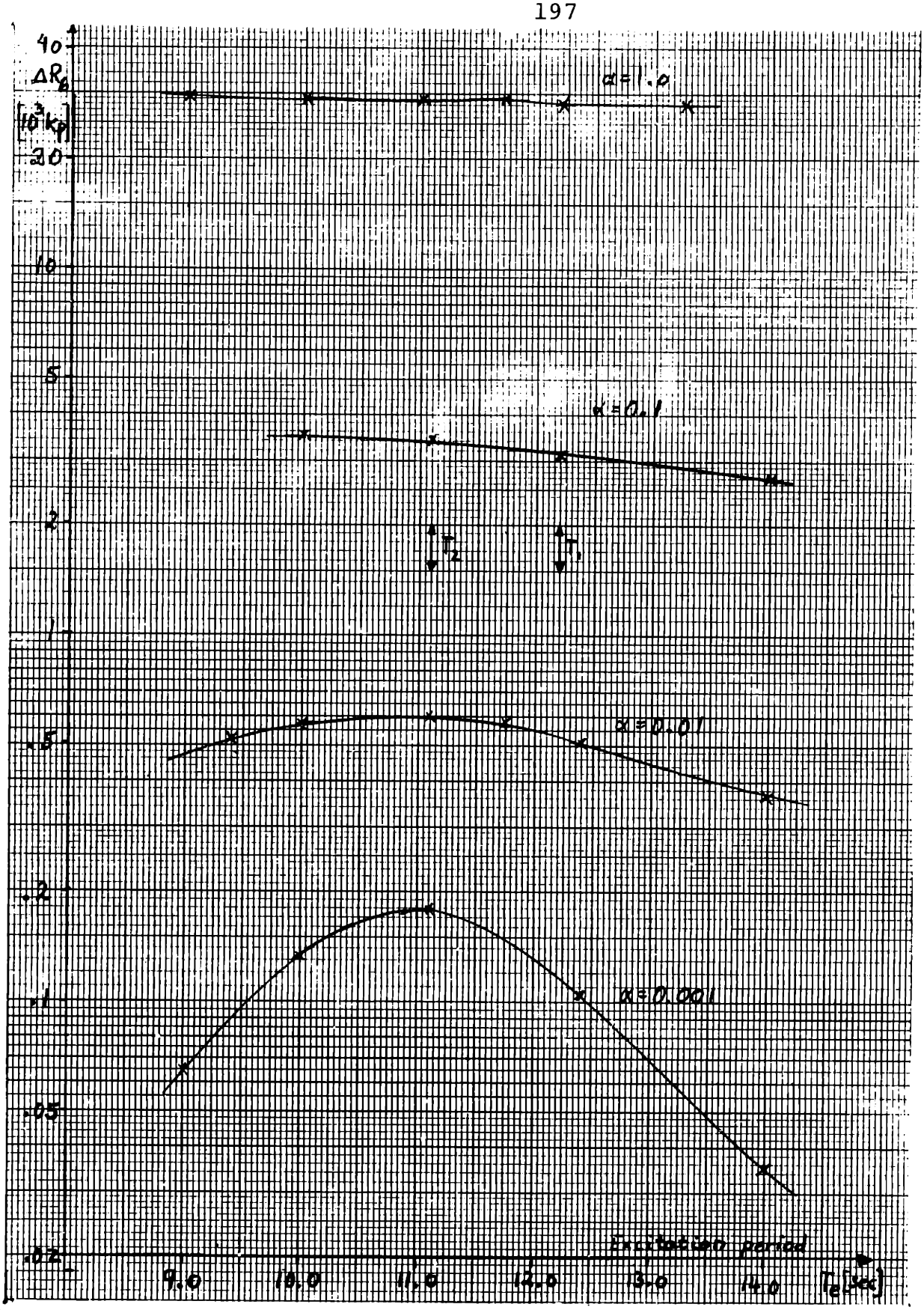

Fig. 9.2.1
Tension response for different excitation amplitudes.

With the amplitudes decreased by a factor of 10 (α=0.1), the behaviour around the natural periods of 11.09 sec and 12.42 sec seemed to have a similar character of Fig. 8.5.8 with no resonance appearance. With the excitation amplitudes decreased by a factor of 100 (α=0.01) there appeared a weak resonance amplification around the natural periods. Finally, with the excitation amplitudes decreased by a factor of 1000 (α=0.001) a still larger amplification appeared around the natural periods. The magnification was largest at the second natural period (11.09 sec). The corresponding normal coordinate has the largest response amplitude, cf. Fig. 8.5.7a. A comparison for the various excitation amplitudes is shown in Fig. 9.2.1.

Fig. 8.5.6 shows the time dependence of the transverse motion at some selected points along the cable. It is somewhat surprising to find that this motion seems to be practically sinusoidal when the drag force varies as the square of the transverse velocity. A complete consideration of this question must include the tension variations, which are shown in the lowest diagram of Fig. 8.5.6. It appears that the tension deviation goes through zero from negative to positive at about 18.5 sec and has a maximum at about 21 sec. The transverse displacements go through zero from negative to positive at about 21.5 sec. Hence the tension deviation is almost at a maximum when the transverse velocity, and conse-

quently the drag force, is a maximum. This tension deviation (i.e. the transverse force component) acts in opposition to the drag force.

An analogous system to this transverse motion is a simple oscillator with velocity squared drag resistance, see Fig. 9.2.2a.

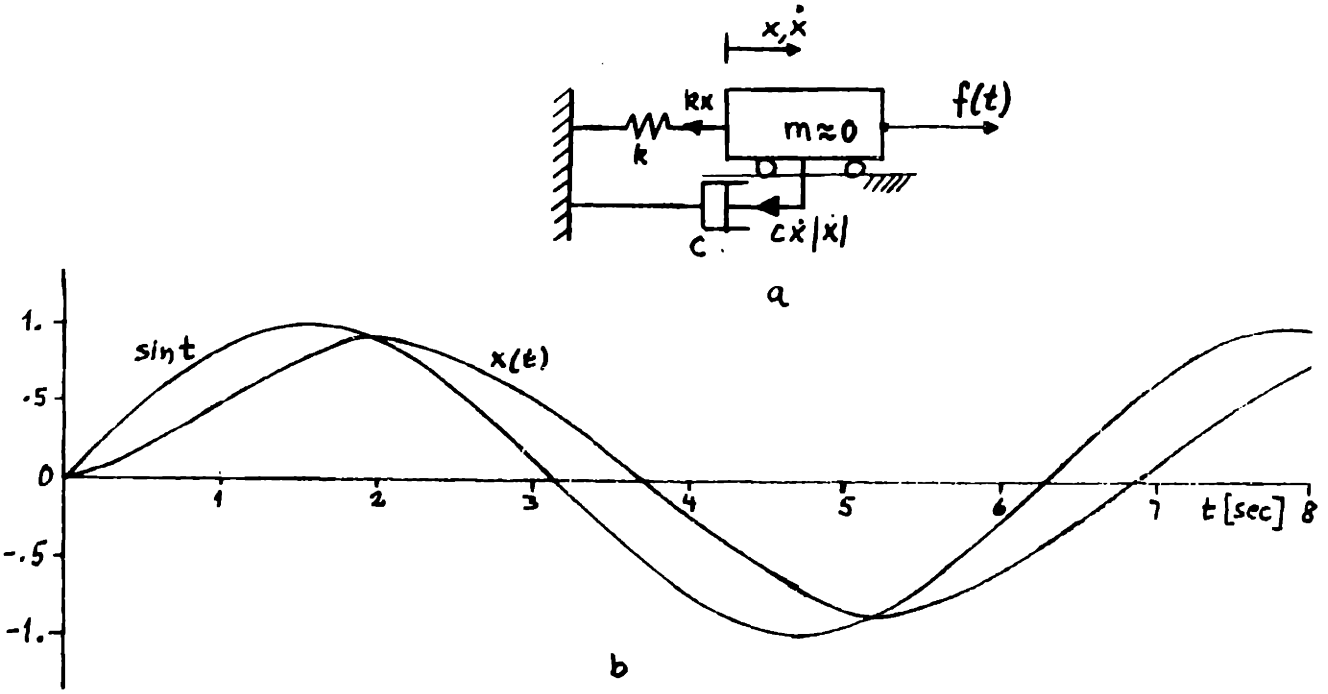

Fig. 9.2.2
Simple oscillator analogy to transverse motion.

The equation of motion for this system may be written

$$m\ddot{x}+c\dot{x}|\dot{x}|+kx-f(t)=0.$$

We let f(t)=sin t and put for simplicity c=k=1. We also assume the inertia forces to be negligible, m=0. Starting from the initial condition x(0)=0, a numerical integration up to t=8 sec gives the response shown in Fig. 9.2.2b. It is seen that the response x(t) has a sinusoidlike shape.

9.3 Suggestions for Further Work.

As the application computer program used in this work was made simple in order to concentrate on the elementary parts of the mechanical finite element model, several improvements must be made in order to expand it into a design program.

A better hydrodynamic model should be implemented, representing the variation of the drag coefficient with the relative velocity between the cable and water. This will involve studying drag forces under non-steady conditions and for complicated cross sections like a chain.

The accuracy obtainable should also be assessed, dependent on the fineness of the model and the time step used in integration. For this one can find some useful results from accuracy studies of other problems analyzed by finite elements, see e.g. Zienkiewicz [9] . The accuracy estimates must be based on comparison with solutions obtained by other, more exact methods. The calculations in Sec. 8.1-4 are examples of such comparisons. Comparisons for simple systems, like the straight string under constant tension, may be taken as indicative of more complex systems, like the mooring cable with initial curvature and variable tension, where exact solutions are not known.

As the computer program was limited to two-dimensional configurations, an extension to three-dimensional analysis may be useful. The programming principles will be similar, but

the computational efforts will be larger, due to the larger number of degrees of freedom.

One may further investigate whether it is feasible to expand the method, here employed for analyzing a single cable, into a complete analysis of a total mooring system. The results obtained from such a model may contain too much detail for practical purposes, so methods should be devised to simplify the analysis to the degree of accuracy needed in design.

Also the interaction between the velocity and acceleration fields of propagating waves and the cable should be included. This will involve adding the velocities induced by the waves to the current velocity for calculation of the drag force, and calculating the forces induced by water acceleration according to Sec. 2.3.

A better representation should be made of the boundary condition at the lower end in many practical cases, where a length of cable (or chain) is lying on the sea floor up to the anchor. It was suggested before to try to represent this by means of a spring-damper system.

On the programming side, the number of elements should be increased, say to 50 or 100, and it should be possible to include concentrated masses, e.g. instrument packages, on the cable.

APPENDIX A

Listing of MAIN program and subroutine TIMINT.

```
      DIMENSION EK(24,24),GK(24,24),MM(24,24),X(12),Y(12),FK(24,24)
      DIMENSION FM(24,24),HK(210),HM(210),AUX(600),D1(20),D2(20),R0(20)
      DIMENSION R1(2,2),R2(2,2),B1(2,2),B2(2,2),RT1(2,2),RT2(2,2)
      DIMENSION RL(11),RM(11),T1(2),T2(2),T3(2),EV(20,20),IND(20)
      DIMENSION COS1(12),COS2(12),XV(12),YV(12),XV0(12),YV0(12)
      DIMENSION RT(11),AR(11),ER(11),RV(11),CM(11),CD(11),DN(11)
      DIMENSION RO(11),WAV(40),MP(2),NMG(10),NML(10)
      DIMENSION RMG(70),RML(70),DC(11)
      DIMENSION XV1(12),YV1(12),XACC(12),YACC(12),FB0(24),FB(24),
     1          EPS1(20),FDIS(20)
      DOUBLE PRECISION HK,HM,AUX,D1,D2,R0,EV,EPS
      DOUBLE PRECISION R1,R2,RT1,RT2,FK,FM,RL,RM
      DOUBLE PRECISION EK,GK,MM,T1,T2,T3,B1,B2
      IDCH=0
      READ(5,10) NEL,ITRANS,ROW,ML,MH,EPS,GRAV,IPM1,IPM2,NTIM
   10 FORMAT(2I4,F8.2,2I4,2F8.2,5I4)
      READ(5,17) IDRA,IDIS,NWAV,NULL,DEPTH
   17 FORMAT(4I4,F8.2)
      MP(1)=IPM1
      MP(2)=IPM2
      NNOD=NEL+1
      WRITE(6,15) NEL,NNOD,ROW,GRAV,IPM1,IPM2,ML,MH,NTIM
   15 FORMAT(5X,14H GENERAL DATA:  ,//,5X,
     1         28H NUMBER OF ELEMENTS:          ,I4,/,5X,
     2         28H NUMBER OF NODES:             ,I4,/,5X,
     3         28H WATER WEIGHT:                ,E10.3,/,5X,
     4         28H GRAVITY ACCELERATION:        ,F8.2,/,5X,
     5         28H NO. OF GLOBAL POINT MASSES:  ,I4,/,5X,
     6         28H NO. OF LOCAL POINT MASSES:   ,I4,/,5X,
     7         28H LOWEST EIGENFREQUENCY:       ,I4,/,5X,
     8         28H HIGHEST EIGENFREQUENCY:      ,I4,/,5X,
     9         28H NO. OF TIME STEPS:           ,I4)
      WRITE(6,16)  IDRA,IDIS,NWAV,DEPTH
   16 FORMAT(5X,28H DRAG INCLUDED. IDRA=         ,I4,/,5X,
     1          28H LARGE DISPLACEMENTS. IDIS=  ,I4,/,5X,
     2          28H NUMBER OF WAVES: NWAV=      ,I4,/,5X,
     3          28H DEPTH TO ORIGIN:            ,E10.3)
      NDOF=2*NNOD
      N1=2*NNOD
      DO 20 I=1,N1
      DO 20 J=1,N1
      EK(I,J)=0.D0
      GK(I,J)=0.D0
      FK(I,J)=0.D0
      FM(I,J)=0.D0
   20 MM(I,J)=0.D0
C
C       COMPUTE STIFFNESS AND MASS MATRICES.
C
      WRITE(6,14)
   14 FORMAT(//,14H ELEMENT DATA:  ,/,117H  N1   N2       X1        Y1
     1  X2        Y2    TENSION   AREA    DIAM     E-MOD.    DENSITY      CM
     2         CD        DC    ,/)
      ROW=ROW/GRAV
      CALL ELEMAT(X,Y,RL,RT,AR,DN,ER,EK,GK,MM,NEL,ROW,RO,GRAV,CM,CD,DC)
      IF (IPM1) 100,100,80
   80 IL=1
      DO 90 I=1,IPM1
      IH=IL+6
```

```
      READ(5,81) NMG(I),(RMG(N),N=NL,NH)
   81 FORMAT(I8,7F8.2)
      WRITE(6,82) NMG(I),(RMG(N),N=NL,NH)
   82 FORMAT(20H POINT MASS AT NODE:    ,I6,2X,5H RMG= ,2X,7(2X,F8.2))
      I1=2*NOD-1
      MM(I1,I1)=XW/GRAV*MM(I1,I1)
      I1=I1+1
      MM(I1,I1)=YW/GRAV*MM(I1,I1)
   90 IL=IL+7
  100 CONTINUE
      DO 150 J=1,NDOF
      DO 150 I=J,NDOF
      EK(I,J)=EK(J,I)
      GK(I,J)=GK(J,I)
      MM(I,J)=MM(J,I)
  150 CONTINUE
C
C      TRANSFORM TO INTRINSIC(LOCAL T-N) CABLE COORDINATES.
C
      CALL MATTRA(X,Y,RL,T1,T2,T3,B1,B2,EK,GK,MM,FK,FM,RT1,RT2,R1,R2,
     1            COS1,COS2,NEL,NDOF)
      IF (IPM2) 390,390,370
  370 NL=1
      DO 380 I=1,IPM2
      NH=NL+6
      READ (5,371) NML(I),(RML(N),N=NL,NH)
  371 FORMAT(I8,7F8.2)
      WRITE(6,372) NML(I),(RML(N),N=NL,NH)
  372 FORMAT(2X,20H POINT MASS AT NODE:   ,I6,2X,5H RML= ,2X,7(2X,F10.4))
      I1=2*NOD-1
      FM(I1,I1)=TW/GRAV*FM(I1,I1)
      I1=I1+1
      FM(I1,I1)=RW/GRAV*FM(I1,I1)
  380 IL=IL+7
  390 CONTINUE
      DO 385 I=1,NDOF
      DO 385 J=1,I
  385 FM(I,J)=FM(J,I)
  351 FORMAT(4H FK=,10(2X,D10.2))
  352 FORMAT(4H FM=,10(2X,D10.2))
C
C      COMPUTE EIGENVALUES AND MODE SHAPES.
C
      CALL EIGCAL(HK,HM,FK,FM,AUX,D1,D2,R0,EV,IND,NNOD,ML,MH)
      IF (NTIM) 1000,1000,480
  480 CONTINUE
      NEV=MH-ML+1
C
C      DO TIME INTEGRATION.
C
      CALL TIMINT(AUX(1),AUX(21),AUX(41),AUX(61),AUX(81),AUX(501),
     1            AUX(521),AUX(541),AUX(561),X,Y,AUX(103),
     2            AUX(105),AUX(107),AUX(133),
     3            AUX(139),AUX(145),AUX(151),AUX(157),AUX(163),
     4            AUX(119),AUX(109),R1,AUX(169),AUX(171),EK,GK,MM,
     5            FK,FM,MP,NMG,NML,RMG,RML,AUX(173),AUX(183),
     6            AUX(193),AUX(233),AUX(257),
     7            AUX(203),AUX(441),EV,R0,D1,D2,HK,COS1,COS2,
     8            XV,YV,XV0,YV0,XV1,YV1,XACC,YACC,
```

```
     9              WAV,AUX(281),AUX(377),FB0,FB,FDIS,
     0              AUX(401),AUX(421),RL,RM,RT,RV,AR,DN,ER,RO,CM,
     1              CD,DC,ROW,GRAV,DEPTH,EPS1,IDRA,IDIS,
     2              NNOD,NEV,NTIM,NWAV,IDCH)
1000 CONTINUE
     END



      SUBROUTINE TIMINT(Y0,YD0,YDD0,Y1,YD1,YDD1,Y2,YD2,YDD2,X10,Y10,
     1                  U,UD,UDD,XG,YG,X1,XD1,XDD1,Y11,YD11,YDD11,B,
     2                  Z,ZG,FK,GK,MM,FK,FM,MP,NMG,NML,RMG,RML,
     3                  FV,FP,F,FDR,FDR0,FN1,FN2,
     4                  EV,R0,X,XD,XDD,COS1,COS2,XV,YV,XV0,YV0,
     5                  XV1,YV1,XACC,YACC,WAV,
     6                  FT,FMA,FB0,FB,FDIS,A,C,RL,RM,RT,RV,AR,DN,
     7                  ER,RO,CM,CD,DC,ROW,GRAV,DEPTH,EPS,
     8                  IDRA,IDIS,NNOD,NEV,NTIME,NWAV,IDCH)
      DIMENSION  Y0(1),YD0(1),YDD0(1),Y1(1),YD1(1),YDD1(1),
     1           Y2(1),YD2(1),YDD2(1),X10(1),Y10(1),U(1),UD(1),
     2           UDD(1),RL(1),RT(1),A(1),C(1),B(2,2),X(1),XD(1),XDD(1)
      DIMENSION  FK(24,24),FM(24,24),FV(1),FP(1),F(1),FN1(1),FN2(1),
     1           FV(20,20),R0(1),COS1(1),COS2(1),RV(1),AR(1),
     2           DN(1),ER(1),RM(1),Z(2),ZG(2),CM(1),CD(1),FDR(1),
     4           FDR0(1),FMA(1),RO(1),WAV(1),MP(1),
     5           NMG(1),NML(1),RMG(1),RML(1),DC(1),FDIS(1)
      DIMENSION X1(1),XD1(1),Y11(1),YD11(1),XDD1(1),YDD11(1),
     1          XV(1),YV(1),XG(1),YG(1),FT(1),XV0(1),YV0(1)
      DIMENSION FK(24,24),GK(24,24),MM(24,24)
      DIMENSION XV1(1),YV1(1),XACC(1),YACC(1),FB0(1),FB(1),EPS(1)
      DIMENSION TIM(5),IPRT(5),CV(20),CW(20),ND(20),OM(20)
      DOUBLE PRECISION  FK,FM,EV,R0,RL,RM,FT,ARG,COST,SINT,R1,R2,ADD
      DOUBLE PRECISION FAC,FK,GK,MM,OM
      DOUBLE PRECISION Y0,YD0,YDD0,Y1,YD1,YDD1,Y2,YD2,YDD2
      R=FB0(1)
      R=FB(1)
      NMAX=50
      ISTOP=0
      NDOF=2*(NNOD-2)
      T1=0.
      DO 20 I=1,NEV
      Y1(I)=0.D0
      YD1(I)=0.D0
      YDD1(I)=0.D0
      C(I)=0.
      EPS(I)=0.1
   20 FN2(I)=0.
      IF (IDIS) 24,24,23
   23 CONTINUE
      CALL TEFNUL(X10,Y10,FT(25),RL,RT,NNOD)
      GO TO 26
   24 DO 25 I=1,NDOF
      FMA(I)=0.
   25 FT(I)=0.0D0
   26 CONTINUE
      IF (IDRA) 27,27,29
```

```
 27 DO 28 I=1,NDOF
 28 FDR(I)=0.
    GO TO 31
 29 CONTINUE
    NTIM=NNOD/5
    IREST=NNOD-5*NTIM
    NL=1
    IF (NTIM) 490,490,485
485 CONTINUE
    DO 500 I=1,NTIM
    NH=NL+4
    READ(5,501) ((XV0(J),YV0(J)),J=NL,NH)
501 FORMAT(10(F8.2))
500 NL=NL+5
490 CONTINUE
    IF (IREST) 520,520,510
510 NH=NL+IREST-1
    READ(5,501) ((XV0(J),YV0(J)),J=NL,NH)
520 CONTINUE
    WRITE(6,491)
491 FORMAT(/,42H WATER VELOCITIES AT NODES IN EQUILIBRIUM:  ,/)
    WRITE(6,492) (XV0(I),I=1,NNOD)
    WRITE(6,493) (YV0(I),I=1,NNOD)
492 FORMAT(5H XV0= ,11(2X,F8.2))
493 FORMAT(5H YV0= ,11(2X,F8.2))
    NL=1
    IF (NTIM) 16,16,14
 14 CONTINUE
    DO 15 I=1,NTIM
    NH=NL+4
    READ(5,501) ((XV1(J),YV1(J)),J=NL,NH)
 15 NL=NL+5
 16 CONTINUE
    IF (IREST) 18,18,17
 17 NH=NL+IREST-1
    READ(5,501) ((XV1(J),YV1(J)),J=NL,NH)
 18 CONTINUE
    WRITE(6,19)
 19 FORMAT(/,28H WATER VELOCITIES AT NODES: ,/)
    WRITE(6,503) (XV1(J),J=1,NNOD)
    WRITE(6,504) (YV1(J),J=1,NNOD)
503 FORMAT(5H XV1= ,11(2X,F8.2))
504 FORMAT(5H YV1= ,11(2X,F8.2))
    CALL DRFNUL(X10,Y10,XV0,YV0,FDR0,MP,NMG,NML,RMG,RML,
   1            Z,ZG,RL,CD,AR,DN,ROW,NNOD)
 31 CONTINUE
    IF (NWAV) 44,44,33
 33 NTIM=NWAV/5
    IREST=NWAV-5*NTIM
    NL=1
    IF (NTIM) 37,37,34
 34 CONTINUE
    DO 36 N=1,NTIM
    NH=NL+9
    READ(5,401) (WAV(I),I=NL,NH)
401 FORMAT(10F8.2)
 36 NL=NL+10
 37 IF (IREST) 43,43,42
 42 NH=NL+2*IREST
```

```
      READ(6,401) (WAV(I),I=NL,NH)
   43 N1=2*NWAV
      WRITE(6,402)  (WAV(I),I=1,N1)
  402 FORMAT(12H TIMINT:WAV= ,10(1X,E10.4))
      GO TO 46
   44 DO 45 N=1,NNOD
      XV(N)=XV1(N)
   45 YV(N)=YV1(N)
   46 CONTINUE
      NEL=NNOD-1
      IVIS=0
      DO 48 I=1,NEL
      IF (DC(I)) 48,48,47
   47 IVIS=1
      GO TO 49
   48 CONTINUE
      N1=2*(NNOD-2)
      DO 481 I=1,N1
  481 FV(I)=0.
   49 CONTINUE
      DO 482 I=1,NEV
  482 CV(I)=0.
      IF (IVIS) 295,295,293
  293 CALL VISCOF(CV,XD1,YD11,X10,Y10,EV,RL,R0,FDR,FN2,COS1,COS2,
     1            Z,ZG,B,DC,NNOD,NEV)
  295 CONTINUE
      IF (IDRA) 605,605,604
  604 CALL DRACOF(CW,X10,Y10,XD1,YD11,XV,YV,EV,COS1,COS2,B,FDR,FN2,R0,
     1            Z,ZG,X1,XG,YG,RL,CD,AR,DN,ROW,NEV,NNOD)
      DO 294 I=1,NEV
  294 CV(I)=CV(I)+CW(I)
  605 CONTINUE
      WRITE(6,651) (CV(I),I=1,NEV)
  651 FORMAT(/,41H TOTAL LINEAR MODAL DAMPING COEFFICIENTS:,/,
     1       10(1X,E10.4))
      DO 596 I=1,NEV
  596 FV(I)=CV(I)/(2*R0(I))
      WRITE(6,597) (FV(I),I=1,NEV)
  597 FORMAT(/,50H TOTAL RELATIVE LINEAR MODAL DAMPING COEFFICIENTS:,
     1       /,10(2X,E10.4))
      DO 620 I=1,NEV
      ARG=R0(I)*R0(I)-CV(I)*CV(I)/4
      IF (ARG) 612,611,610
  610 ND(I)=1
      OM(I)=DSQRT(ARG)
      GO TO 620
  611 ND(I)=2
      OM(I)=0.
      GO TO 620
  612 ND(I)=3
      ARG=-ARG
      OM(I)=DSQRT(ARG)
  620 CONTINUE
      DO 705 I=1,NEV
      FN1(I)=0.
  705 FN2(I)=0.
      IT=0
      TL=0.
      DO 200 NIT=1,NTIME
```

```
      READ(5,301) LTYP,PER,AM1,FI1,AM2,FI2,DFAC,NSTEP
  301 FORMAT(I8,6F8.2,I8)
      IF (DFAC) 291,290,291
  290 DFAC=1.
  291 CONTINUE
      WRITE(6,302) LTYP,DFAC,NSTEP
  302 FORMAT(//,6H LTYP=,I4,6H DFAC=,1X,E10.4,14H NO. OF STEPS:,I4)
      IF (LTYP-1) 312,311,312
  311 OME=6.2831853/PER
      WRITE(6,303) PER,OME,AM1,FI1,AM2,FI2
  303 FORMAT(/,9H PERIOD= ,E10.4,2X,7H FREQ= ,E10.4,2X,8H X-AMPL= ,
     1       F10.4,10H X-PHASE= ,F10.4,16H (DEG)  Y-AMPL= ,F10.4,
     2       2X,10H Y-PHASE= ,F10.4,6H (DEG))
      FI1=FI1/57.29578
      FI2=FI2/57.29578
      IRE=6
  312 CONTINUE
      DO 200 IIT=1,NSTEP
      IT=IT+1
      IF (IT-31) 310,305,310
  305 DO 306 I=1,NEV
  306 EPS(I)=0.1*EPS(I)
  310 CONTINUE
      NUMA=0
      DO 30 I=1,NEV
      Y0(I)=Y1(I)
      YD0(I)=YD1(I)
      YDD0(I)=YDD1(I)
   30 FN1(I)=FN2(I)
      IF (LTYP-1) 340,321,330
  321 IF (IRE-6) 323,322,322
  322 READ(5,304) ((TIM(I),IPRT(I)),I=1,5)
  304 FORMAT(5(F8.2,I8))
      IRE=1
  323 T=TIM(IRE)
      IPR=IPRT(IRE)
      IRE=IRE+1
      DELT=T-TL
      IF (IIT-NSTEP) 702,701,701
  701 TL=T
  702 CONTINUE
      CALL DISGEN(DELT,OME,AM1,FI1,AM2,FI2,U,UD,UDD)
      GO TO 335
  330 IF (LTYP-2) 331,331,340
  331 READ(5,10) T,(U(I),I=1,2),(UD(I),I=1,2),(UDD(I),I=1,2),IPR
   10 FORMAT(F8.2,6E8.2,I4)
  335 GO TO 342
  340 WRITE(6,341) LTYP
  341 FORMAT(/,6H LTYP=,I4,37H IS NOT ALLOWED. CALCULATION STOPPED.)
      STOP
  342 CONTINUE
      WRITE(6,11)
   11 FORMAT(/,101H TIMESTEP       TIME     XDISP        YDISP        XVEL
     1       YVEL         XACC         YACC          IPR    )
      WRITE(6,12)  IT,T,(U(I),I=1,2),(UD(I),I=1,2),(UDD(I),I=1,2),IPR
   12 FORMAT(I6,3X,7(2X,E10.4),3X,I3)
      DT=T-T1
      T1=T
      X1(1)=X10(1)
```

```
      Y11(1)=Y10(1)
      XG(1)=0.
      YG(1)=0.
      XD1(1)=0.
      YD11(1)=0.
      XDD1(1)=0.
      YDD11(1)=0.
      X1(NNOD)=U(1)+X10(NNOD)
      Y11(NNOD)=U(2)+Y10(NNOD)
      XG(NNOD)=U(1)
      YG(NNOD)=U(2)
      XD1(NNOD)=UD(1)
      YD11(NNOD)=UD(2)
      XDD1(NNOD)=UDD(1)
      YDD11(NNOD)=UDD(2)
      CALL DISFOR(FK,FM,FDIS,U,UDD,NNOD)
   40 CONTINUE
      IND=0
      IF (NUMB) 41,41,143
   41 CALL TIMSTP(Y0,YD0,YDD0,Y2,YD2,YDD2,C,FN1,FN2,R0,CV,OM,DT,N  NEV)
      GO TO 149
  143 CONTINUE
      DO 50 I=1,NEV
      Y2(I)=Y1(I)
      YD2(I)=YD1(I)
   50 YDD2(I)=YDD1(I)
  149 CONTINUE
      IW=0
      CALL NEWPOS(X,Y2,XD,YD2,XDD,YDD2,EV,XG,YG,X10,Y10,COS1,COS2,Z,ZG,
     1            B,X1,Y11,XD1,YD11,XDD1,YDD11,NNOD,NEV,IW)
      CALL ELETEN(RT,RV,AR,FR,RL,RM,X10,Y10,XG,YG,NNOD,IW)
      IF (IDRA) 52,52,51
   51 CONTINUE
      IF (NWAV) 54,54,53
   53 CALL WATVEL(X1,Y11,XV,YV,XV1,YV1,XACC,YACC,T,GRAV,DEPTH,
     1            WAV,NNOD,NWAV)
   54 CONTINUE
      CALL DRAFOR(X1,Y11,XD1,YD11,XV,YV,MP,NMG,NML,RMG,RML,
     1            COS1,COS2,B,FDR,FDR0,Z,ZG,RM,CD,AR,DN,ROW,NNOD)
   52 CONTINUE
      IF (IDIS) 57,57,56
   56 CONTINUE
      CALL TENFOR(X1,Y11,XG,YG,COS1,COS2,B,FT,FT(25),FT(49),
     1            FT(73),RM,RT,RV,EK,GK,Z,ZG,NNOD,IDIS)
      CALL MASFOR(X1,Y11,XDD1,YDD11,MM,MP,NMG,NML,RMG,RML,COS1,COS2,
     1            B,FMA,FT(49),FT(61),Z,ZG,RL,RM,CM,AR,ROW,R0,NNOD)
   57 CONTINUE
      IF (IVIS) 59,59,58
   58 CALL VISFOR(X1,Y11,XD1,YD11,COS1,COS2,B,FV,RM,DC,
     1            Z,ZG,NNOD)
   59 CONTINUE
      DO 60 I=1,NDOF
   60 F(I)=FT(I)+FDR(I)+FMA(I)+FV(I)+FDIS(I)
      CALL TRAFOR(EV,F,FN2,NNOD,NEV)
      DO 61 I=1,NEV
   61 FN2(I)=FN2(I)+CV(I)*YD2(I)
      CALL TIMSTP(Y0,YD0,YDD0,Y1,YD1,YDD1,C,FN1,FN2,R0,CV,OM,DT,ND,NEV)
      DO 90 I=1,NEV
      SUM=DABS((Y2(I)+Y1(I))/2.)
```

```
      DIFF=DABS(Y2(I)-Y1(I))
      IN=NUMB/2
      IRES=NUMB-2*IN
      IF (IRES) 75,75,74
   74 CONTINUE
      Y1(I)=0.5*(Y1(I)+Y2(I))
      YD1(I)=0.5*(YD1(I)+YD2(I))
      YDD1(I)=0.5*(YDD1(I)+YDD2(I))
   75 CONTINUE
      IF (DIFF) 76,76,77
   76 QUOT=0.
      GO TO 78
   77 QUOT=DIFF/SUM
   78 CONTINUE
      IF (QUOT-EPS(I)) 90,90,80
   80 IND=1
   90 CONTINUE
      IF (IND) 190,190,120
  120 NUMB=NUMB+1
      IF (NUMB-NMAX) 40,40,140
  140 ISTOP=ISTOP+1
      IF (ISTOP-5) 190,190,189
  189 WRITE(6,141) IT,T,NMAX,ISTOP
  141 FORMAT(//,10H TIMESTEP:,I4,2X,6H TIME:,1X,F8.2,/,
     1       10H MORE THAN,I4,25H ITERATIONS HAVE OCCURRED,I4,
     2       28H TIMES. CALCULATION STOPPED.)
      STOP
  190 CONTINUE
      WRITE(6,191) IT,NUMB
  191 FORMAT(11H TIMESTEP: ,I4,2X,22H NUMBER OF ITERATIONS: ,I4)
      WRITE(6,192) (Y1(I),I=1,NEV)
  192 FORMAT(4H Y1=,10(2X,D10.4))
      IF (IPR) 195,194,195
  194 IPR=1
  195 IW=IPR
      CALL NEWPOS(X,Y1,XD,YD1,XDD,YDD1,EV,XG,YG,X10,Y10,COS1,
     1            COS2,Z,ZG,A,X1,Y11,XD1,YD11,XDD1,YDD11,NNOD,NEV,IW)
      CALL ELETEN(RT,RV,AR,FR,RL,RM,X10,Y10,XG,YG,NNOD,IW)
  200 CONTINUE
      RETURN
      END
```

REFERENCES

[1] Lamb, H.: Hydrodynamics, 6th e d., Cambridge University Press, 1945.

[2] Gautmacher: Matrix Theory I, II, Chelsea Publ. Co., 1974.

[3] Hildebrand, F. B.: Advanced Calculus for Engineers, Prentice Hall, 1962.

[4] Batchelor, G. K.: An Introduction to Fluid Dynamics, Cambridge University Press, 1967.

[5] Routh, E. J.: Dynamics of a System of Rigid Bodies, Advanced Part, 6th ed. (1905). Reprint by Dover Publications.

[6] Jahnke, E. and F. Emde: Tables of Functions, Dover publications, 1945.

[7] Przemieniecki, J. S.: Theory of Matrix Structural Analysis, McGraw-Hill Book Company, 1968.

[8] Zurmühl, R.: Matrizen, Springer Verlag, 1950.

[9] Zienkiewicz, O. C.: The Finite Element Method in Engineering and Science, McGraw-Hill, 1971.

[10] Pode, L.: Tables for Computing the Equilibrium Configuration of a Flexible Cable in a Uniform Stream, David Taylor Model Basin, Report 687 (March 1951).

[11] Berteaux, H. O.: Buoy Engineering, to be published.

[12] Dominguez, R. F. and C. E. Smith: Dynamic Analysis of Cable Systems, Journal of the Structural Division, ASCE, Vol. 98, no. ST8, paper 9127, Aug. 1972, pp. 1817-1834.

[13] Patton, K. T.: The Response of Cable-Moored Axisymmetric Buoys to Ocean Wave Excitation, NUSC TP 4331, June 1972, Naval Underwater Systems Center.

[14] Reid, R. O.: Dynamics of Deep-Sea Mooring Lines, Final Report, Project 204, Ref. 68-11F, Dept. of Oceanography, Texas A&M University, July 1968.

[15] Hoffman, D., E. S. Geller and C. S. Niederman: Mathematical Simulation and Model Tests in the Design of Data Buoys, SNAME, 1973.

[16] Tsai, N.-T.: Analysis of Non-Linear Transient Motion of Cables Using Bond Graph Method, ASME Paper no. 71-Vibr-21, 1971.

[17] Leonard, J. W. and W. W. Recker: Non-linear Dynamics of Cables with Low Initial Tension, Proceedings ASCE, Engineering Mechanics Division, April 1972.

[18] Leonard, J. W.: Curved Finite Element Approximation to Non-linear Cables, Offshore Technology Conference Houston, Texas, 1972.

[19] Webster, R. L.: Nonlinear Static and Dynamic Response of Underwater Cable Structures Using the Finite Element Method, Offshore Technology Conference, Houston, Texas, paper OTC 2322, 1975.

[20] Hsu, F. H. and U. A. Blenkarn: Analysis of Peak Mooring Force Caused by Slow Vessel Drift Oscillation in Random Seas, Offshore Technology Conference, Houston, Texas, 1970.

[21] Smith, C. E., T. Yamamoto and J. H. Nath: Longitudinal Vibration in Taut-line Moorings, Marine Technology Society Journal, Vol. 18, no. 5, June 1974.

[22] Goeller, J. E. and P. A. Laura: A Theoretical and Experimental Investigation of Impact Loads in Stranded Steel Cables During Longitudinal Excitation, in Proceedings of the Fifth Southeastern Conference on Theoretical and Applied Mechanics, ed. G. L. Rogers, the University of North Carolina Press, 1970.

[23] Kawashima, S. and H. Kimura: Measurement of the Internal Friction of Metal Wires and Metal Wire Ropes through the Longitudinal Vibration, Mem. Fac. Engr., Kyushu University, 13(1), 1952.

[24] Skop, R. A. and G. J. O'Hara: The Method of Imaginary Reactions, Marine Technology Society Journal, Vol. 4 (1970), no. 1.

[25] Choo, Y. and M. J. Casarella: A Survey of Analytical Methods for Dynamic Simulation of Cable-Body Systems, Journal of Hydronautics, Vol. 7, no. 4 (Oct. 1973).

[26] Walton, T. S. and H. Palacheck: Calculation of Nonlinear Transient Motion of Cables, David Taylor Model Basin, Report 1279, July 1959.

[27] Argyris, J. H. and A. S. L. Chan: Applications of Finite Elements in Space and Time, Ingenieur-Archiv 41 (1972), pp. 235-257.

[28] Argyris, J. H., P. C. Du-ne and T. Angelopoulos: Non-linear Oscillations Using the Finite Element Technique, Computer Methods in Applied Mechanics and Engineering, Vol. 2 (1973), pp. 203-250.

[29] Newmark, N. M.: A Method of Computation for Structural Dynamics, Proceedings ASCE, July 1959.

[30] Newman, J.N.: Marine Hydrodynamics, Lecture Notes, Department of Ocean Engineering, MIT, 1972.

[31] Griffin, O.M.: Vortex-Induced Lift and Drag on Stationary and Vibrating Bluff Bodies, Journal of Hydronautics, Vol. 9, No. 4, Oct 1975.

[32] Williams, H.E.: Motion of a Cable Used as a Mooring, Journal of Hydronautics, Vol. 9, No. 7, July 1975.

BIOGRAPHICAL NOTE

Per I. Johansson was born 14 February 1942 in Oslo, Norway.

After graduating from the Gymnasium (High School) in 1960, he had one year of practical work in a shipyard before entering the Department of Shipbuilding and Marine Engineering at the Technical University of Norway. Later he did studies at the University of Oslo. He finally graduated from the Technical University in 1969, and started working in the Research Department of Det norske Veritas. Simultaneously, he continued his studies of physics at the University of Oslo and graduated in 1972. He entered the Department of Ocean Engineering, MIT in September 1973.